
6 COLLAPS3.3D COMPUTER CODE DESCRIPTION

The version of the Westinghouse BWR cladding creep collapse code, COLLAPS-II, described in Sections 6 and 7 of Reference (1-1) is referred to as COLLAPS-3.2S. This section describes a revised version of COLLAPS-II referred to as COLLAPS-3.3D.

The COLLAPS-II code is used to predict cladding ovalization, which ultimately leads to creep collapse, as a function of irradiation time. The modifications of COLLAPS-3.2S resulting in COLLAPS-3.3D can be summarized as follows:

- (1) The "S" in COLLAPS-3.2S refers to single precision. The "D" in COLLAPS-3.3D refers to double precision,
- (2) COLLAPS-3.2S assumed an infinite length hollow tube with no internal support due to pellets. [

] and

- (3) The improved BWR cladding creep correlation described in Section 2.2.3 has been incorporated into COLLAPS-3.3D.

For current nuclear fuel rod and pellet designs and fabrication processes, only small pellet-to-pellet axial gaps are expected to occasionally occur in the fuel pellet stack during operation. With the exception of cladding locations adjacent to these gaps, the pellets will provide support for the cladding and prevent cladding collapse. In effect, the pellet supports the cladding from any significant increase in ovality resulting in a reduction in the rate of ovalization. [

]

6.1 Introduction

6.1.1 Background

Six assumptions are listed in Section 6.1.1 of Reference (1-1). With the exception of assumption (6), these assumptions continue to be appropriate for COLLAPS-3.3D. Assumption (6) should be modified for COLLAPS-3.3D as follows:

(6) [

]

6.1.2 Basic Assumptions and Definitions

Section 6.1.2 remains unchanged relative to Reference (1-1).

6.1.3 The Stress Resultants

Section 6.1.3 remains unchanged relative to Reference (1-1).

6.1.4 Axial Strain ϵ_z

Section 6.1.4 remains unchanged relative to Reference (1-1).

6.2 Integration of Equilibrium Equations

All sections of Section 6.2 (Sections 6.2.1 through 6.2.3) are unchanged relative to Reference (1-1).

6.3 Calculation of the Neutral Line Shape from Generalized Strains

All sections of Section 6.3 (Sections 6.3.1 through 6.3.4) are unchanged relative to Reference (1-1).

6.4 Calculation of the Indeterminate Reaction, M_B

All sections of Section 6.4 (Sections 6.4.1 through 6.4.3) are unchanged relative to Reference (1-1).

6.5 Creep and Solution of the Time-Dependent Collapse Problem

Section 6.5 of Reference (1-1) (Sections 6.5.1 through 6.5.5) is unchanged relative to Reference (1-1). Section 6.5.6 is a new section [

]

6.5.1 Elastic Stresses

Section 6.5.1 is unchanged relative to Reference (1-1).

6.5.2 Strain Increments Due to Creep

Section 6.5.2 is unchanged relative to Reference (1-1).

6.5.3 The Automatic Time Step Selection

Section 6.5.3 is unchanged relative to Reference (1-1).

6.5.4 Data Preparation for the Next-Time-Step

Section 6.5.4 is unchanged relative to Reference (1-1).

6.5.5 The Geometry of the Un-deflected Line

Section 6.5.5 is unchanged relative to Reference (1-1).

6.5.6 Finite Length Axial Pellet to Pellet Gap Model

[

]

[

]

(6.5.6-1)

6.6 Summary

Section 6.6 is unchanged relative to Reference (1-1).

6.7 Collapse Criteria

Section 6.7 is unchanged relative to Reference (1-1).

6.8 References

No references in addition to those in Reference (1-1) are required.

7 COLLAPS-3.3D CODE QUALIFICATION

As discussed in Section 6, predictions of COLLAPS-3.3D will differ from those of COLLAPS-3.2S due to implementation of the improved BWR creep correlation described in Section 2.2.3 and the finite length axial pellet to pellet gap treatment.

Utilization of the new BWR creep correlation described in Section 2.2.3 in COLLAPS-3.3D is qualified in this section by comparisons of predicted collapse results with corresponding creep correlation results in Section 7 of Reference (1-1). Repetition of the parametric evaluations in Section 7 of Reference (1-1) for the new creep correlation described in Section 2.2.3 is not considered to be necessary because of the relatively minor impact of the new creep correlation on collapse results. The relative sensitivities of COLLAPS-3.3D will be very similar to those of COLLAPS-3.2S.

[

] In addition, the impact on cladding collapse of the finite length axial gap approximation is provided for COLLAPS-3.3D.

7.1 Introduction

Section 7.1 remains unchanged relative to Reference (1-1).

7.1.1 Model Overview

Section 7.1.1 remains unchanged relative to Reference (1-1).

7.1.2 Numerical Solution

[

]

7.2 Creep Model for Zircaloy

7.2.1 General

The general description of the creep model in Section 7.2.1 of Reference (1-1) continues to apply to the creep correlations referred to in Reference (1-1). The new "RXA Creep Correlation" described in Sections 7.2.6 and 2.2.3 of this report will be used in BWR design and licensing analysis using COLLAPS-3.3D in place of the "ABB Atom Correlation" described in Section 7.2.2 of Reference (1-1).

COLLAPS-3.3D includes four Zircaloy creep correlations which can be selected by the user in the code input file. These creep correlations are described below. Only the correlation identified as the RXA (Recrystallization Annealed) Creep Correlation in Section 7.2.6 will be used for design and licensing analysis of BWR fuel with COLLAPS-3.3D.

7.2.2 ABB Atom Correlation

Section 7.2.2 is unchanged relative to Reference (1-1).

7.2.3 Hagrman Correlation

Section 7.2.3 is unchanged relative to Reference (1-1).

7.2.4 CEPAN Correlation

Section 7.2.4 is unchanged relative to Reference (1-1).

7.2.5 Creep Hardening Rules

Section 7.2.5 is unchanged relative to Reference (1-1).

7.2.6 RXA (Recrystallization Annealed) Creep Correlation

An improved Zircaloy creep correlation, referred to in this section as the "RXA Creep Correlation," was added to STAV7.2 as described in Section 2.2.3. Therefore, this new correlation has also been included in COLLAPS-3.3D.

7.3 Qualification of COLLAPS-3.3D

Section 7.3 is unchanged relative to Reference (1-1) with the exception of an additional Section 7.3.5 which describes qualification measures for COLLAPS-3.3D.

[

]

7.3.1 Selection of Initial Parameters

Section 7.3.1 applies to COLLAPS-3.3D and is unchanged relative to Reference (1-1).

7.3.2 Discussion of the Effect of Meshing

Section 7.3.2 applies to COLLAPS-3.3D and is unchanged relative to Reference (1-1).

7.3.3 The Ovality in Mechanical Equilibrium

Section 7.3.3 applies to COLLAPS-3.3D and is unchanged relative to Reference (1-1).

7.3.4 Comparison of Collapse Times

Section 7.3.4 applies to COLLAPS-3.3D and is unchanged relative to Reference (1-1).

7.3.5 RXA Creep Correlation for an Infinite Length Axial Pellet to Pellet Gap

[

]

[

]

7.3.6 Finite Length Axial Pellet-to-Pellet Gap

The standard test case described in Section 7.3.1 of Reference (1-1) was used to demonstrate the impact of the finite length axial pellet to pellet gap capability of COLLAPS-3.3D. [

]

[

]

7.4 Summary

The summary in Section 7.4 of Reference (1-1) is applicable to COLLAPS-3.3D. In addition, the following conclusions are applicable:

The finite length axial pellet-to-pellet axial gap treatment and the use of the RXA Creep Correlation in conjunction with the COLLAPS-3.3D code have been qualified and found to have a reasonable and modest impact on cladding collapse relative to COLLAPS-3.2S.

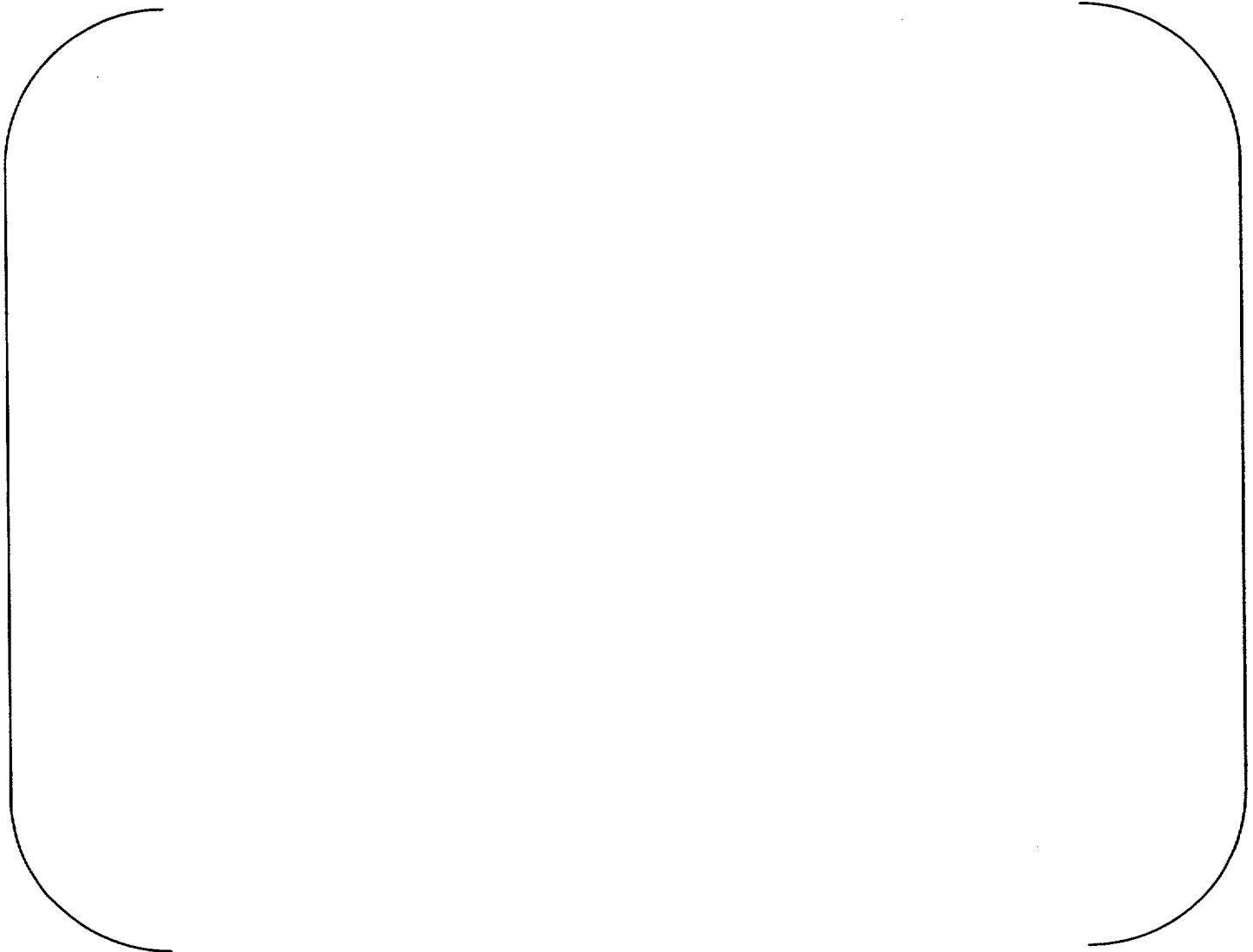
COLLAPS-3.3D includes additional phenomenological models that provide more realistic predictions of the cladding collapse phenomenon under varying conditions.

COLLAPS-3.3D has been demonstrated to be acceptable for analysis of BWR cladding collapse.

7.5 References

- (7-1) W. M. Adams, et al., CEPAN Method of Analyzing Creep Collapse of Oval Cladding Vol. 5. Evaluation of Interpellet Gap Formation and Clad Collapse in Modern PWR Fuel Rods, EPRI Report, EPRI NP-3966, 1985.

Table 7-1: Actual and Predicted (with finite length model) Collapse Times



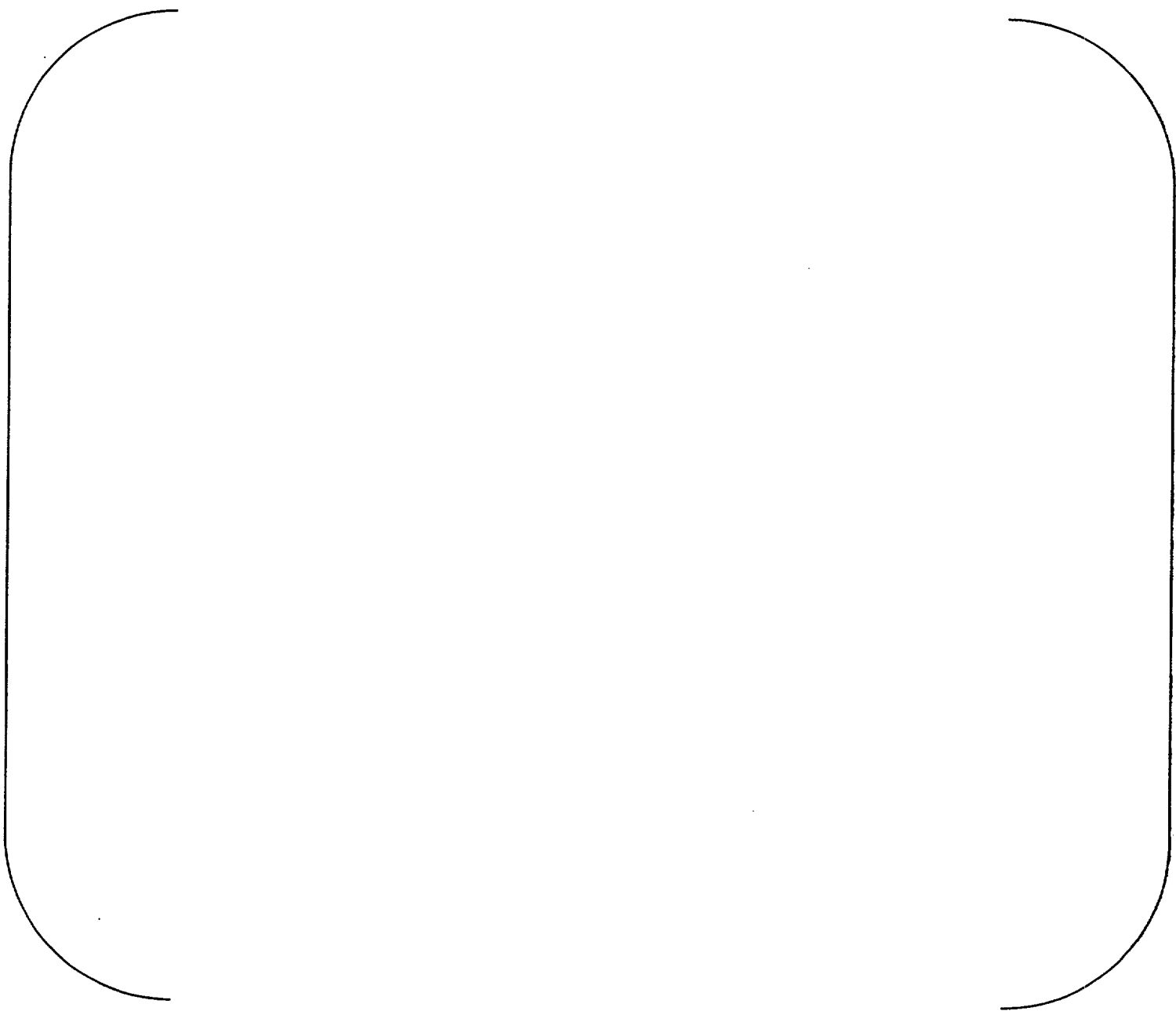


Figure 7-1: Calculated Infinite Length Pellet-pellet Axial Gap Ovality as a Function of Time

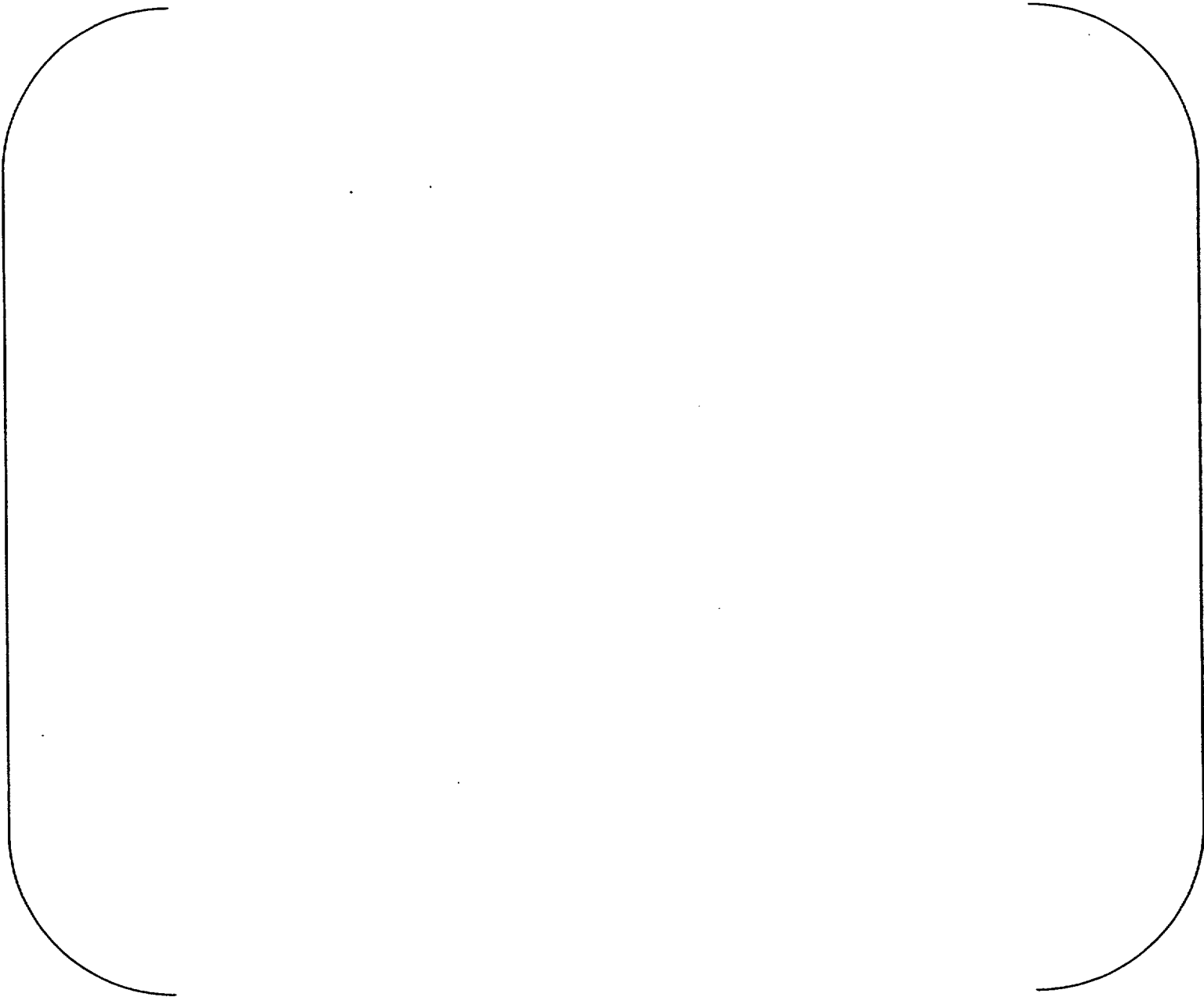


Figure 7-2: Ovality as a Function of Time (Finite Length Model Sensitivity)

APPENDIX A THERMAL AND MECHANICAL MATERIAL PROPERTIES

A.1 Fuel Rod Pellet Thermal Properties

A.1.1 Pellet Thermal Conductivity

The general description of Section A.1.1 of Reference (1-1) provided by the text through Equation (A.1-7) of Reference (1-1) is unchanged. However, the specific expressions for the UO_2 and $(U,Gd)O_2$ fuel thermal conductivity have been reformulated to explicitly treat the decrease in fuel conductivity with burnup. Therefore, the revised treatment of UO_2 and $(U,Gd)O_2$ fuel thermal conductivity are provided in Sections A.1.1.1 and A.1.1.2 of this document, respectively. Section A.1.1.3 provides a discussion of comparisons with thermal conductivity measurements.

A.1.1.1 UO_2 Fuel Thermal Conductivity in STAV7.2

The fuel thermal-conductivity models in STAV7.2 have been improved relative to those in Reference (1-1) by the introduction of a burnup dependence.

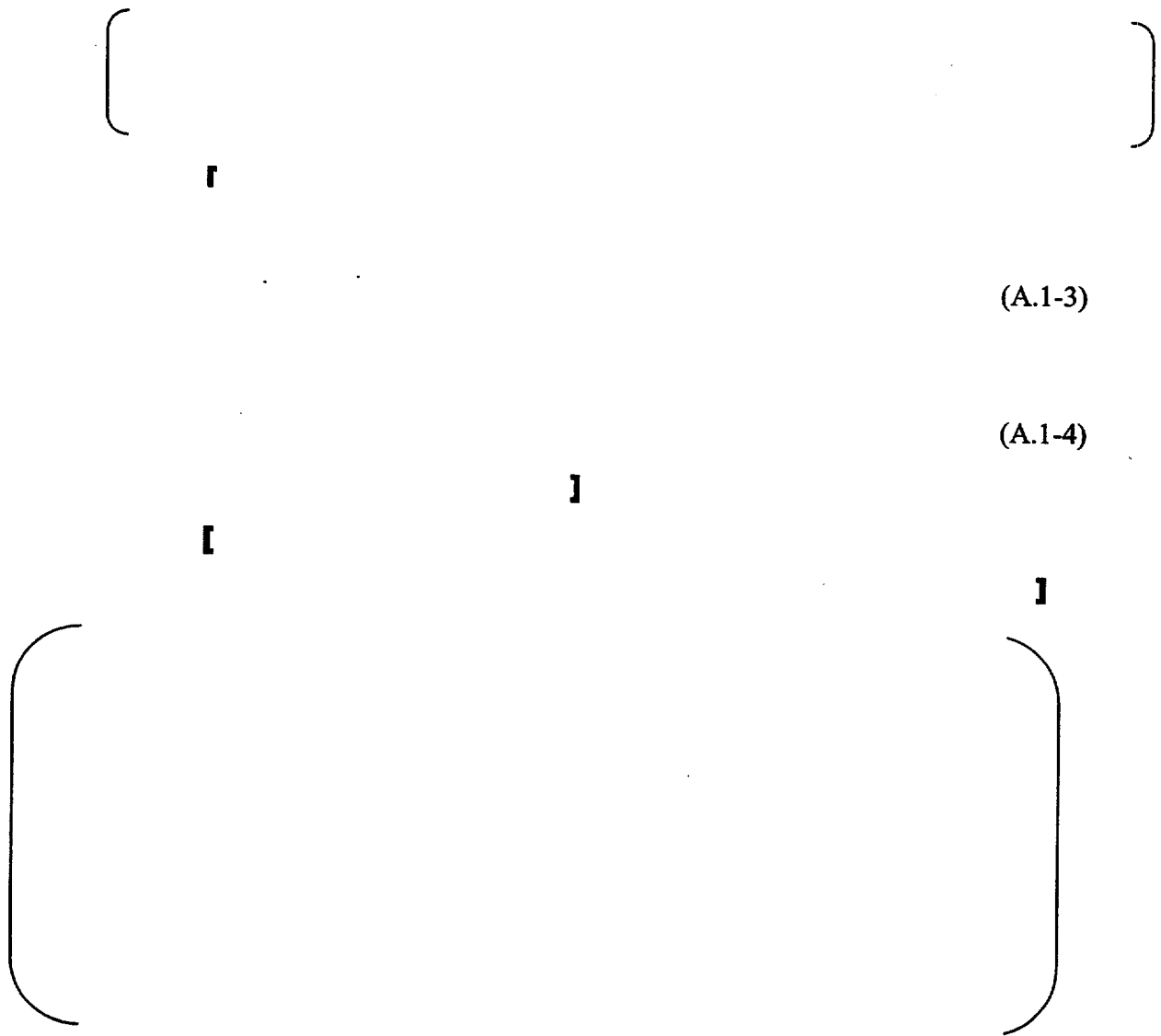
[

(A.1-1)

(A.1-2)

]

Table A.1-1: Values of the Constant Used in Equation (A.1-1)



Fraction of theoretical density

Figure A.1-1: Porosity correction factor, P, to thermal conductivity of UO₂ fuel as a function of fuel density. The factor is normalized to one for 95% dense fuel.



[

]

Equation (A.1-1) reduces to Equations (A-8) and (A-9) in Section A.1.1 of Reference (1-1) for UO_2 unirradiated fuel.

A.1.1.2 Gadolinia Fuel Thermal Conductivity

The thermal conductivity of unirradiated $(\text{U,Gd})\text{O}_2$ has been a subject of several measurements as reported in References (A-3) through (A-6). In these studies, the laser-flash technique is used to measure the thermal diffusivity of the material. In this method a short-duration (about 1 ms) heat pulse from a laser is deposited on one face of a slab sample, and the temperature rise as a function of time in the opposite face of the sample is monitored. Diffusivity, h , is then calculated from the thickness of the slab sample and half-time of temperature rise.

Having determined h , the thermal conductivity, k , is calculated using the relation:

$$k = h C_p \rho \quad (\text{A.1-6})$$

where ρ is the material density, and C_p is the heat capacity of the material at constant pressure. In References (A-3) and (A-5) through (A-7), heat capacities were calculated by combining the values for UO_2 and Gd_2O_3 using the thermodynamic rules of mixture. On the other hand, in Reference (A-4), calorimetric measurements were made to determine specific heat of $(\text{U,Gd})\text{O}_2$ samples as a function of temperature.

[

(A.1-7)

(A.1-8)

]

Equation (A.1-7) reduces to Equations (A-14) and (A-15) in Section A.1.1 of Reference (1-1) for unirradiated $(\text{U,Gd})\text{O}_2$ fuel.

A.1.1.3 Comparison of Thermal Conductivity Equations with Experimental Data

[

]

[

]

A.1.2 Pellet Heat Capacity

The heat capacity treatment described in Section A.1.2 of Reference (1-1) is used in STAV7.2.

A.1.3 Pellet Thermal Expansion

The pellet thermal expansion treatment described in Section A.1.3 of Reference (1-1) is used in STAV7.2.

A.2 Fuel Rod Cladding Thermal Properties

A.2.1 Cladding Thermal Conductivity

The cladding thermal conductivity model described in Section A.2.1 of Reference (1-1) is used in STAV7.2.

A.2.2 Cladding Heat Capacity

The cladding heat capacity model described in Section A.2.2 of Reference (1-1) is used in STAV7.2.

A.2.3 Cladding Thermal Expansion

The cladding thermal expansion models described in Section A.2.3 of Reference (1-1) is used in STAV7.2.

A.3 Fuel Rod Cladding Elastoplastic Material Properties

Section A.3 of Reference (1-1) remains applicable to STAV7.2 with exception of the following changes:

(1) []

(2) []

]

(3) []

]

(4) While they do not represent differences in the STAV6.2 and STAV7.2 codes, two typographical corrections of Reference (1-1) are required:

(a) []

]

(b) []


]

A.4 Fuel Rod Void Gas Properties

[

]

Table A.4-1: Accommodation Coefficients



A.5 Extension of Gadolinia Burnup Application to 9 w/o

A.5.1 Summary

The Safety Evaluation Report for Reference (1-1) limited the application of STAV6.2 to fuel rods with gadolinia concentrations less than or equal to 8 w/o. It is our understanding that this limitation was based on a lack of irradiation data for fuel rods with higher concentrations. **[**

]
Consequently, it is concluded that application of STAV7.2 to fuel rods containing gadolinia concentrations less than or equal to 9 w/o is acceptable, and NRC concurrence with this conclusion is requested.

A.5.2 Reactor Operation with 9 w/o Gadolinia Fuel Rods

[

]

[

]

[

]

A.5.3 Acceptability of STAV7.2 Models for 9 w/o Gadolinia

(U,Gd)O₂ Pellet Power Distribution

[

]

[

]

[

]

[

]

(U,Gd)O₂ Thermal Conductivity

[

]

Therefore, it is concluded that there will be no significant decrease in reliability of thermal conductivity predictions associated with the model described in Section A.1.1.2 for concentrations of 9 w/o gadolinia relative to 8 w/o gadolinia.

(U,Gd)O₂ Heat Capacity (Specific Heat)

[

Therefore, it is concluded that the UO₂ correlation for the specific heat will continue to be applicable to (U,Gd)O₂ fuel for gadolinia concentrations up to 9 w/o.

(U,Gd)O₂ Thermal Expansion (Section A.1.3)

[

] Therefore, the UO₂ STAV7.2 thermal expansion model will provide acceptable predictions of thermal conductivity for (U,Gd)O₂ to 9 w/o (U,Gd)O₂.

A.6 References

- (A-1) D. L. Hagrman and G. A. Reymann, *MATPRO-version II- A handbook of materials properties for use in the analysis of light water reactor fuel behavior*, NUREG/CR-0497, 1979.
- (A-2) Y. Kosaka, Thermal conductivity degradation analysis of the ultra high burnup experiment (IFA-562), OECD Halden Project Report HWR-341 (1993).
- (A-3) S. Fukushima et al, "The Effect of Gadolinium Content in Thermal Conductivity of Near Stoichiometric (U,Gd)O₂ Solid Solution," *J. Nucl. Mater.*, Vol. 105, pg. 201, (1982).
- (A-4) L. W. Newman, "Development and Demonstration of an Advanced Extended Burnup Fuel Assembly Incorporating Urania - Gadolinia," DOE/ET/34212-36 (BAW-1681-2), August 1982.
- (A-5) R. H. Watson, "Properties of Urania-Gadolinia System (Part II)," EPRI NP-5862-LD, June 1988.
- (A-6) R.A. Busch, "Properties of Urania-Gadolinia System (Part I)," Draft, NFIR-RP-03-06D, December 1986.
- (A-7) T. Wada, K. Noro, and K. Tsukui, "Behavior of UO₂-Gd₂O₃ Fuel," Proceedings of the International Conference on Fuel Performance, British Nuclear Energy Society, 15-19 October 1973, London, England.
- (A-8) A. R. Massih, S. Persson and Z. Weiss, Modelling of (U,Gd)O₂ fuel behavior in boiling water reactors, *J. Nucl. Mater.*, 188 (1992) 323-330.

APPENDIX B FUEL TEMPERATURE COMPARISONS

Appendix B of Reference (1-1) is a discussion of the power distribution calculation and neutron diffusion treatment for (U,Gd)O₂ fuel in STAV6.2. Sections 2.1.2.3 and 2.1.5.2 of this document address the applicability of the information in Appendix B of Reference (1-1) to STAV7.2. In addition, Section A.5 of Appendix A is a new section providing justification for extending the limit on gadolinia concentration established in Reference (1-1) from 8 w/o to 9 w/o.

Therefore, it is not necessary to repeat the information in Appendix B of Reference (1-1). Consequently, Appendix B of this document contains comparisons of STAV7.2 fuel temperature predictions with experimental data as discussed in Section 3.

Beginning of Life (BOL) Temperatures

Table B-1: BOL Centerline Temperature in Rod 432-1

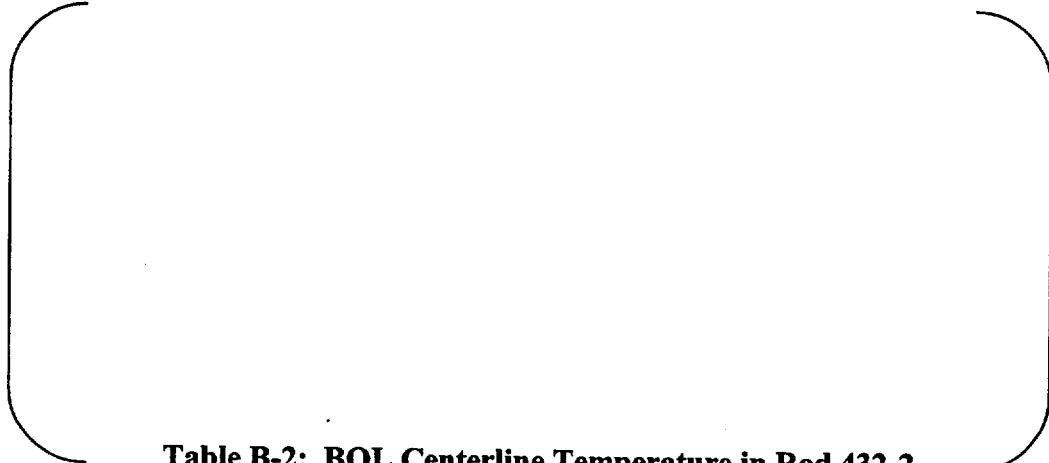


Table B-2: BOL Centerline Temperature in Rod 432-2

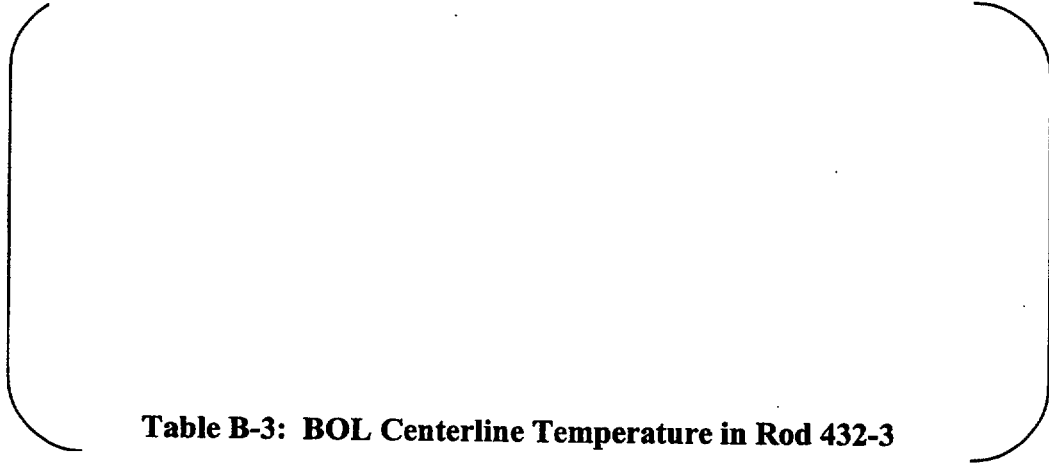


Table B-3: BOL Centerline Temperature in Rod 432-3



Table B-4: BOL Centerline Temperature in Rod 432-5



Table B-5: BOL Centerline Temperature in Rod 504-1-ar

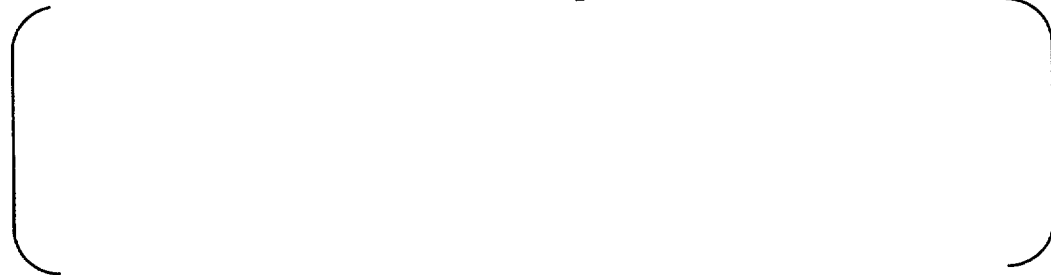


Table B-6: BOL Centerline Temperature in Rod 504-1-he



Table B-7: BOL Centerline Temperature in Rod 504-1-xe

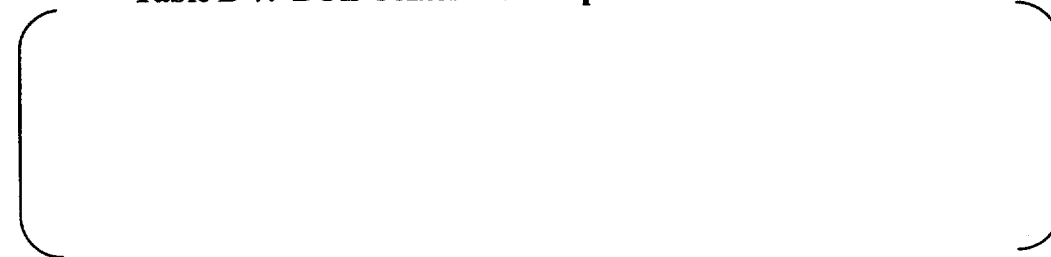


Table B-8: BOL Centerline Temperature in Rod 505-911A

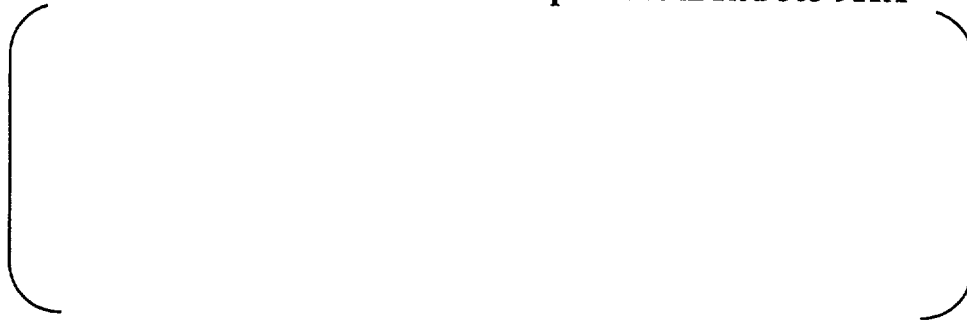


Table B-9: BOL Centerline Temperature in Rod 505-911B



Table B-10: BOL Centerline Temperature in Rod 505-912A



Table B-11: BOL Centerline Temperature in Rod 505-913A



Table B-12: BOL Centerline Temperature in Rod 505-913B



Table B-13: BOL Centerline Temperature in Rod 505-914A

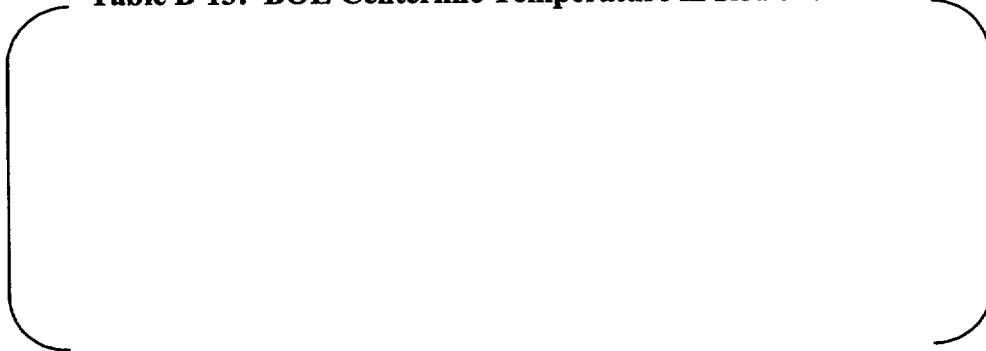


Table B-14: BOL Centerline Temperature in Rod 505-915A

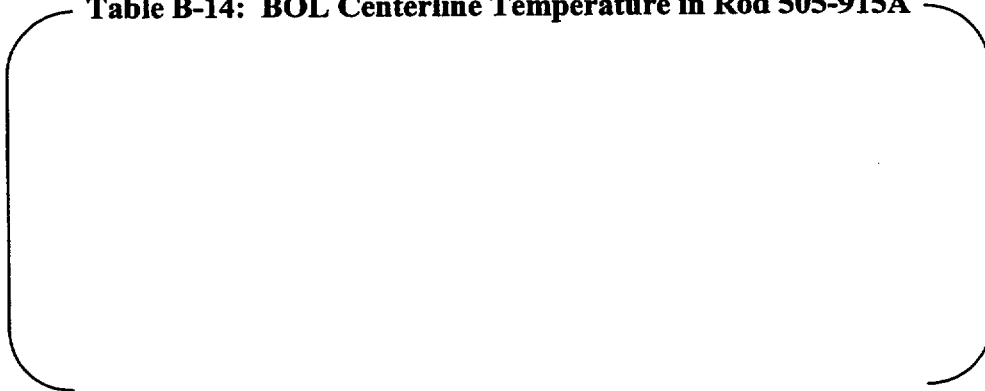


Table B-15: BOL Centerline Temperature in Rod 505-915B

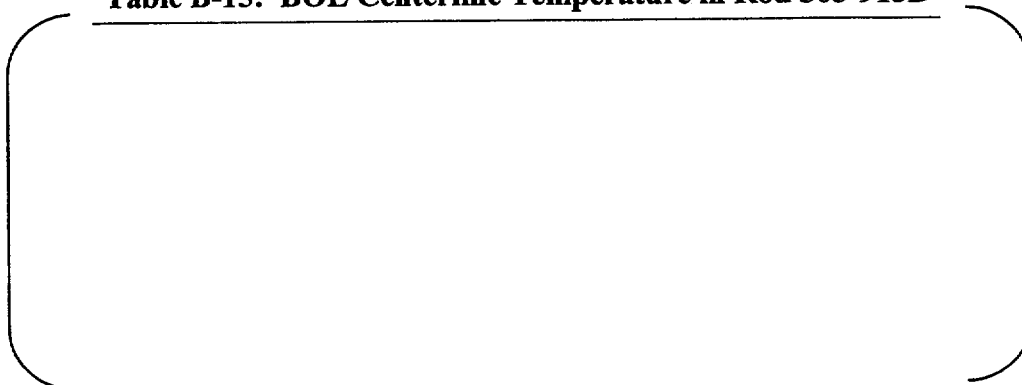


Table B-16: BOL Centerline Temperature in Rod 505-916A

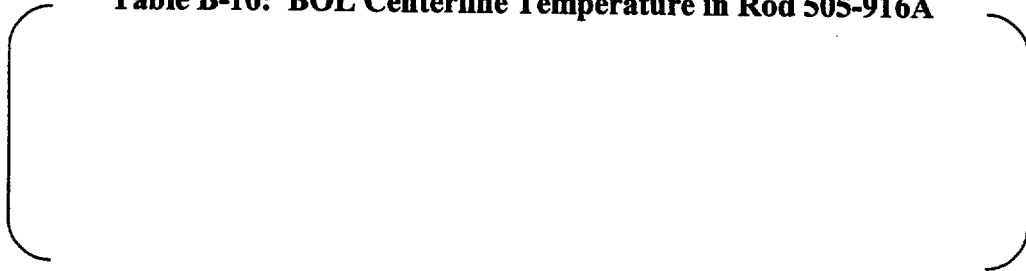


Table B-17: BOL Centerline Temperature in Rod 505-922C

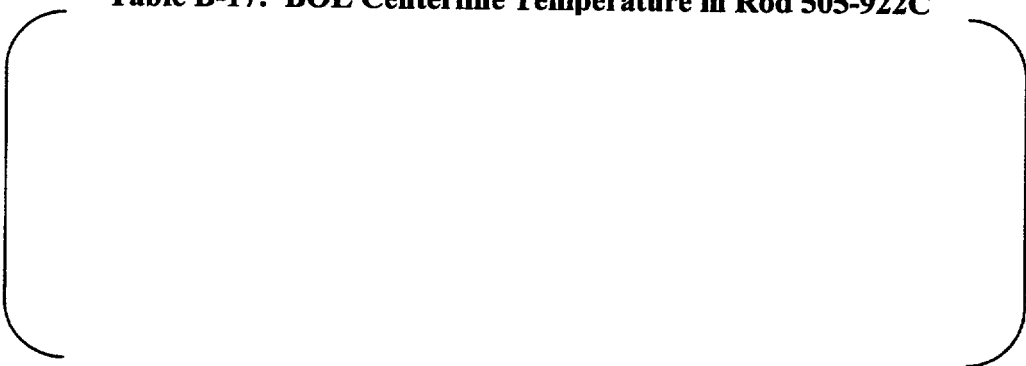


Table B-18: BOL Centerline Temperature in Rod 505-922D

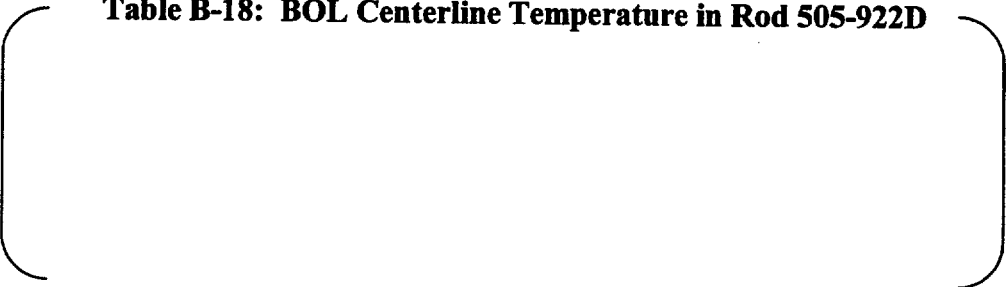


Table B-19: BOL Centerline Temperature in Rod 505-923D

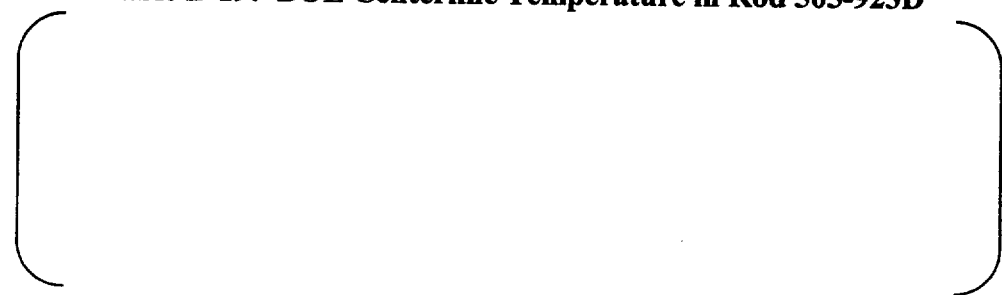


Table B-20: BOL Centerline Temperature in Rod 505-924C

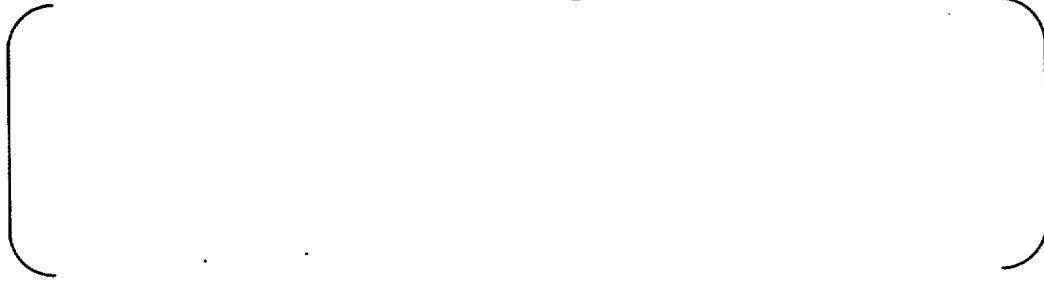


Table B-21: BOL Centerline Temperature in Rod 505-924D

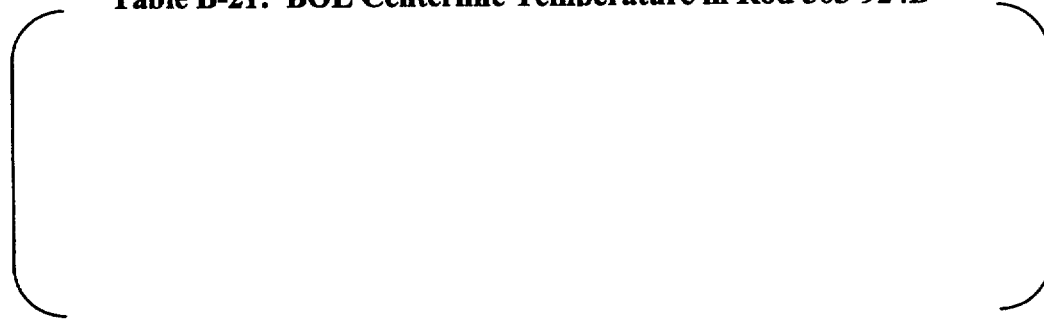


Table B-22: BOL Centerline Temperature in Rod 505-926C



Table B-23: BOL Centerline Temperature in Rod 505-926D



Table B-24: BOL Centerline Temperature in Rod 507-1_3_5

Table B-25: BOL Centerline Temperature in Rod 507-2_4_6

Table B-26: BOL Centerline Temperature in Rod 513-1

Table B-27: BOL Centerline Temperature in Rod 513-2

Table B-28: BOL Centerline Temperature in Rod 513-6

**Table B-29: Rod Average Centerline Temperature in Rod
515-a1**

**Table B-30: Rod Average Centerline Temperature in Rod
515-a2**

Table B-31: BOL Centerline Temperature in Rod 522-1

Table B-32: BOL Centerline Temperature in Rod 522-2

**Table B-33: Rod Average Centerline Temperature in Rod
562-1r1**

**Table B-34: Rod Average Centerline Temperature in Rod
562-1r5L**

In-Life Temperatures

Table B-35: Temperature in Rod 432-1 at Bottom Node: TCBOT

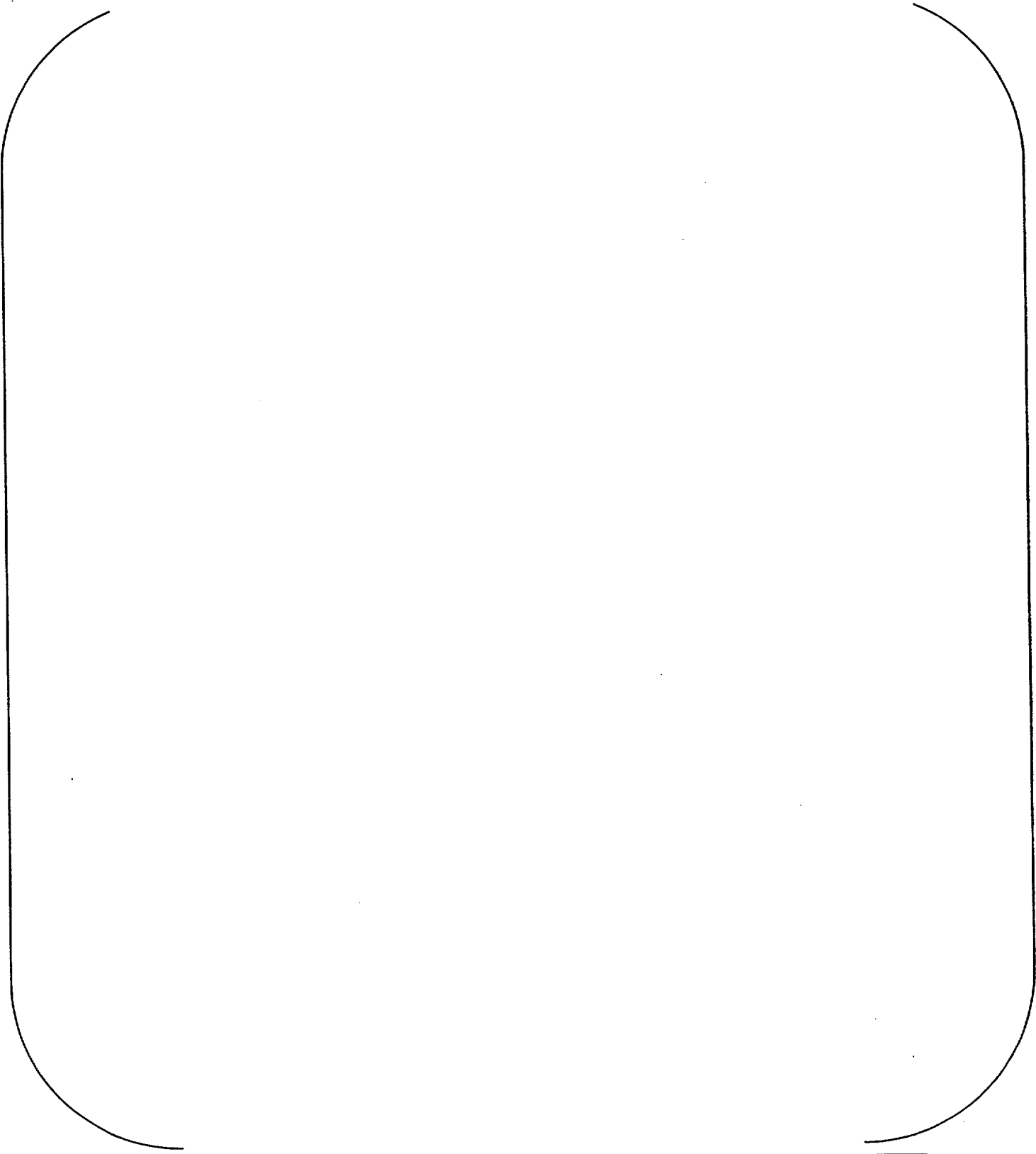


Table B-35: Temperature in Rod 432-1 at Bottom Node: TCBOT (Continued)

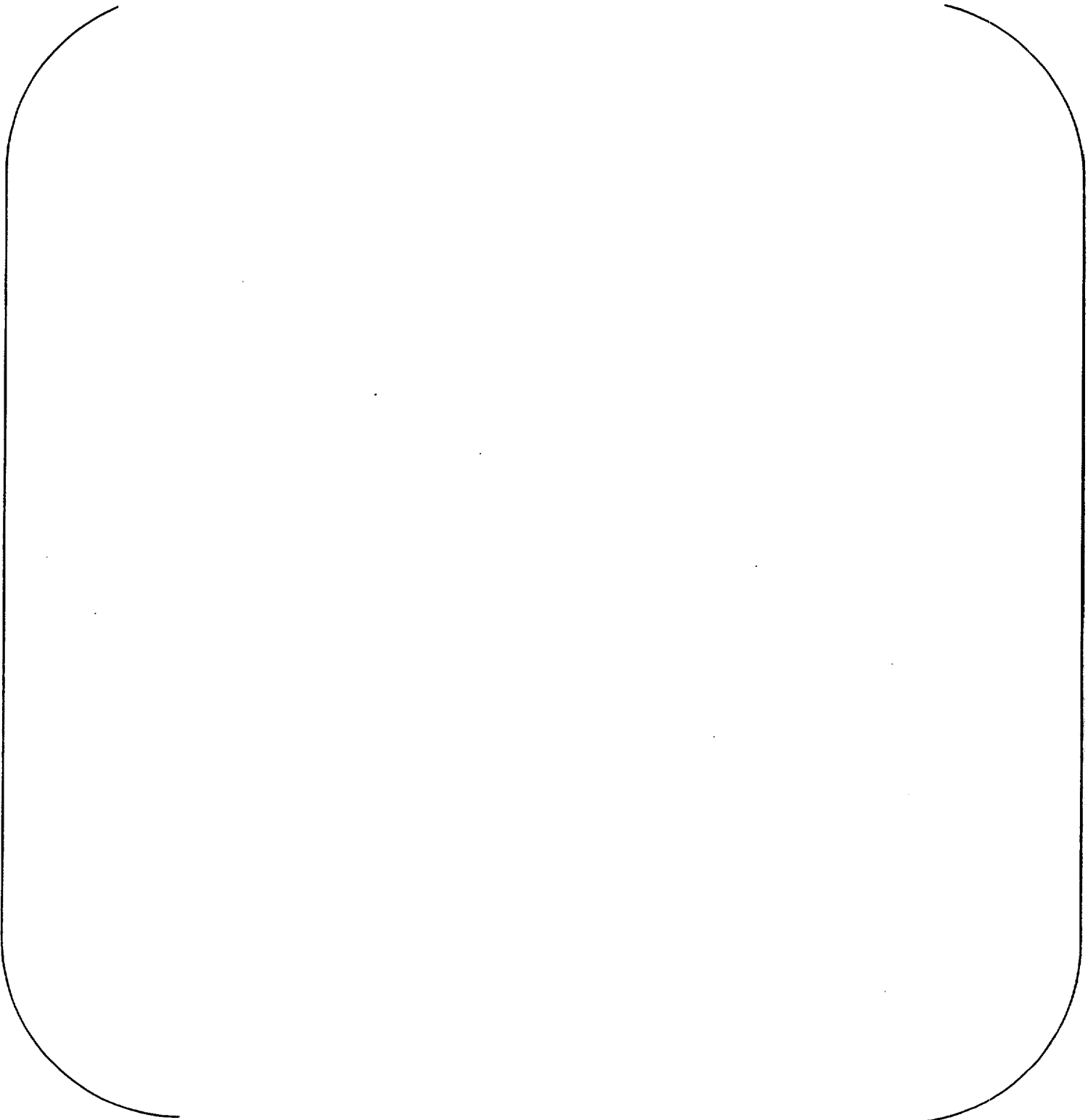
A large, empty rounded rectangular frame that occupies most of the page. It is defined by a single black line with rounded corners, and it is currently blank.

Table B-35: Temperature in Rod 432-1 at Bottom Node: TCBOT (Continued)

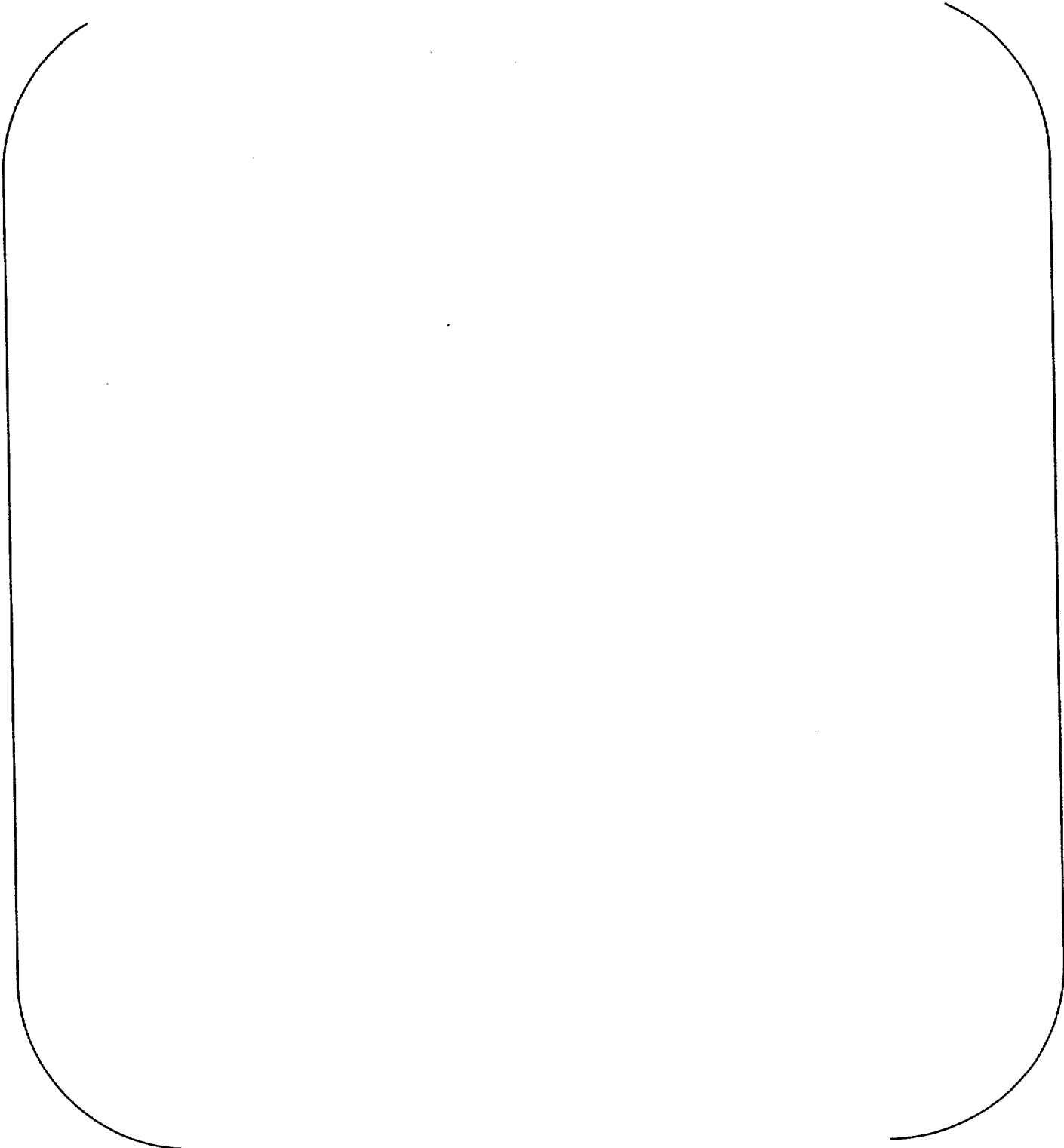


Table B-35: Temperature in Rod 432-1 at Bottom Node: TCBOT (Continued)

Table B-35: Temperature in Rod 432-1 at Bottom Node: TCBOT (Continued)

A large, empty rounded rectangular frame with a thin black border, occupying the central portion of the page. It is intended for the content of Table B-35.

Table B-36: Temperature in Rod 432-1 at Top Node: TCTOP

A large, empty rounded rectangular frame that occupies most of the page. It is defined by a single black line with rounded corners, and it is currently empty of any data or text.

Table B-37: Temperature in Rod 432-2 at Bottom Node: TCBOT

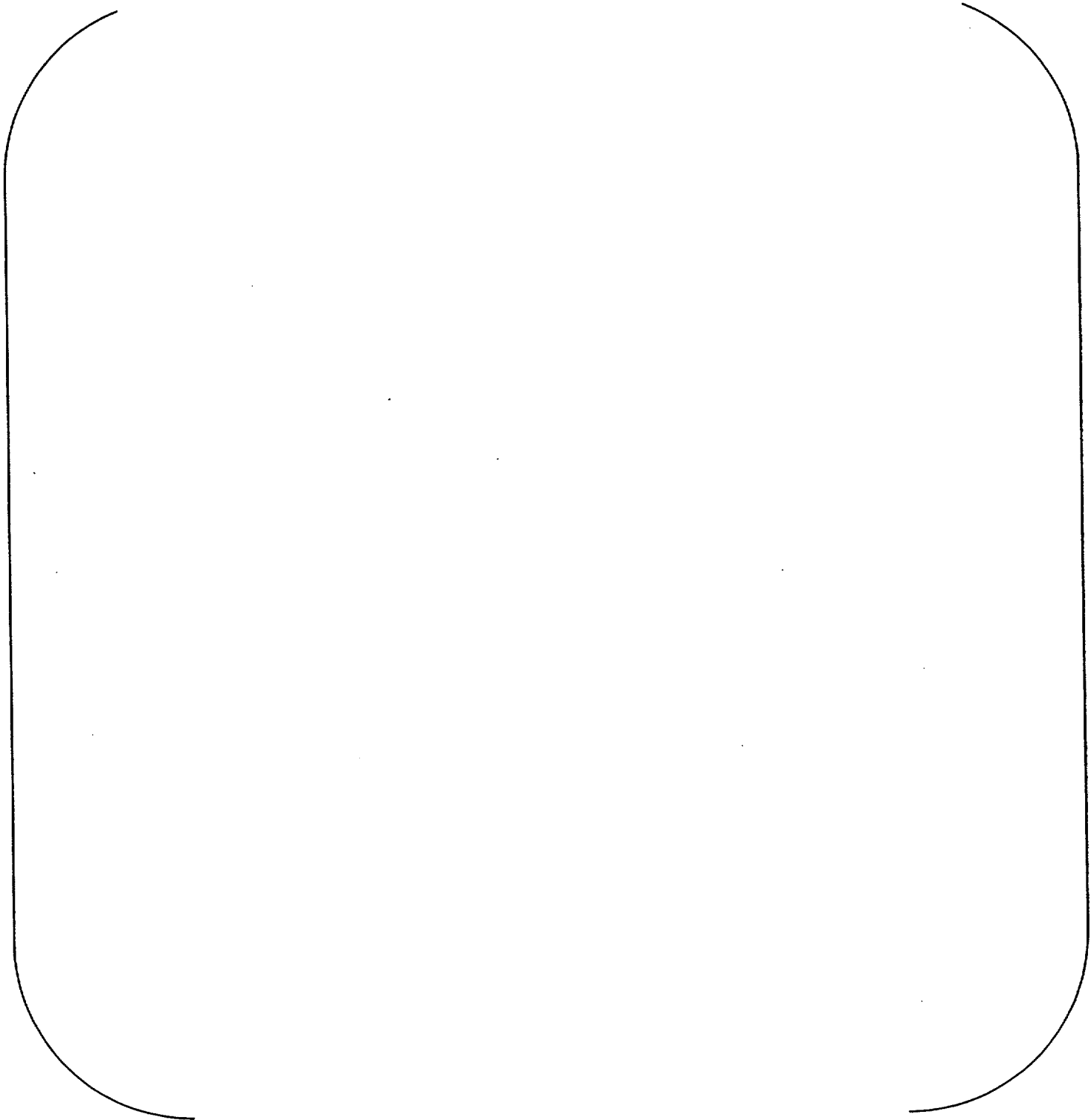
A large, empty rounded rectangular frame with a thin black border, occupying the central portion of the page. It is intended for the content of Table B-37.

Table B-37: Temperature in Rod 432-2 at Bottom Node: TCBOT (continued)

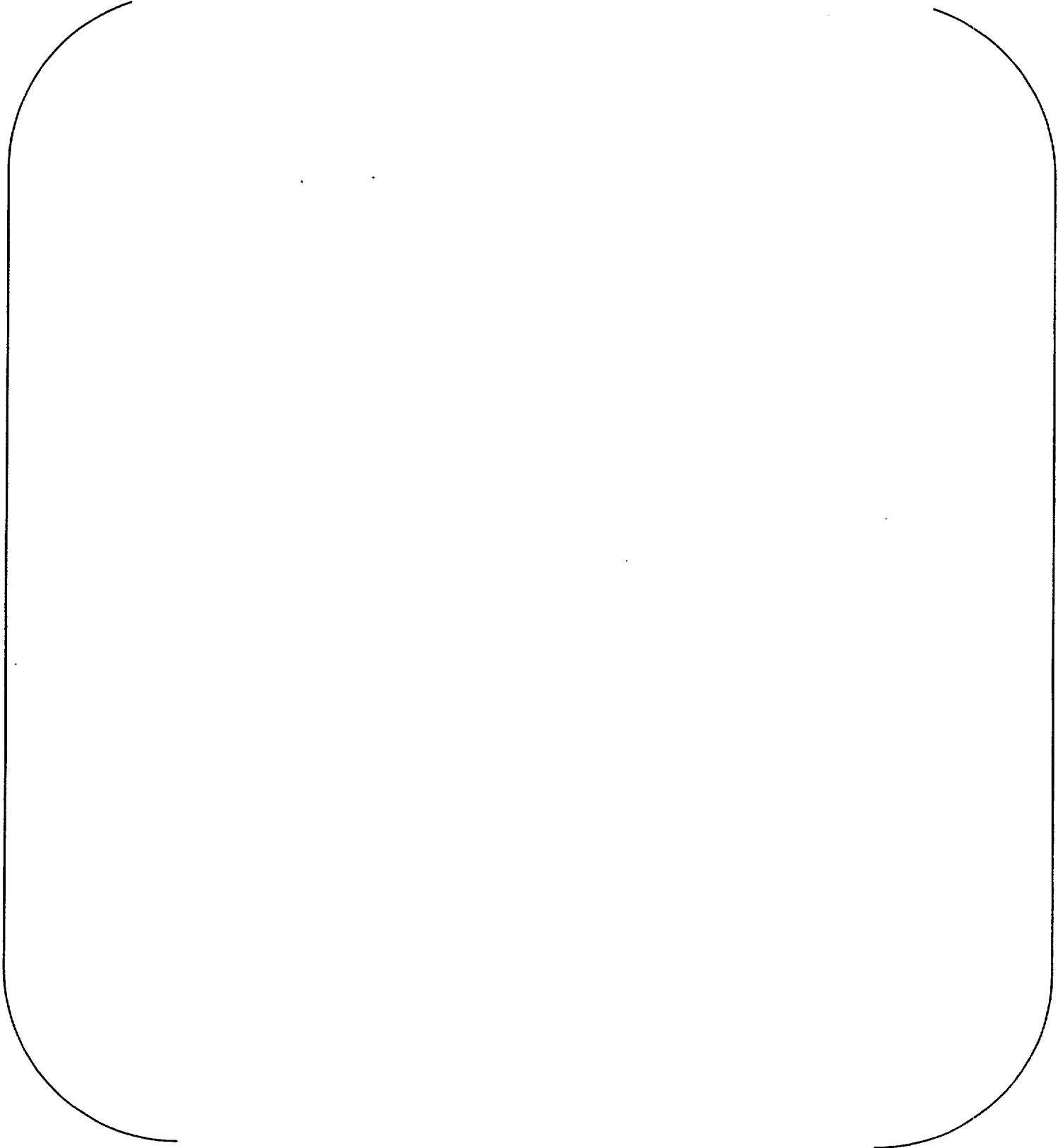


Table B-37: Temperature in Rod 432-2 at Bottom Node: TCBOT (continued)

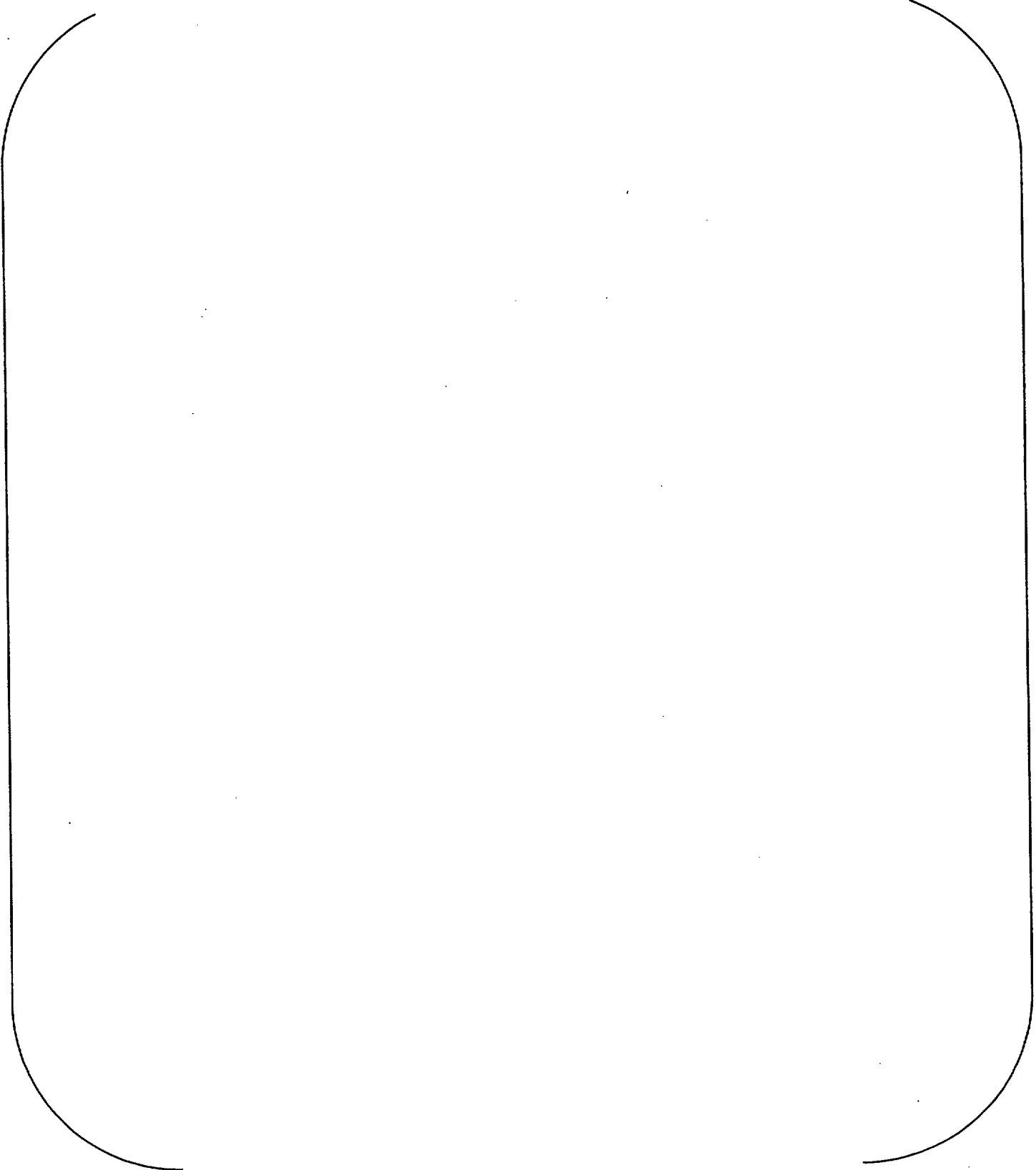


Table B-37: Temperature in Rod 432-2 at Bottom Node: TCBOT (continued)

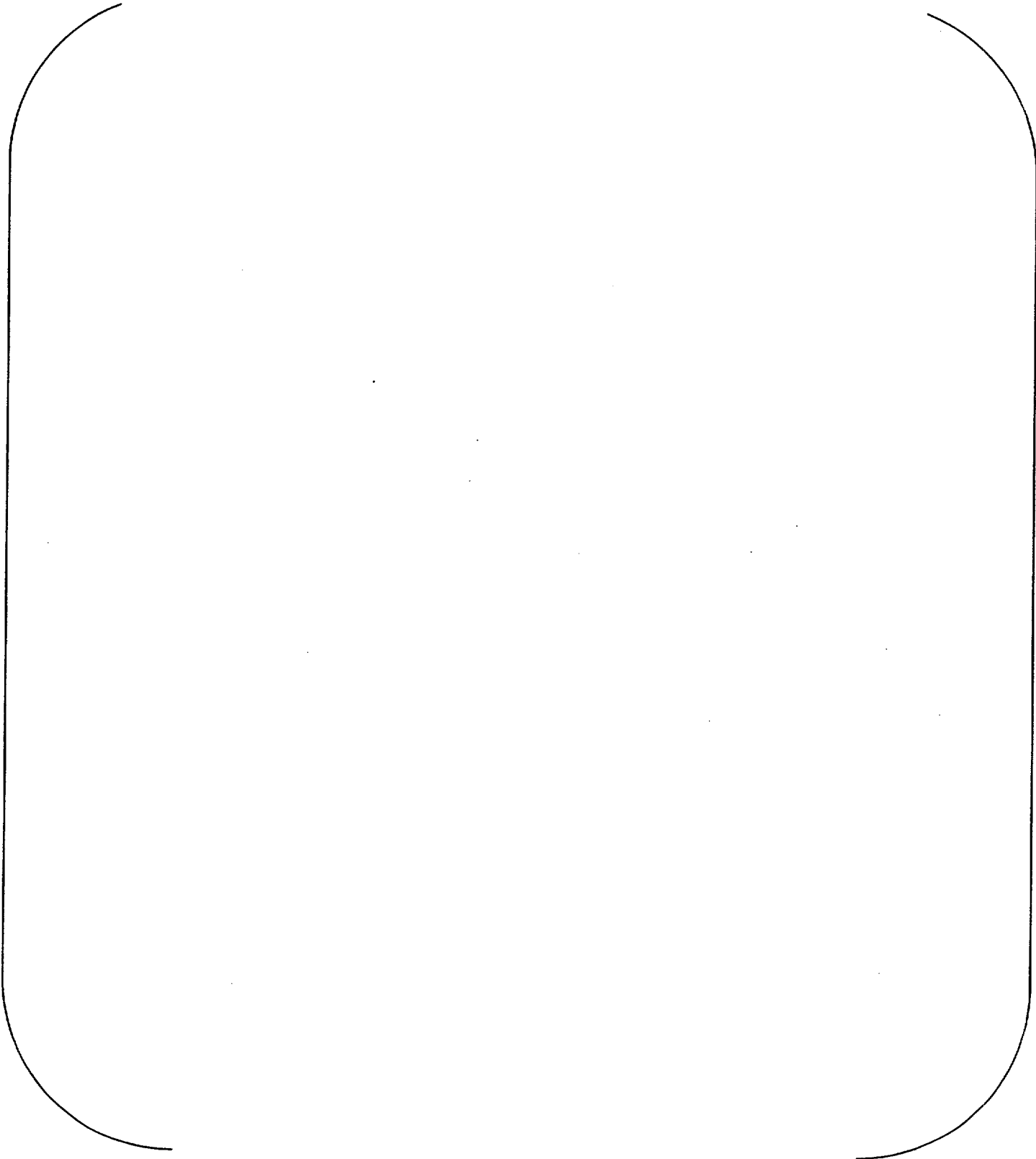
A large, empty rounded rectangular frame with a thin black border, occupying the central portion of the page. It is intended for the content of Table B-37.

Table B-37: Temperature in Rod 432-2 at Bottom Node: TCBOT (continued)

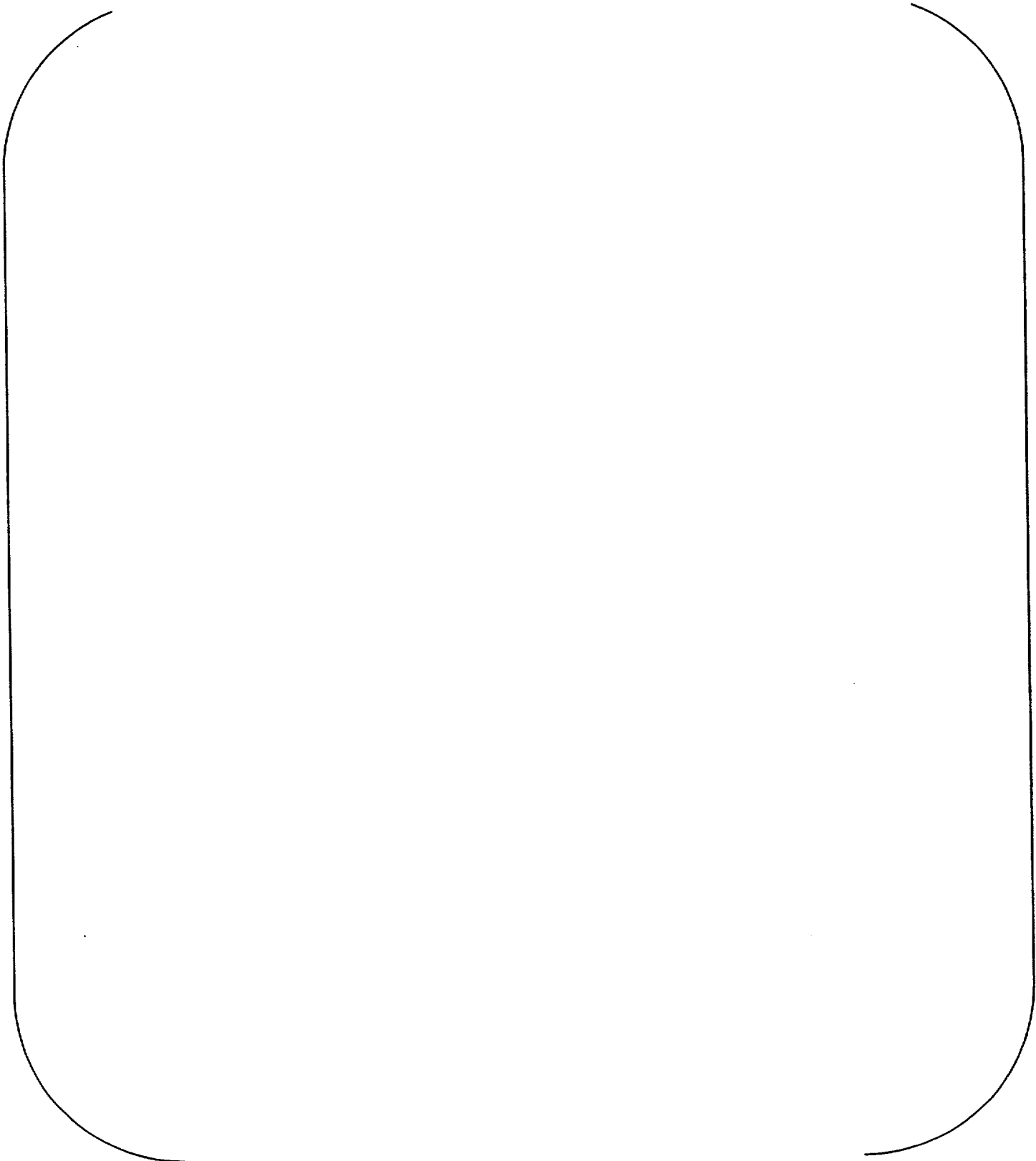
A large, empty rounded rectangular frame with a thin black border, occupying most of the page. It is intended for a table but contains no data.

Table B-37: Temperature in Rod 432-2 at Bottom Node: TCBOT (continued)

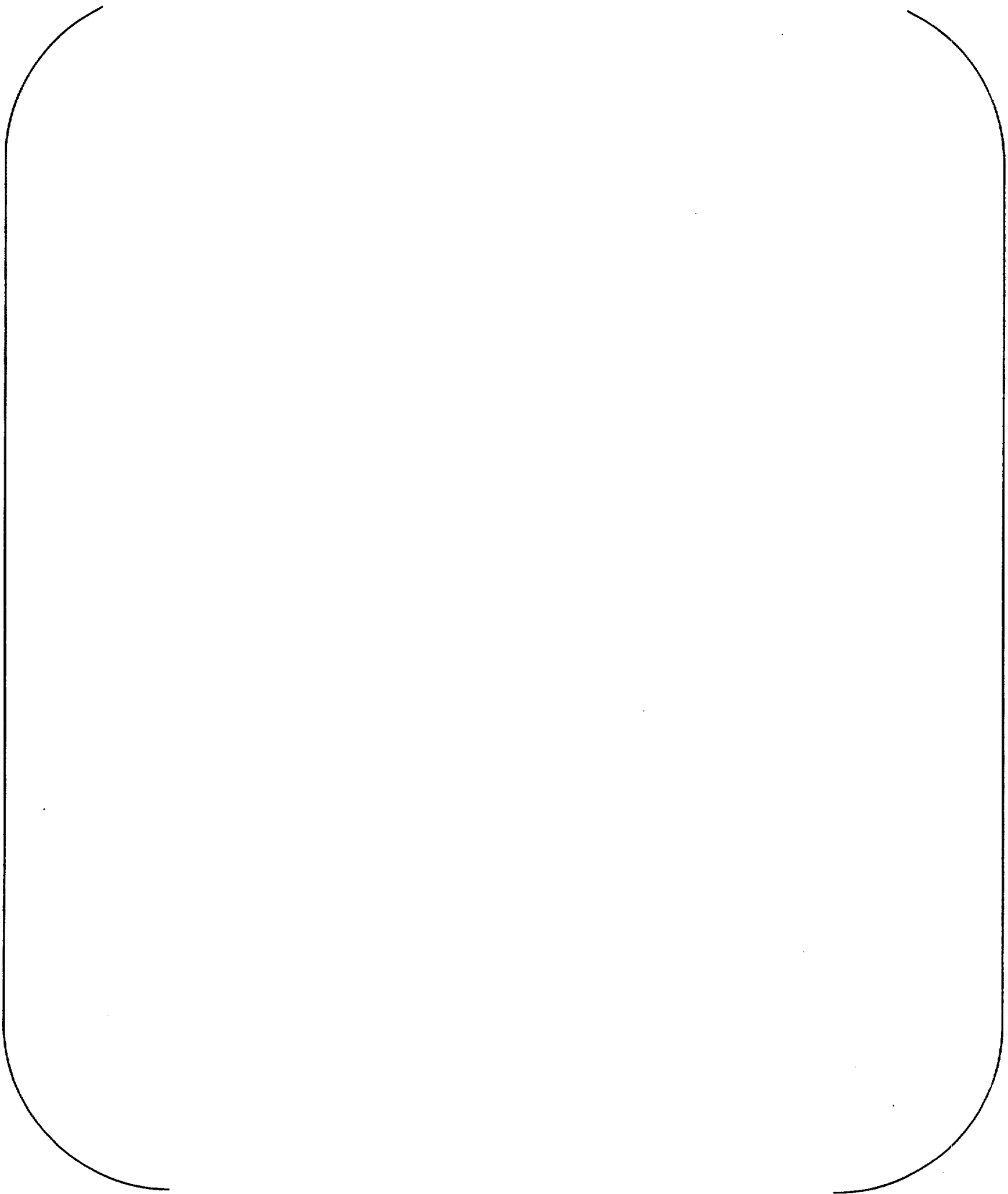


Table B-37: Temperature in Rod 432-2 at Bottom Node: TCBOT (continued)

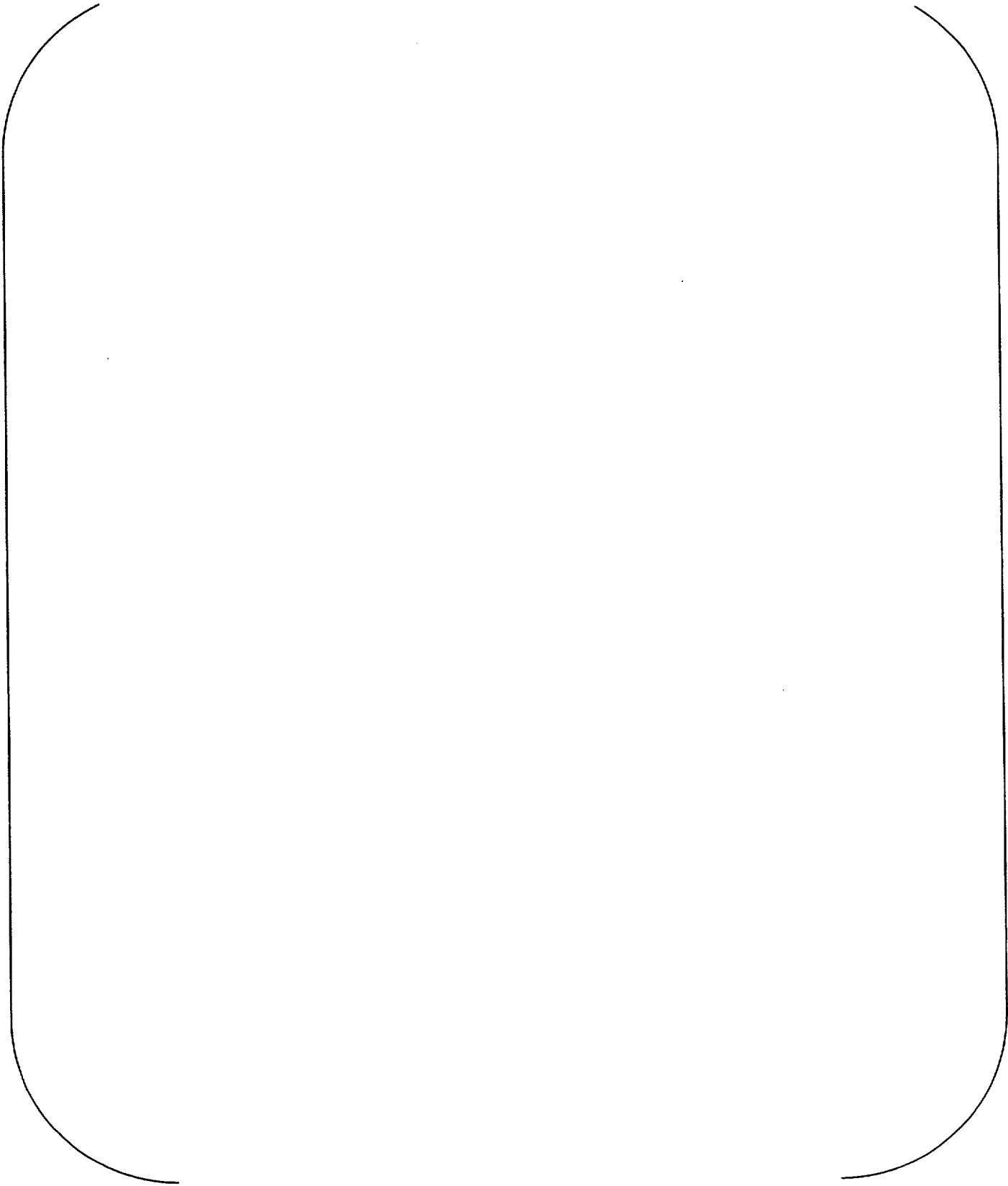
A large, empty rounded rectangular frame with a thin black border, occupying most of the page. It is intended for the data from Table B-37.

Table B-37: Temperature in Rod 432-2 at Bottom Node: TCBOT (continued)

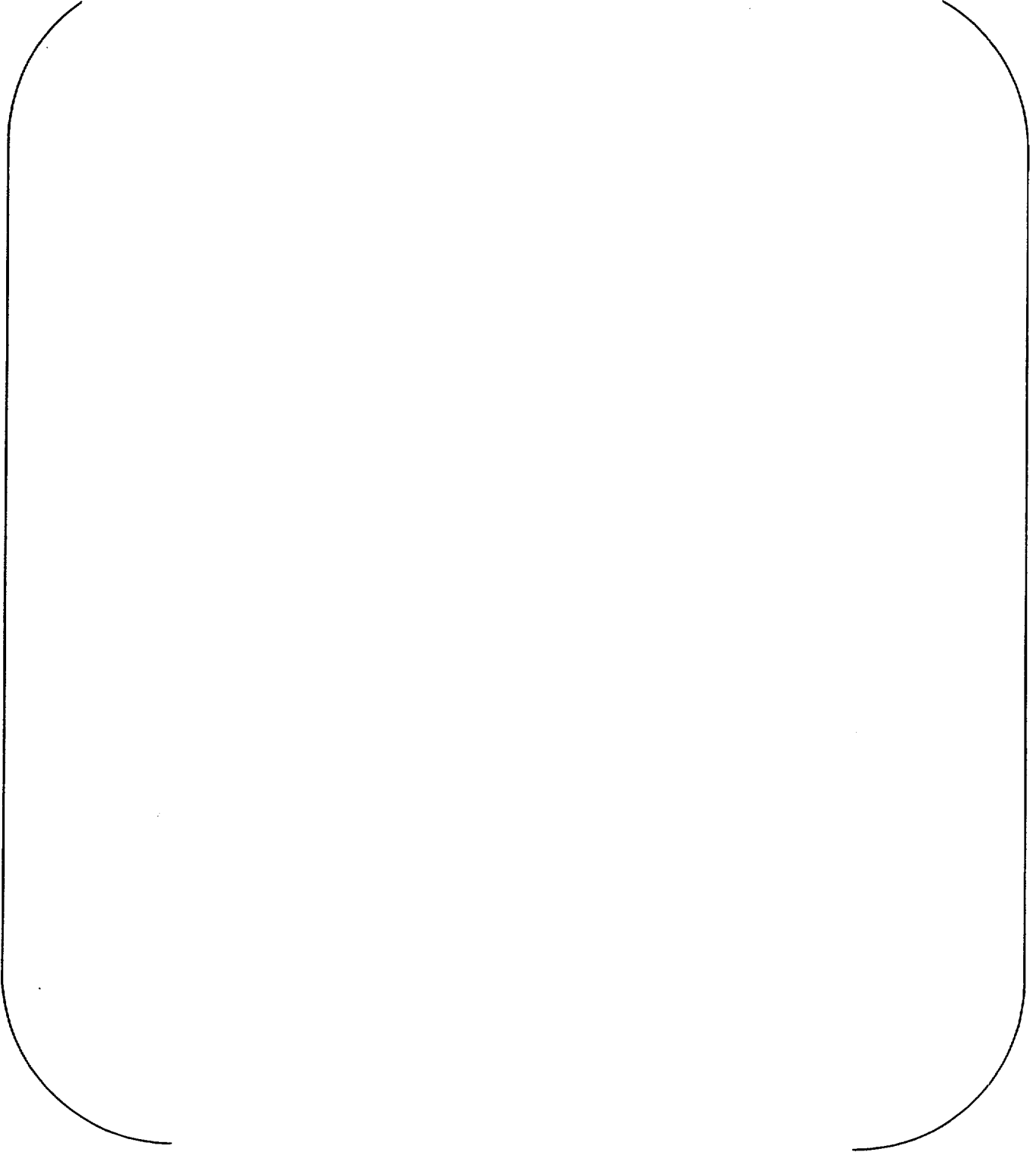
A large, empty rounded rectangular frame with a thin black border, occupying the central portion of the page. It is intended for the content of Table B-37.

Table B-37: Temperature in Rod 432-2 at Bottom Node: TCBOT (continued)

A large, empty rounded rectangular box with a thin black border, positioned centrally on the page. It appears to be a placeholder for a table or data that is not present in this version of the document.

Table B-38: Temperature in Rod 432-3 at Bottom Node: TCBOT

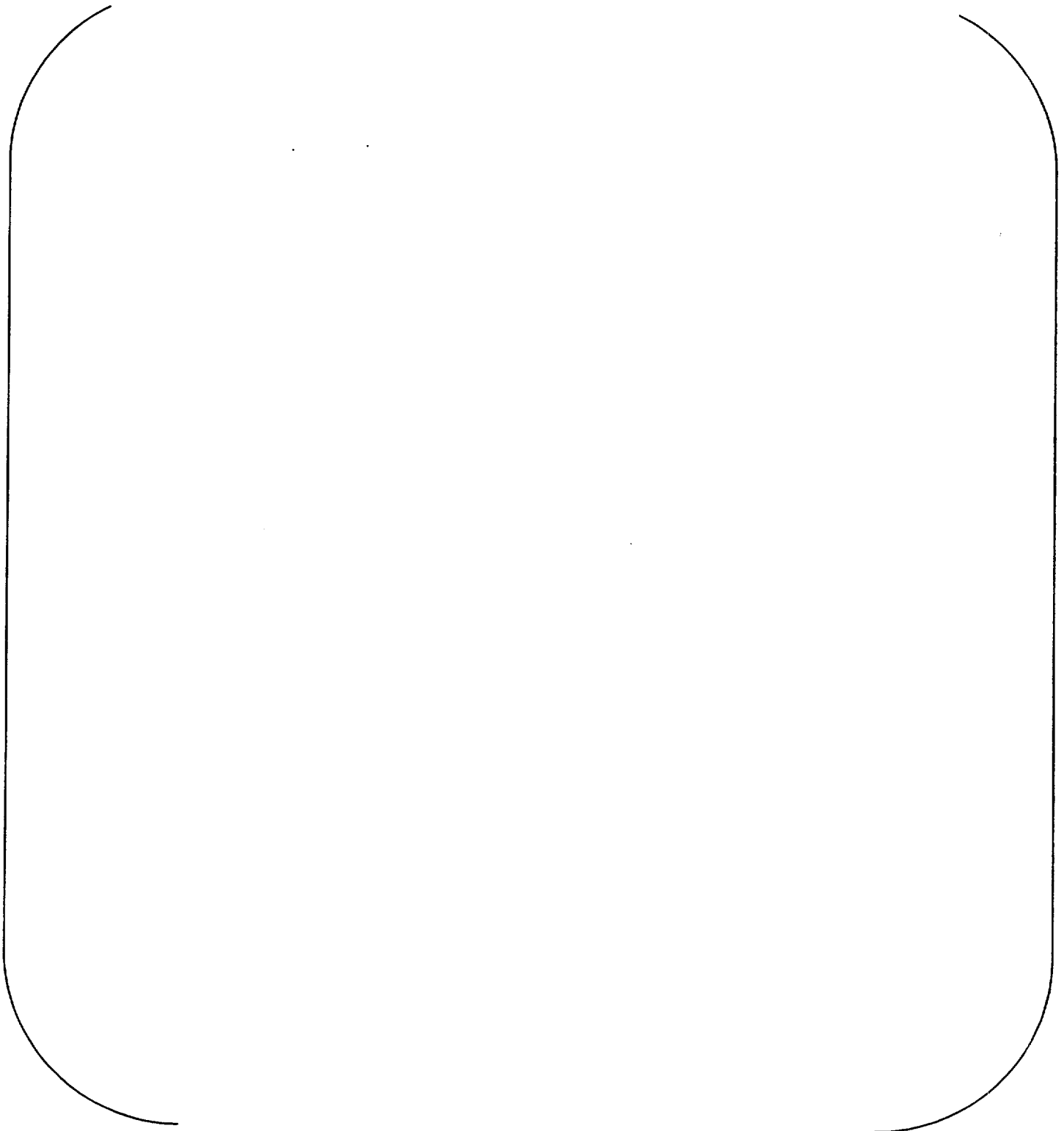


Table B-38: Temperature in Rod 432-3 at Bottom Node: TCBOT (continued)

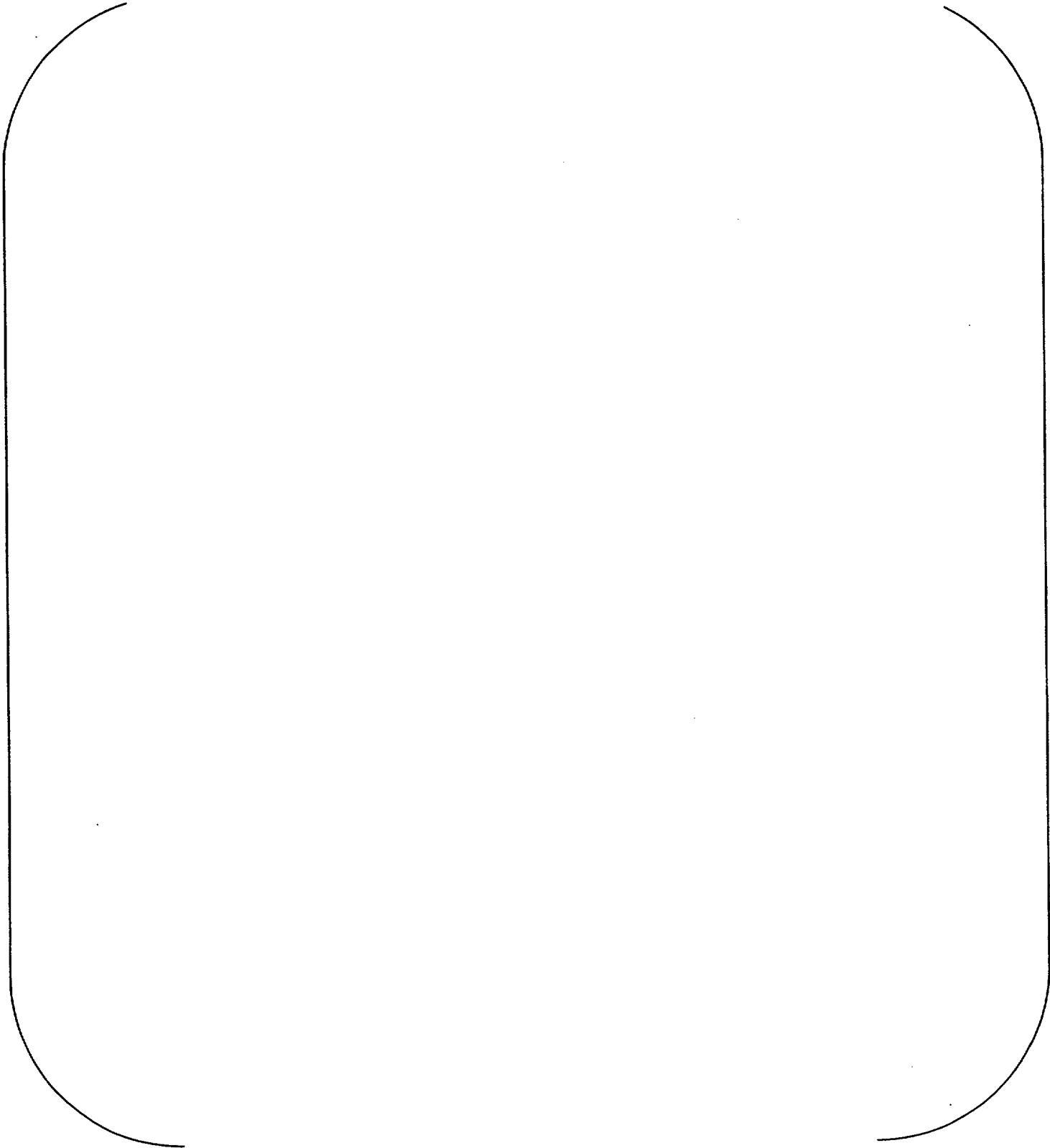
A large, empty rounded rectangular frame with a thin black border, occupying most of the page. It is intended for the content of Table B-38.

Table B-38: Temperature in Rod 432-3 at Bottom Node: TCBOT (continued)

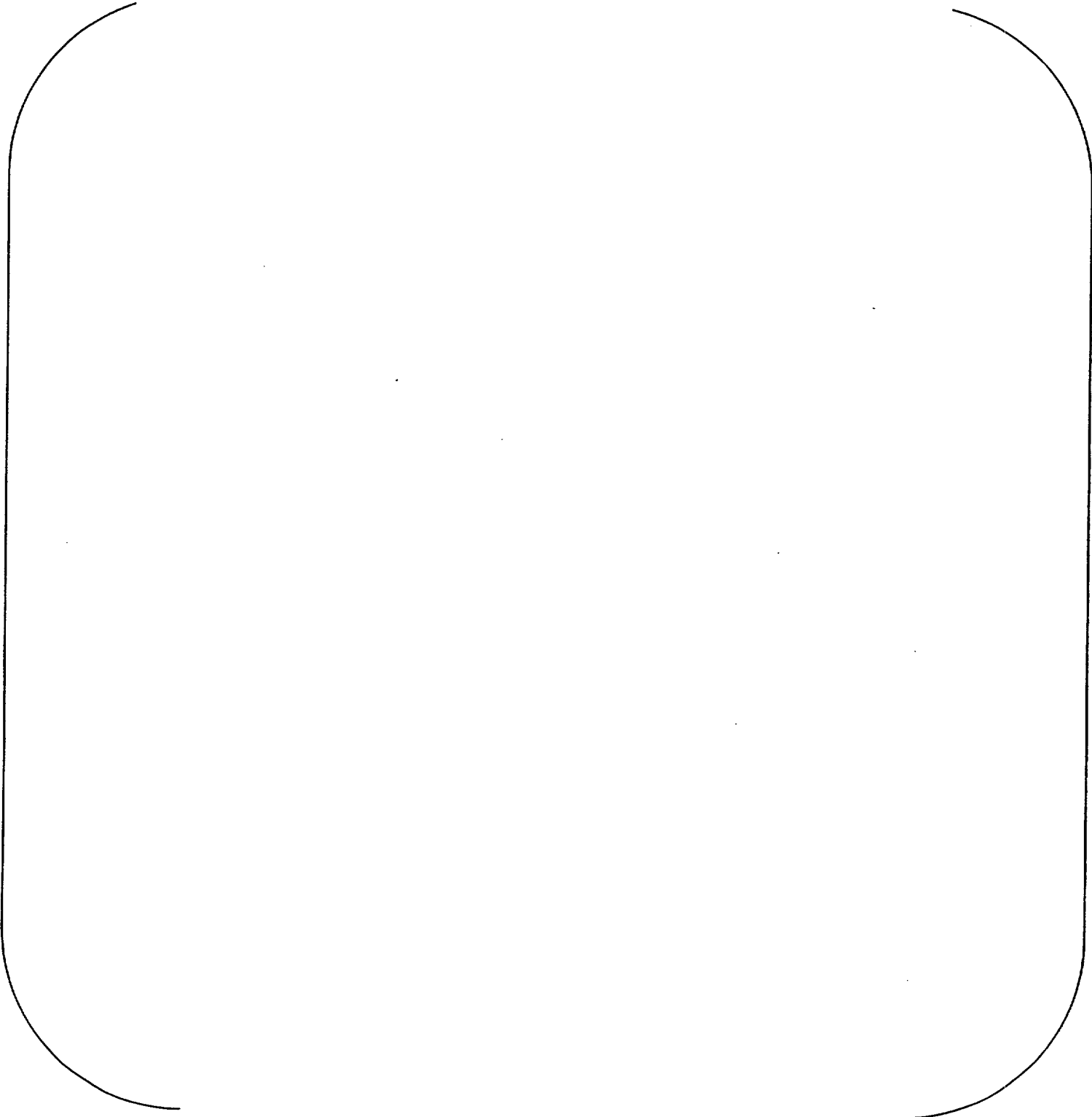


Table B-38: Temperature in Rod 432-3 at Bottom Node: TCBOT (continued)

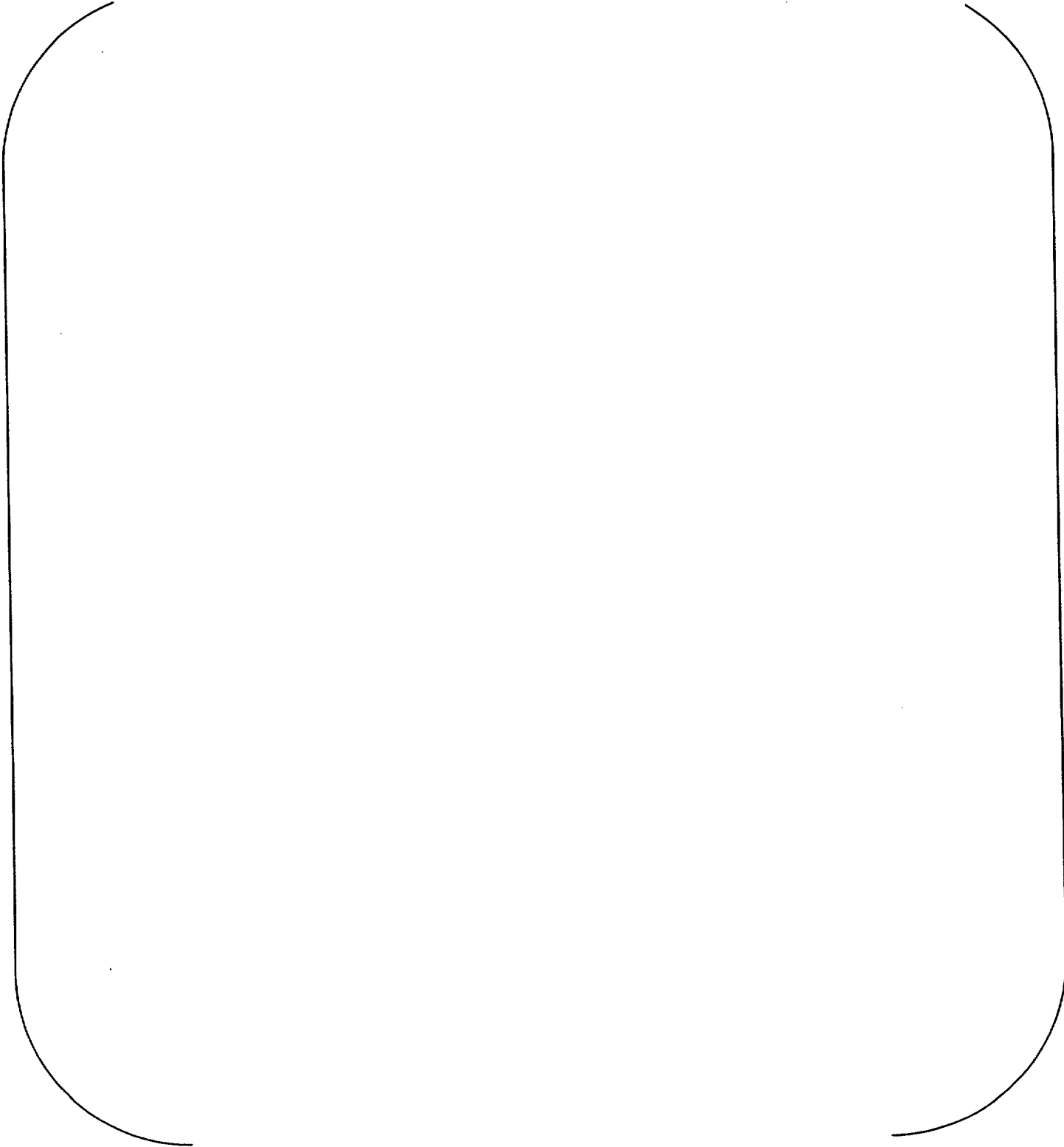
A large, empty rounded rectangular frame with a thin black border, occupying the central portion of the page. It is intended for the content of Table B-38.

Table B-38: Temperature in Rod 432-3 at Bottom Node: TCBOT (continued)

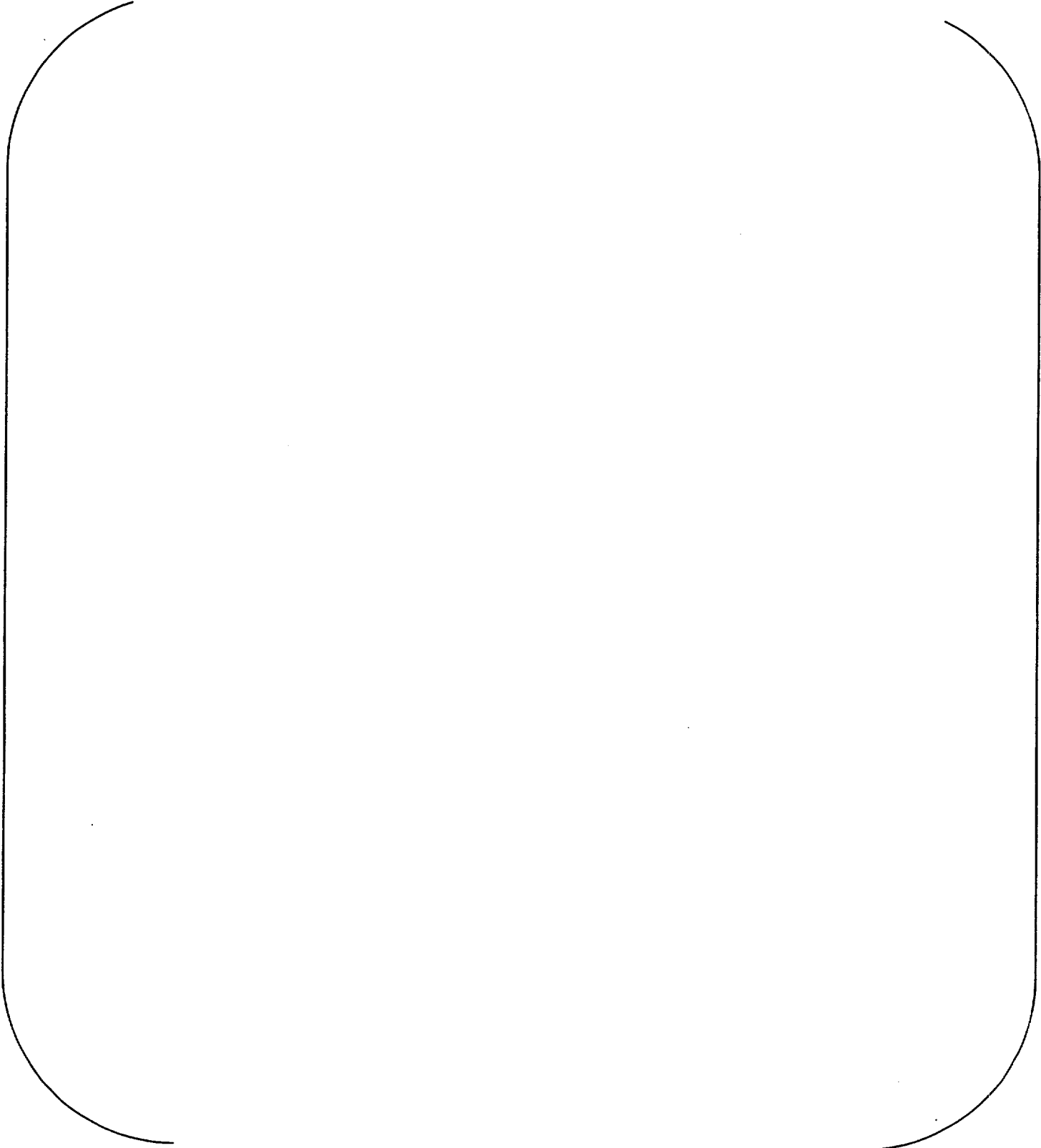
A large, empty rounded rectangular frame with a thin black border, occupying most of the page. It is intended for the content of Table B-38.

Table B-38: Temperature in Rod 432-3 at Bottom Node: TCBOT (continued)

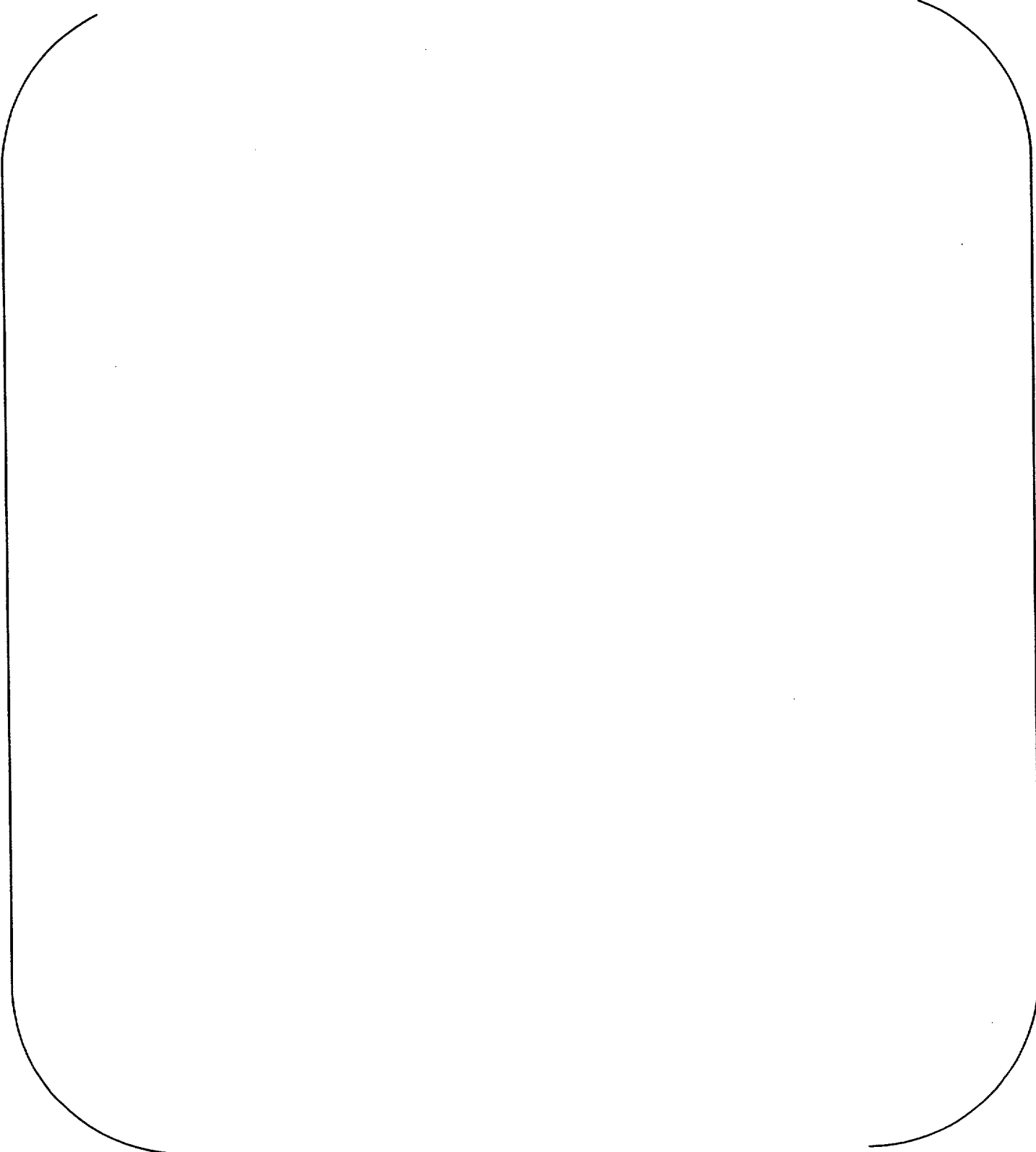


Table B-38: Temperature in Rod 432-3 at Bottom Node: TCBOT (continued)

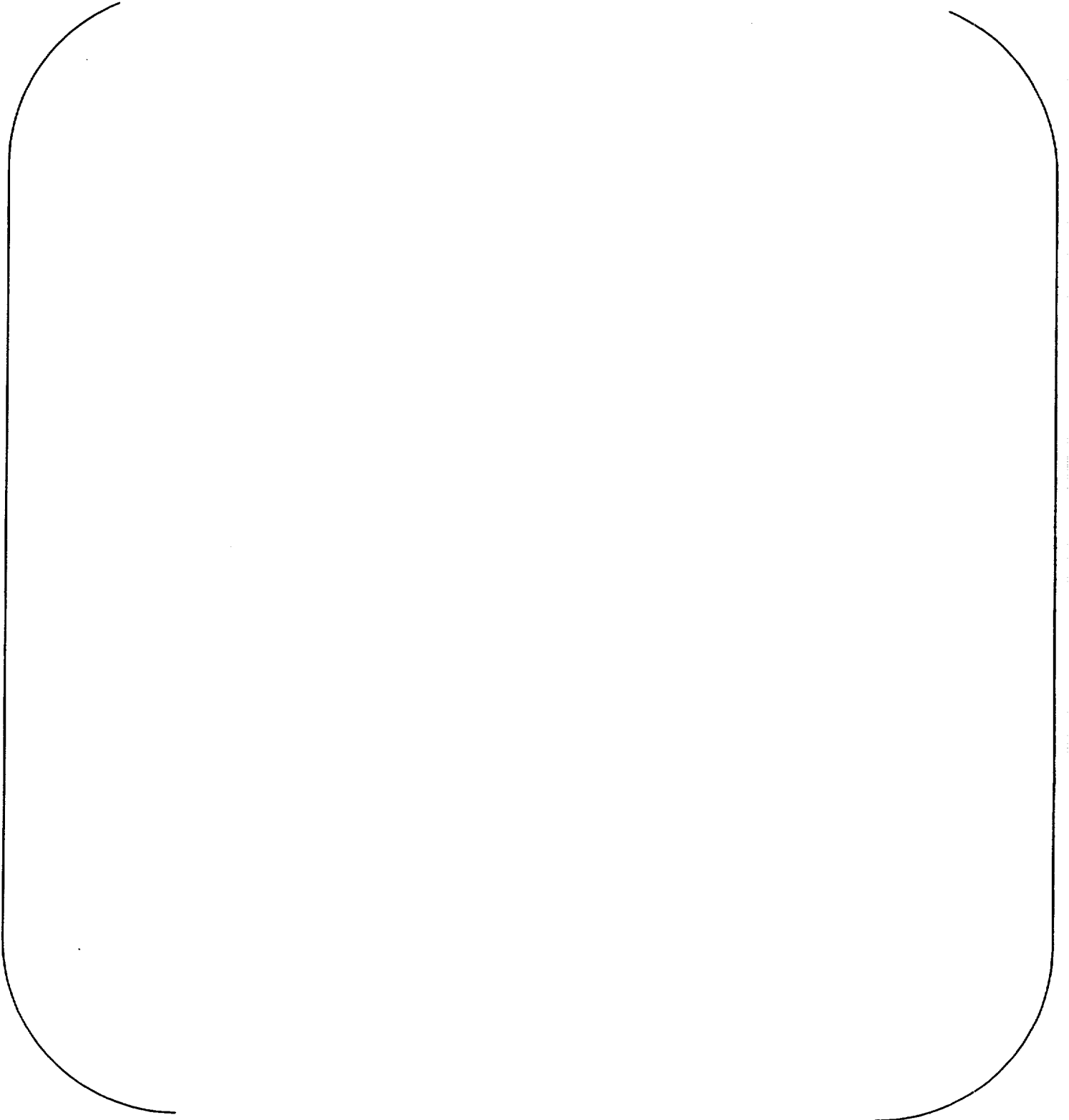
A large, empty rounded rectangular frame with a thin black border, occupying the central portion of the page. It is intended for the content of Table B-38.

Table B-38: Temperature in Rod 432-3 at Bottom Node: TCBOT (continued)

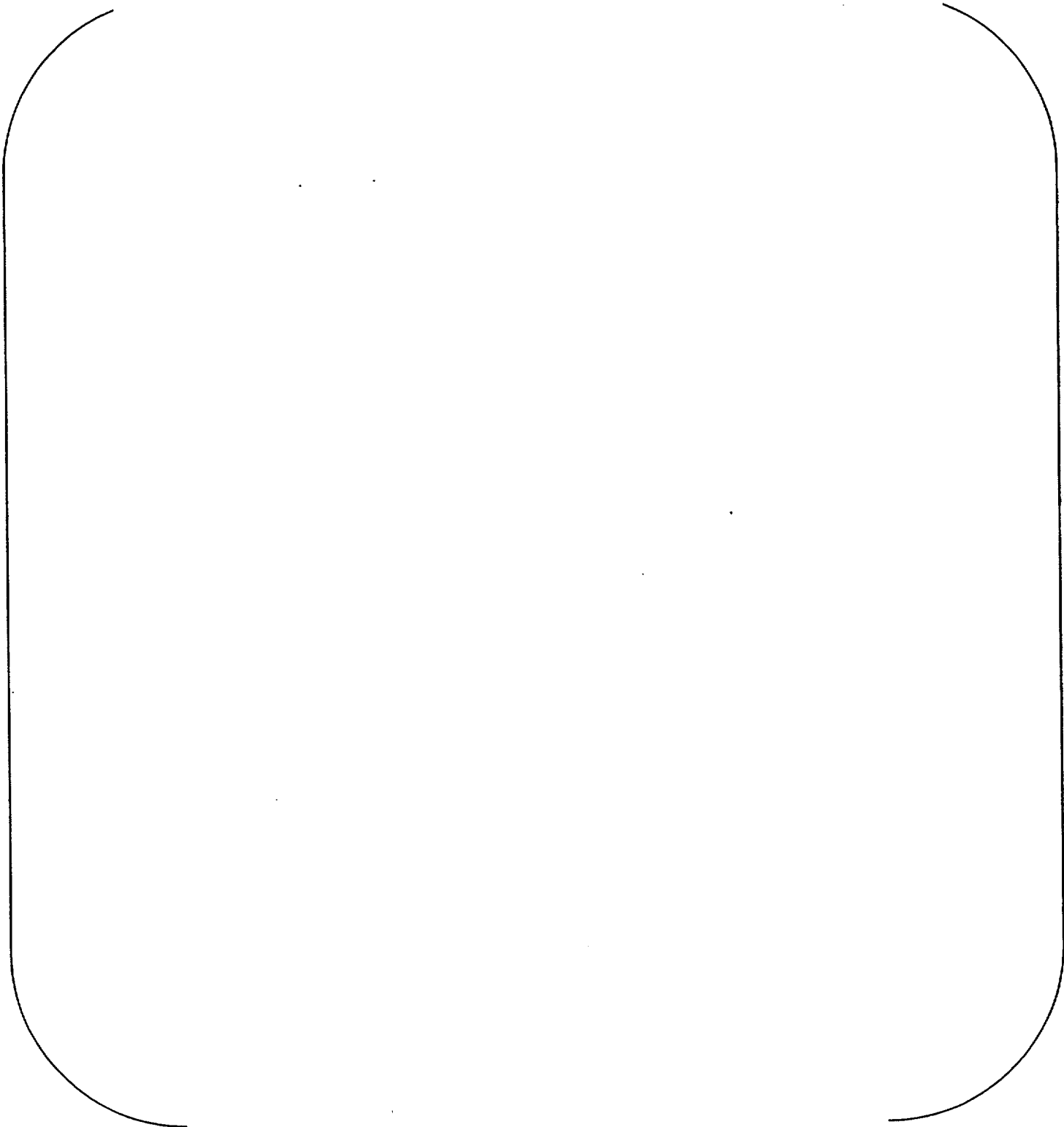
A large, empty rounded rectangular frame that occupies most of the page. It is defined by a single black line with rounded corners. The interior of the frame is completely blank, suggesting that the data for Table B-38 is either missing or has been redacted.

Table B-38: Temperature in Rod 432-3 at Bottom Node: TCBOT (continued)



Table B-39: Temperature in Rod 432-3 at Top Node: TCTOP

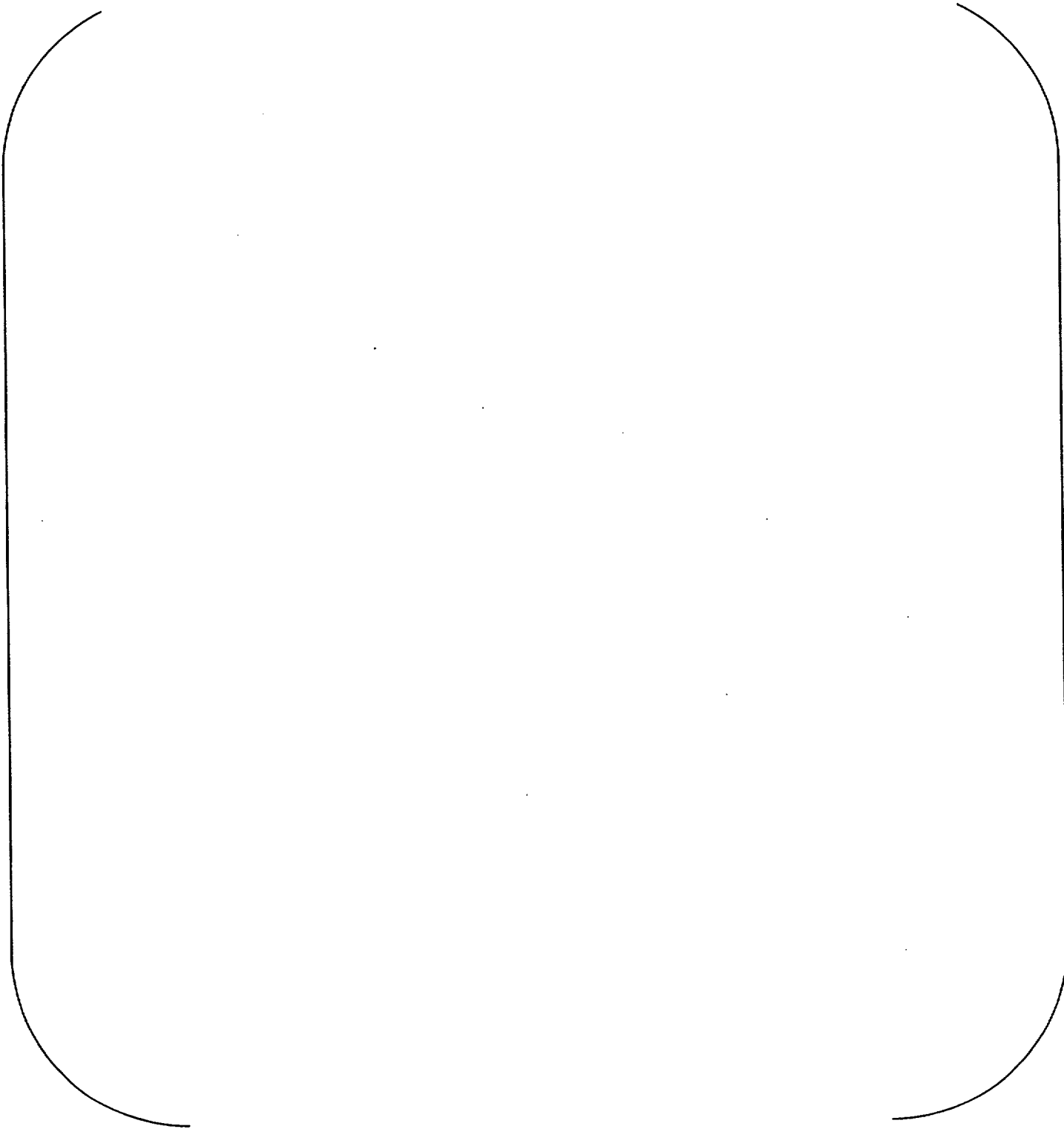
A large, empty rounded rectangular frame with a thin black border, occupying the central portion of the page. It is intended for the content of Table B-39.

Table B-39: Temperature in Rod 432-3 at Top Node: TCTOP (continued)

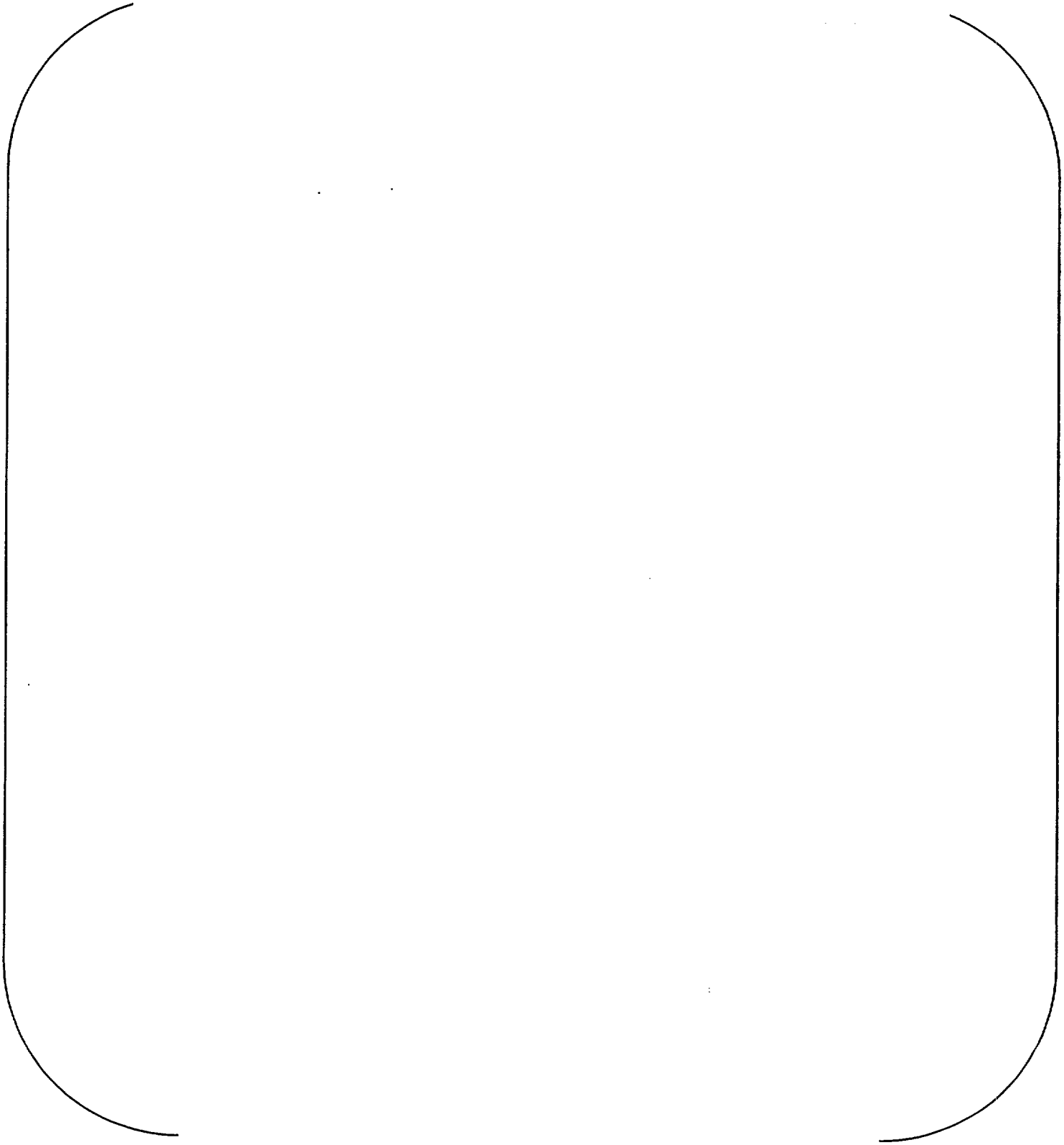
A large, empty rounded rectangular frame that occupies most of the page. It is defined by a thin black line with rounded corners. The interior of the frame is completely blank, suggesting that the data for Table B-39 is either missing or has been redacted.

Table B-39: Temperature in Rod 432-3 at Top Node: TCTOP (continued)

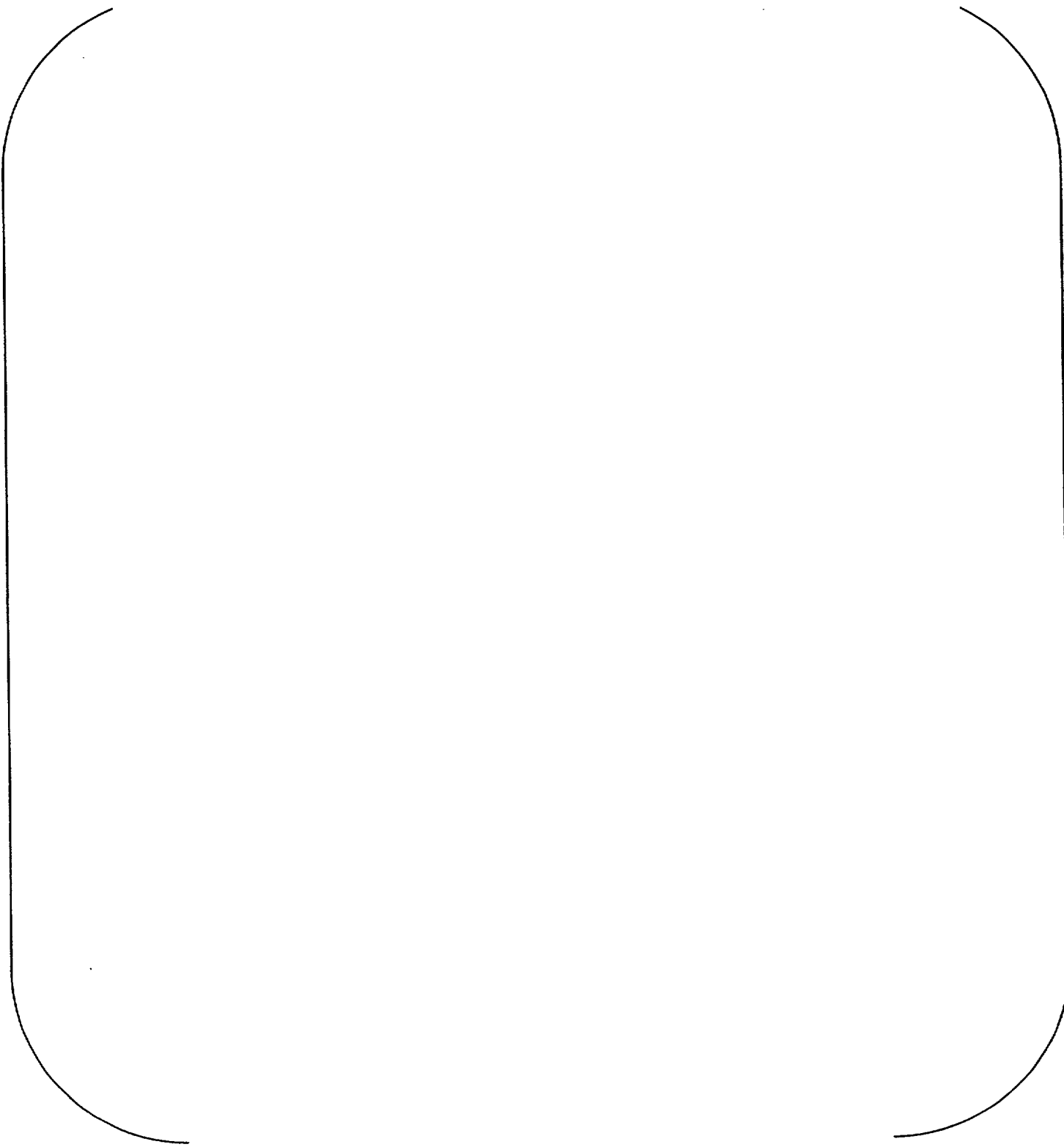
A large, empty rounded rectangular frame with a thin black border, occupying the central portion of the page. It is intended for the content of Table B-39.

Table B-39: Temperature in Rod 432-3 at Top Node: TCTOP (continued)

A large, empty rounded rectangular frame with a thin black border, occupying the central portion of the page. It is intended for the content of Table B-39.

Table B-40: Temperature in Rod 432-5 at Bottom Node: TCBOT

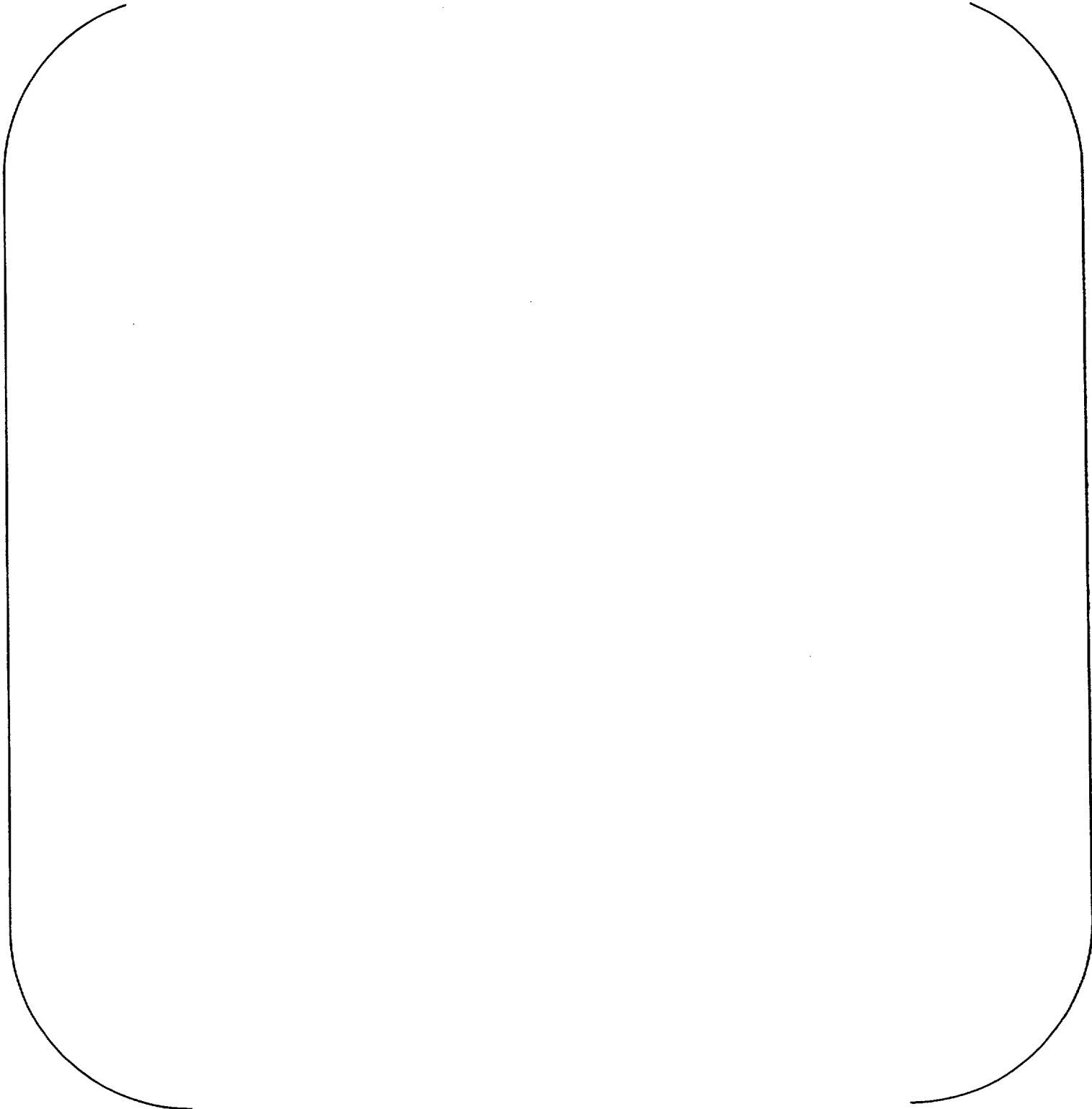
A large, empty rounded rectangular frame with a thin black border, occupying the central portion of the page. It is intended for the content of Table B-40.

Table B-40: Temperature in Rod 432-5 at Bottom Node: TCBOT (continued)

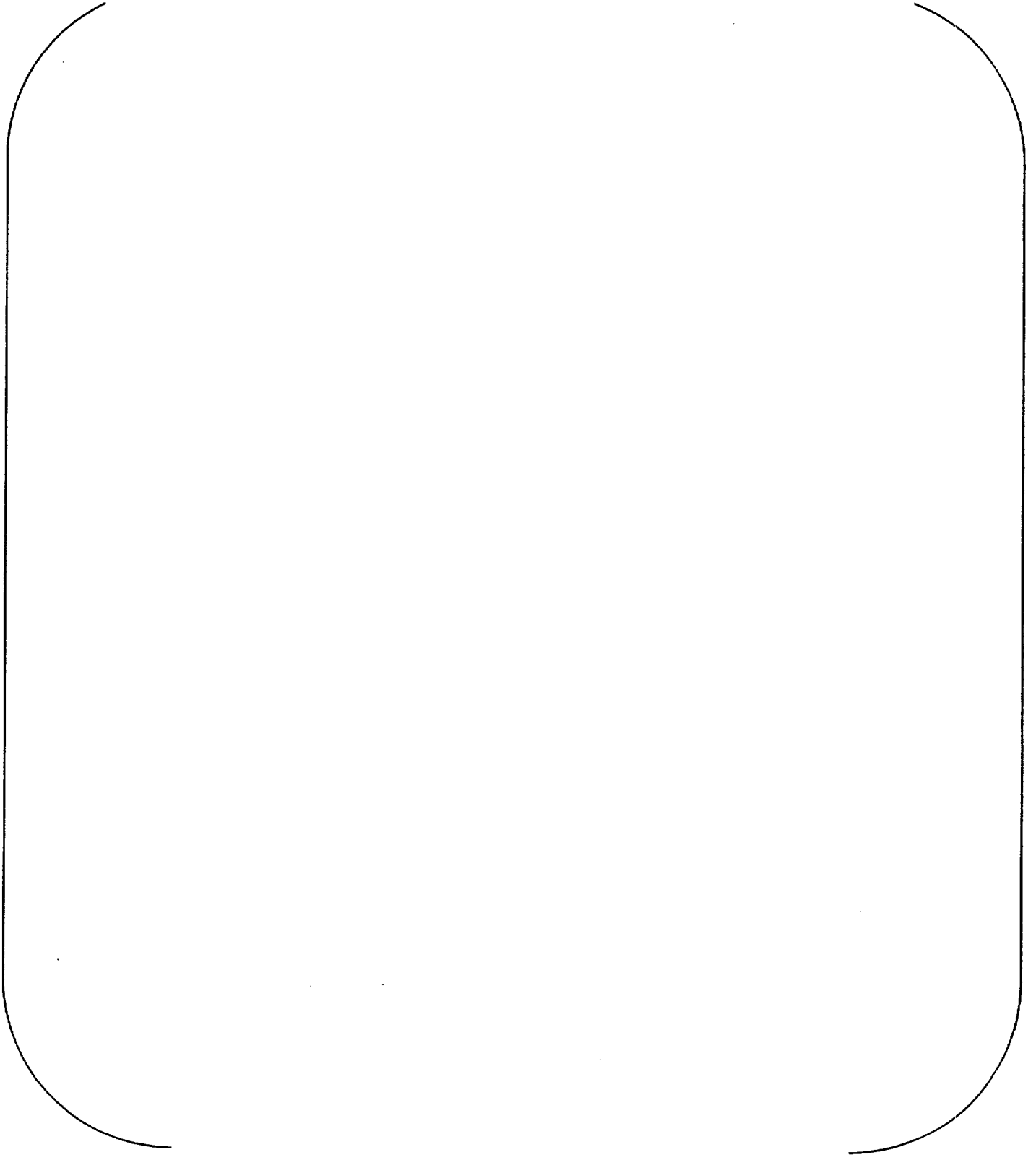


Table B-40: Temperature in Rod 432-5 at Bottom Node: TCBOT (continued)

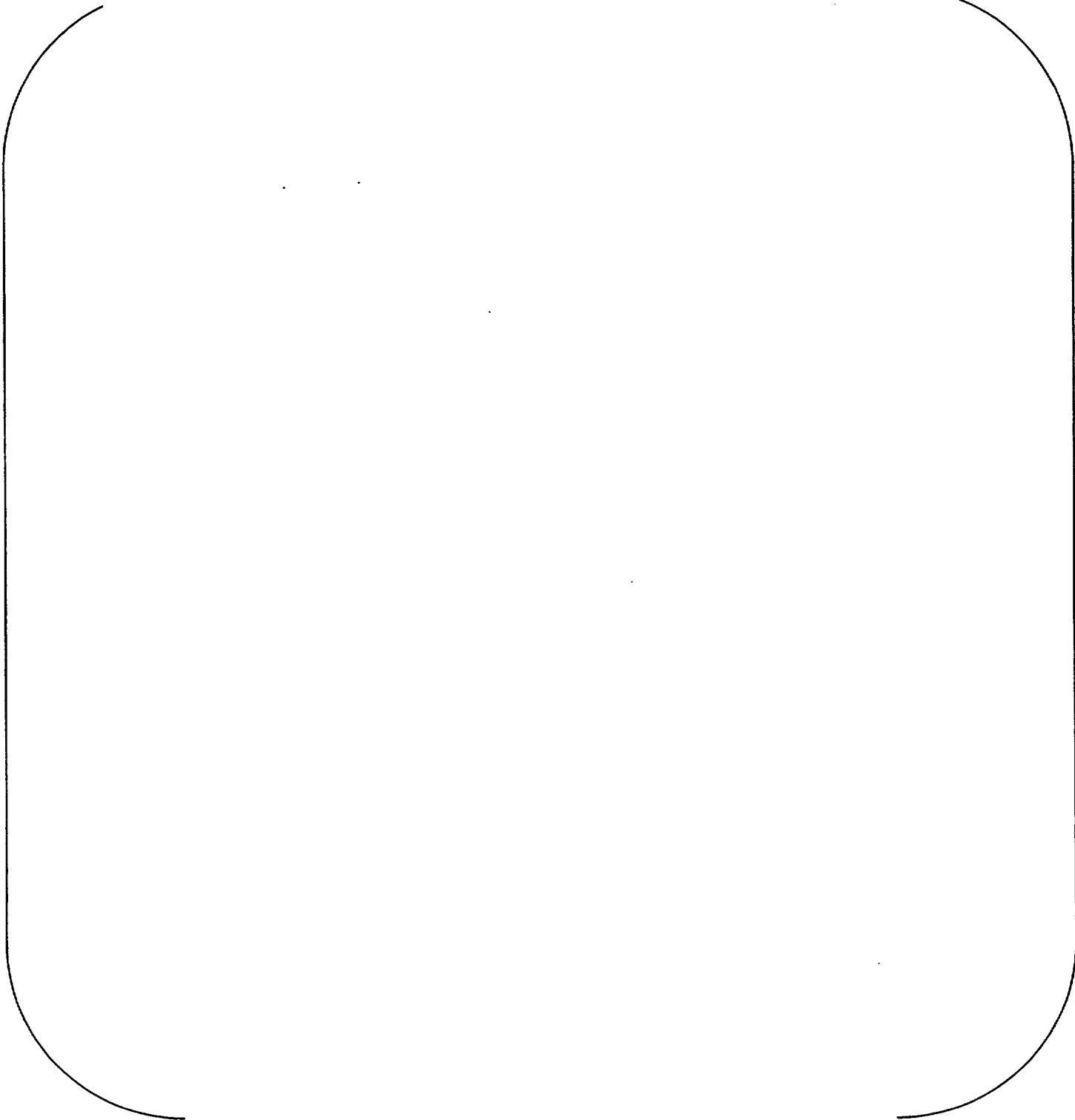
A large, empty rounded rectangular frame with a thin black border, occupying the central portion of the page. It is intended for the content of Table B-40.

Table B-40: Temperature in Rod 432-5 at Bottom Node: TCBOT (continued)

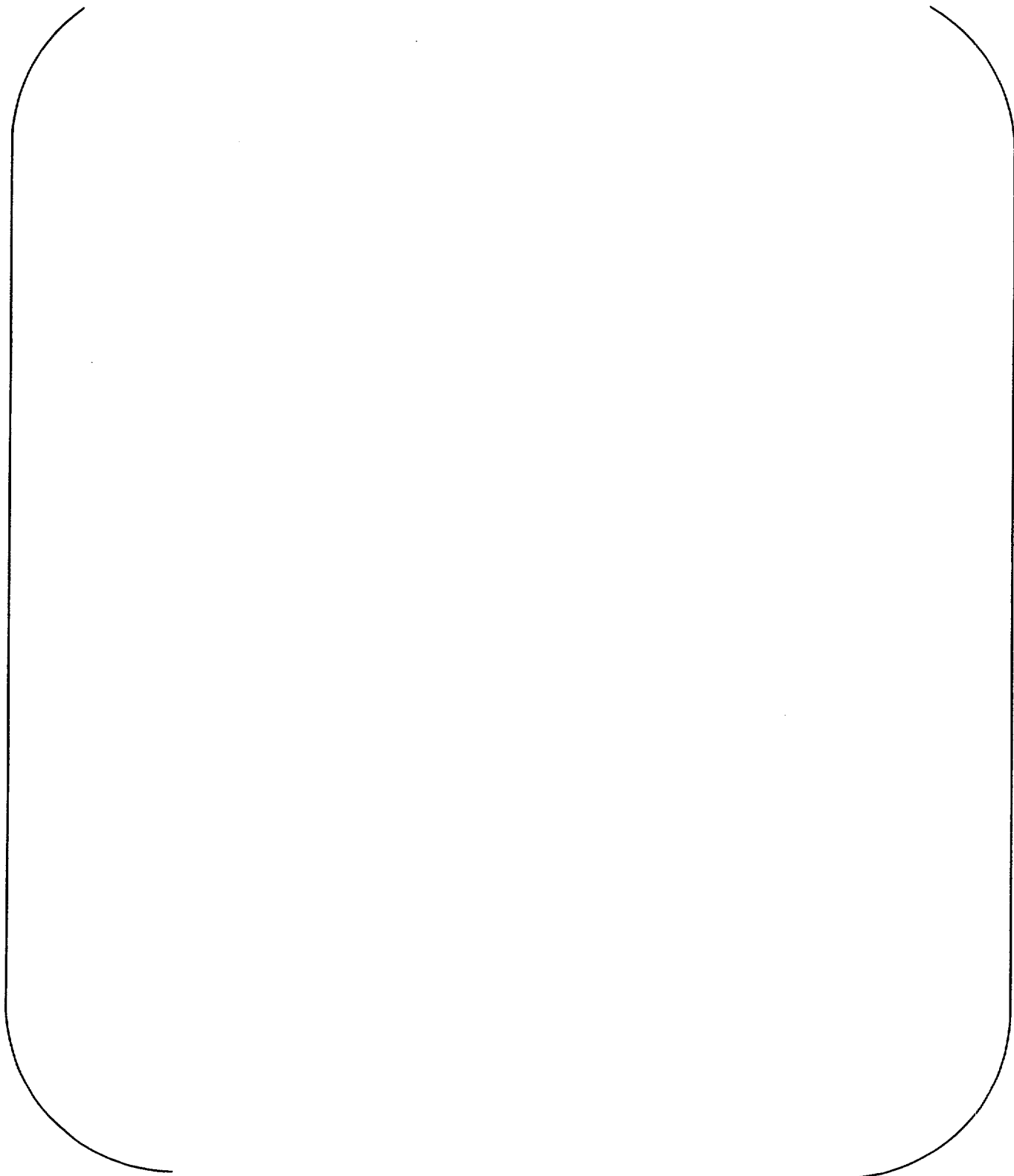
A large, empty rounded rectangular frame with a thin black border, occupying most of the page. It is intended for a table but contains no data.

Table B-40: Temperature in Rod 432-5 at Bottom Node: TCBOT (continued)

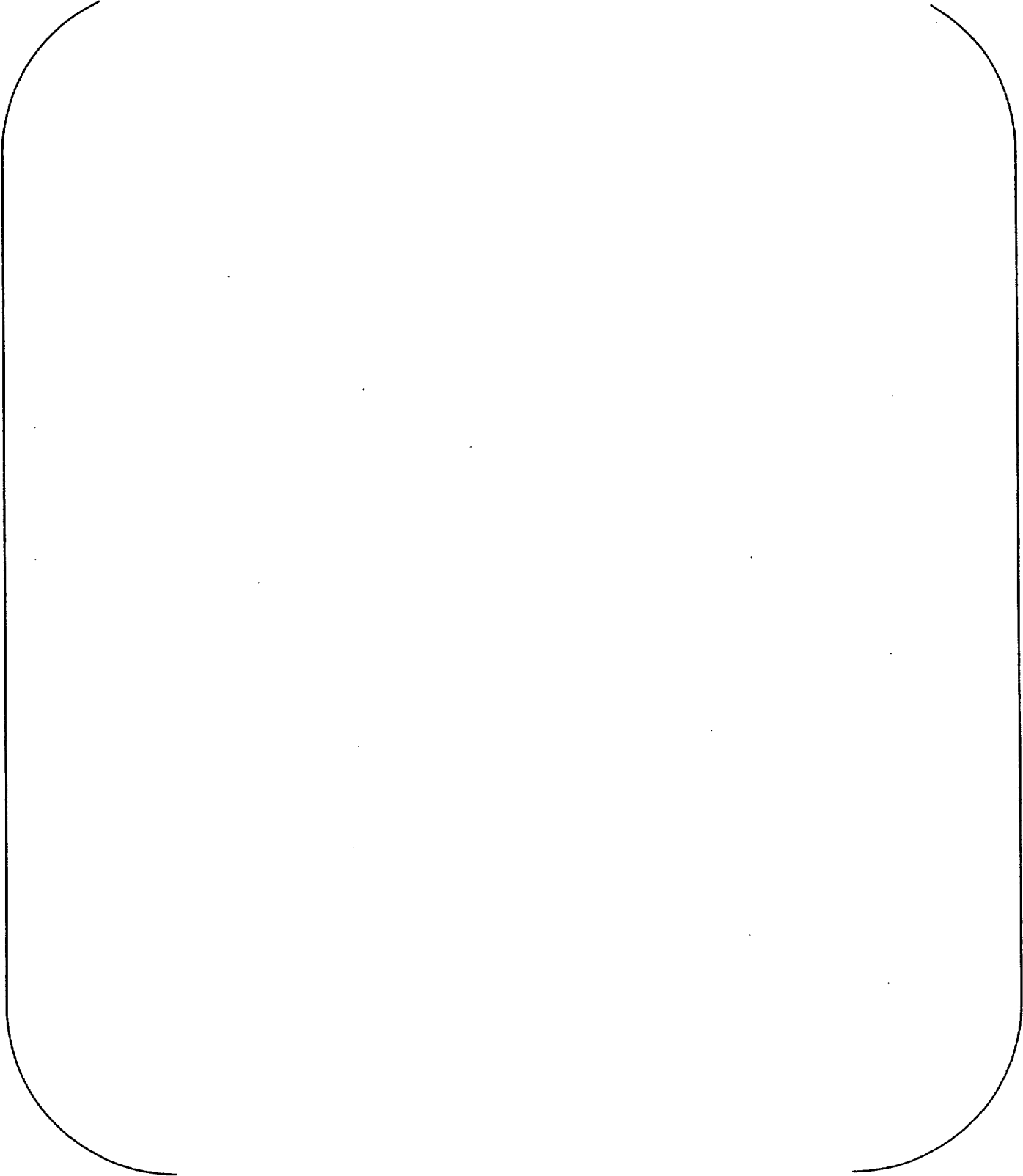
A large, empty rounded rectangular frame with a thin black border, occupying most of the page. It is intended for a table but contains no data.

Table B-40: Temperature in Rod 432-5 at Bottom Node: TCBOT (continued)

Table B-40: Temperature in Rod 432-5 at Bottom Node: TCBOT (continued)

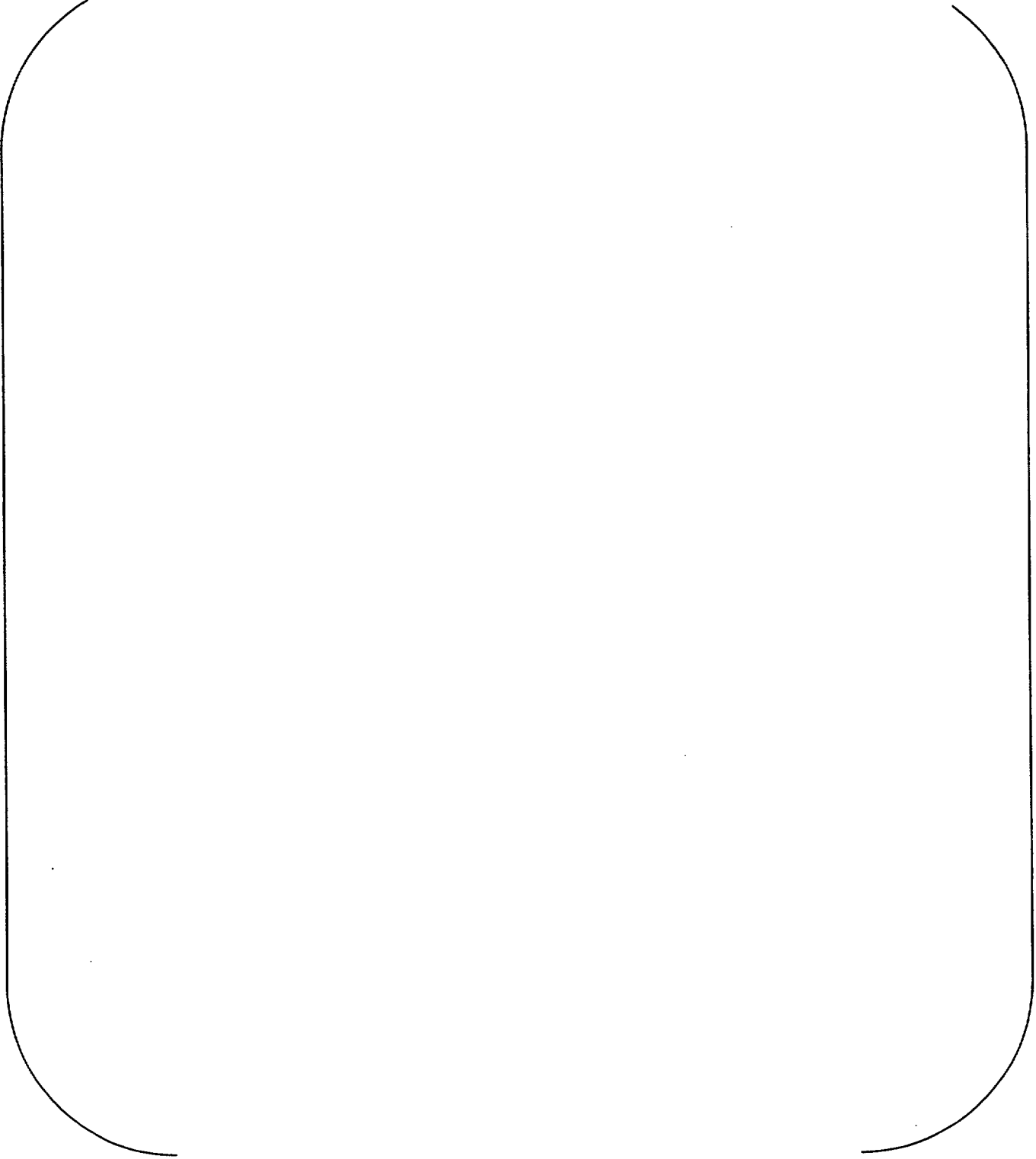
A large, empty rounded rectangular frame with a thin black border, occupying the central portion of the page. It is intended for the content of Table B-40.

Table B-40: Temperature in Rod 432-5 at Bottom Node: TCBOT (continued)

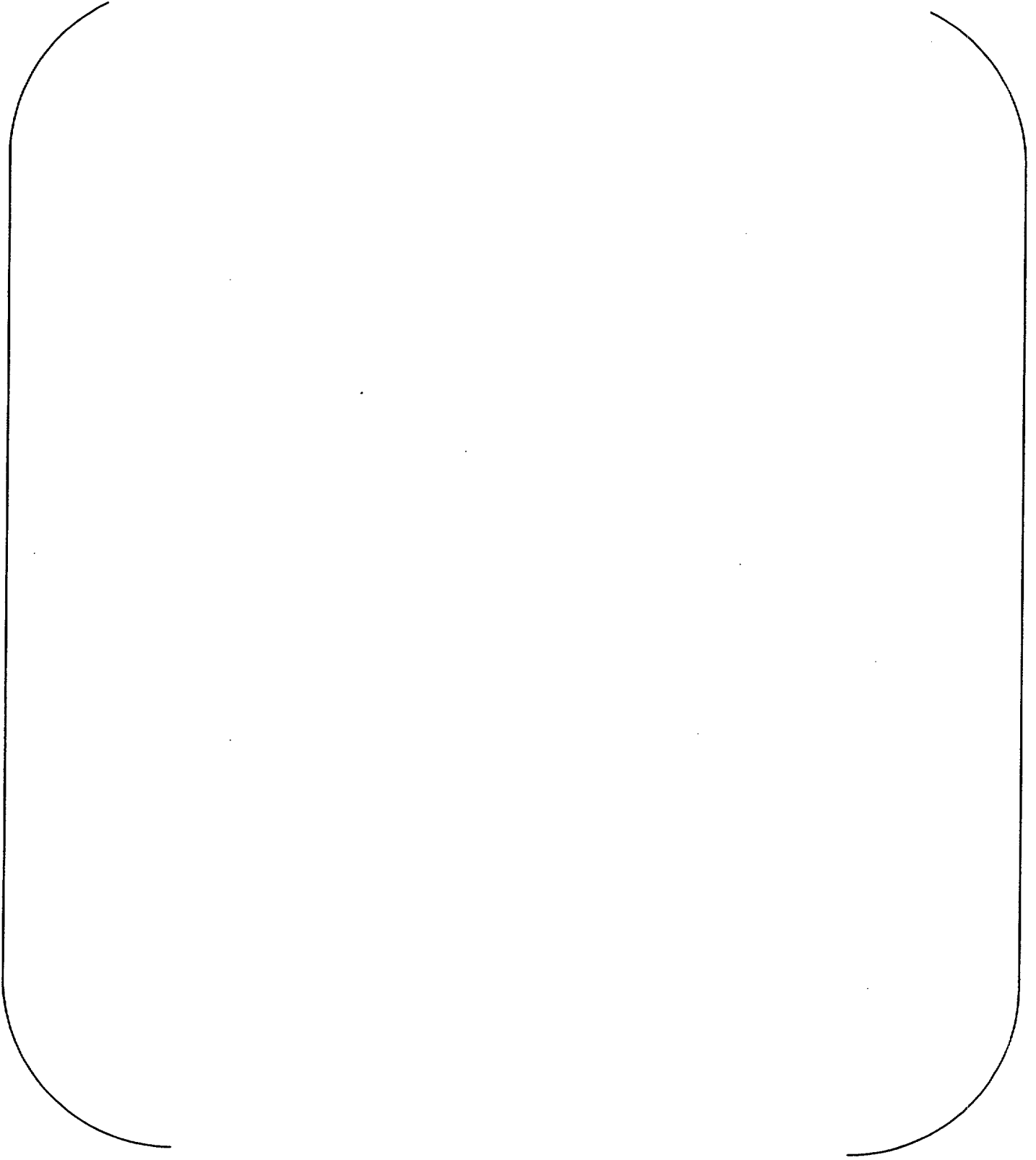


Table B-40: Temperature in Rod 432-5 at Bottom Node: TCBOT (continued)



Table B-41: Temperature in Rod 432-5 at Top Node: TCTOP

A large, empty rounded rectangular frame with a thin black border, centered on the page. It appears to be a placeholder for a table or figure.

Table B-42: Temperature in Rod 513-1 at Bottom Node: TCBOT

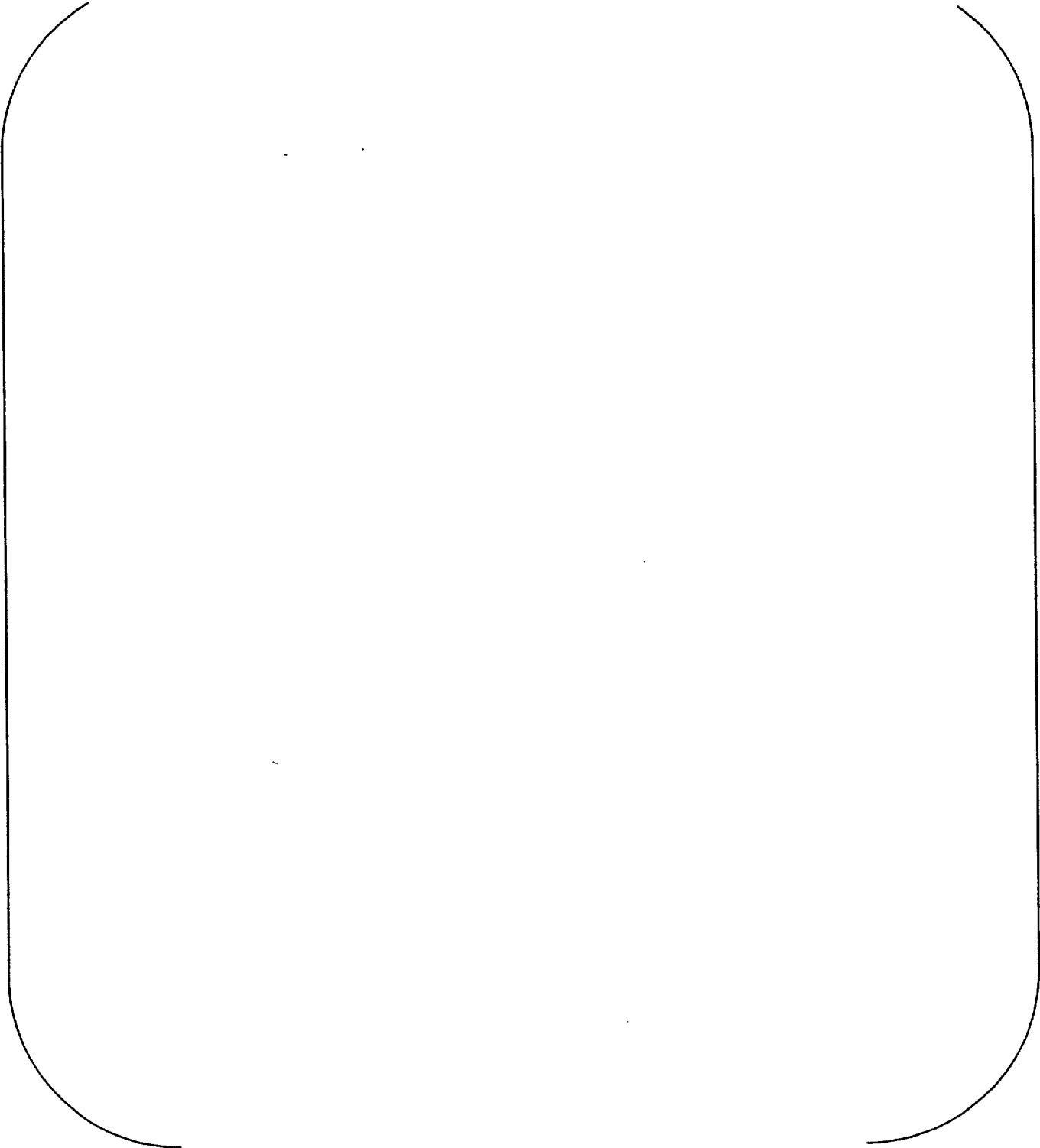
A large, empty rounded rectangular frame with a thin black border, occupying the central portion of the page. It is intended for the content of Table B-42.

Table B-42: Temperature in Rod 513-1 at Bottom Node: TCBOT (continued)

Table B-43: Temperature in Rod 513-1 at Top Node: TCTOP

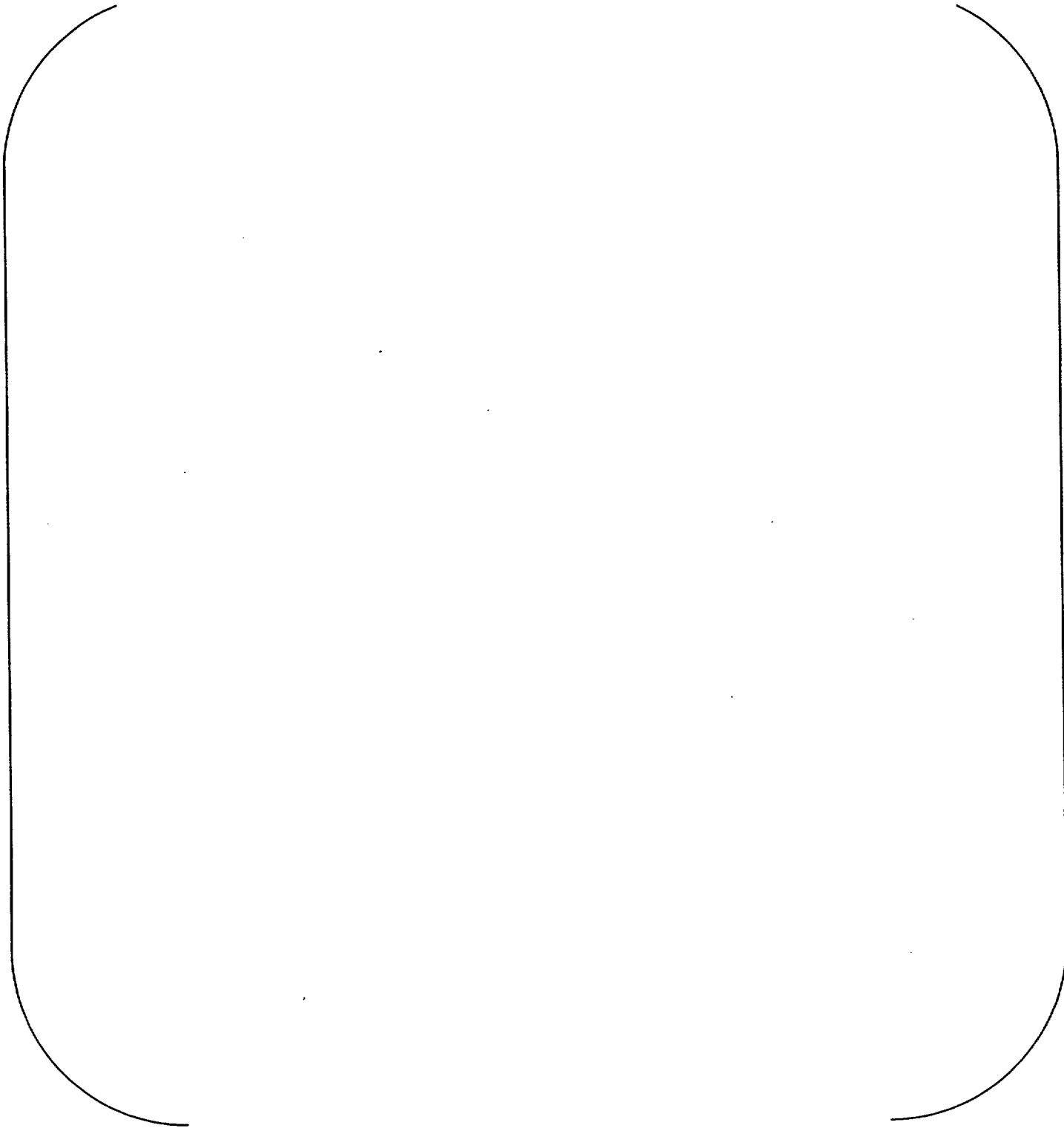
A large, empty rounded rectangular frame with a thin black border, occupying the central portion of the page. It is intended for the content of Table B-43.

Table B-43: Temperature in Rod 513-1 at Top Node: TCTOP (continued)

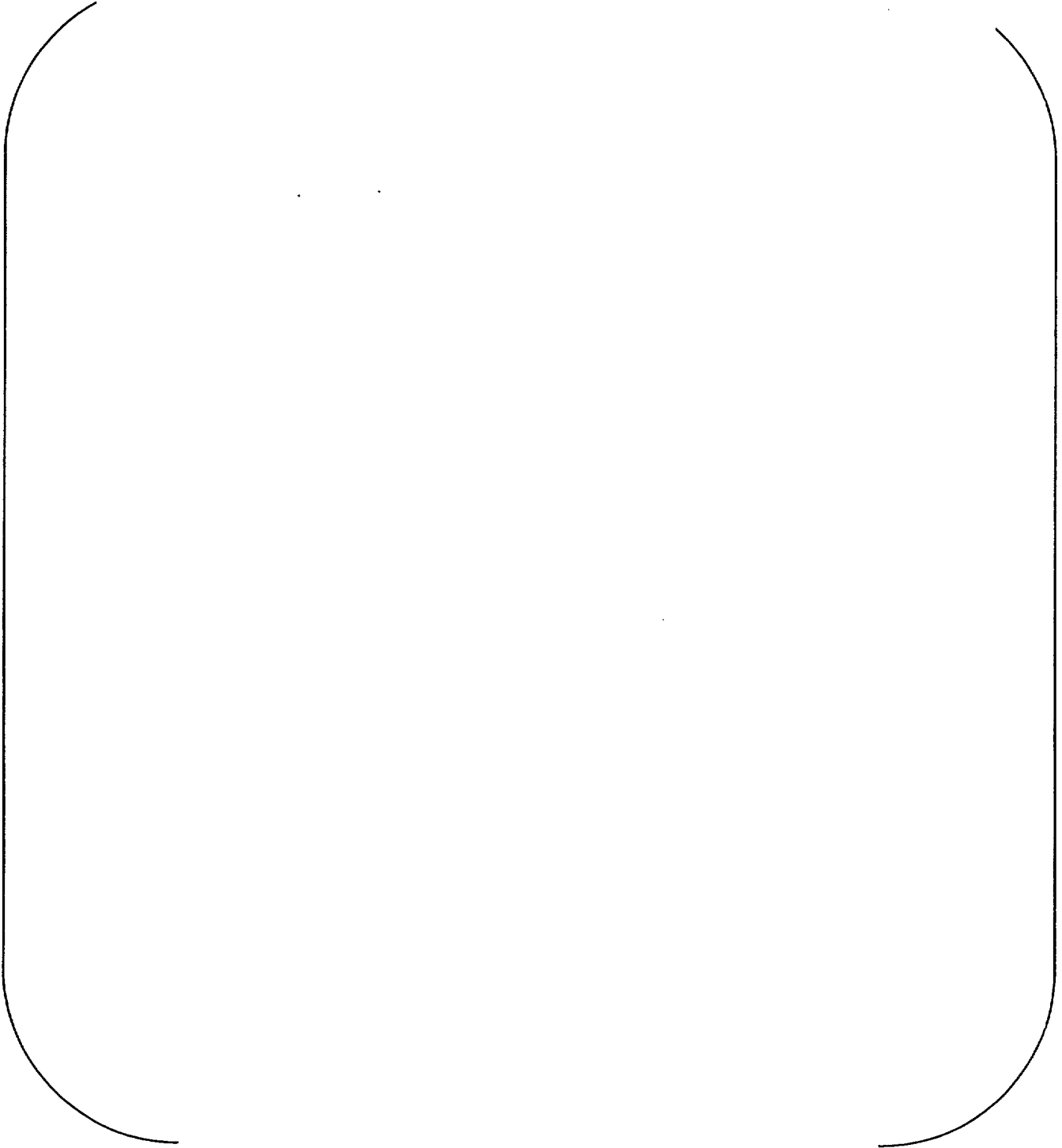


Table B-44: Temperature in Rod 513-2 at Bottom Node: TCBOT

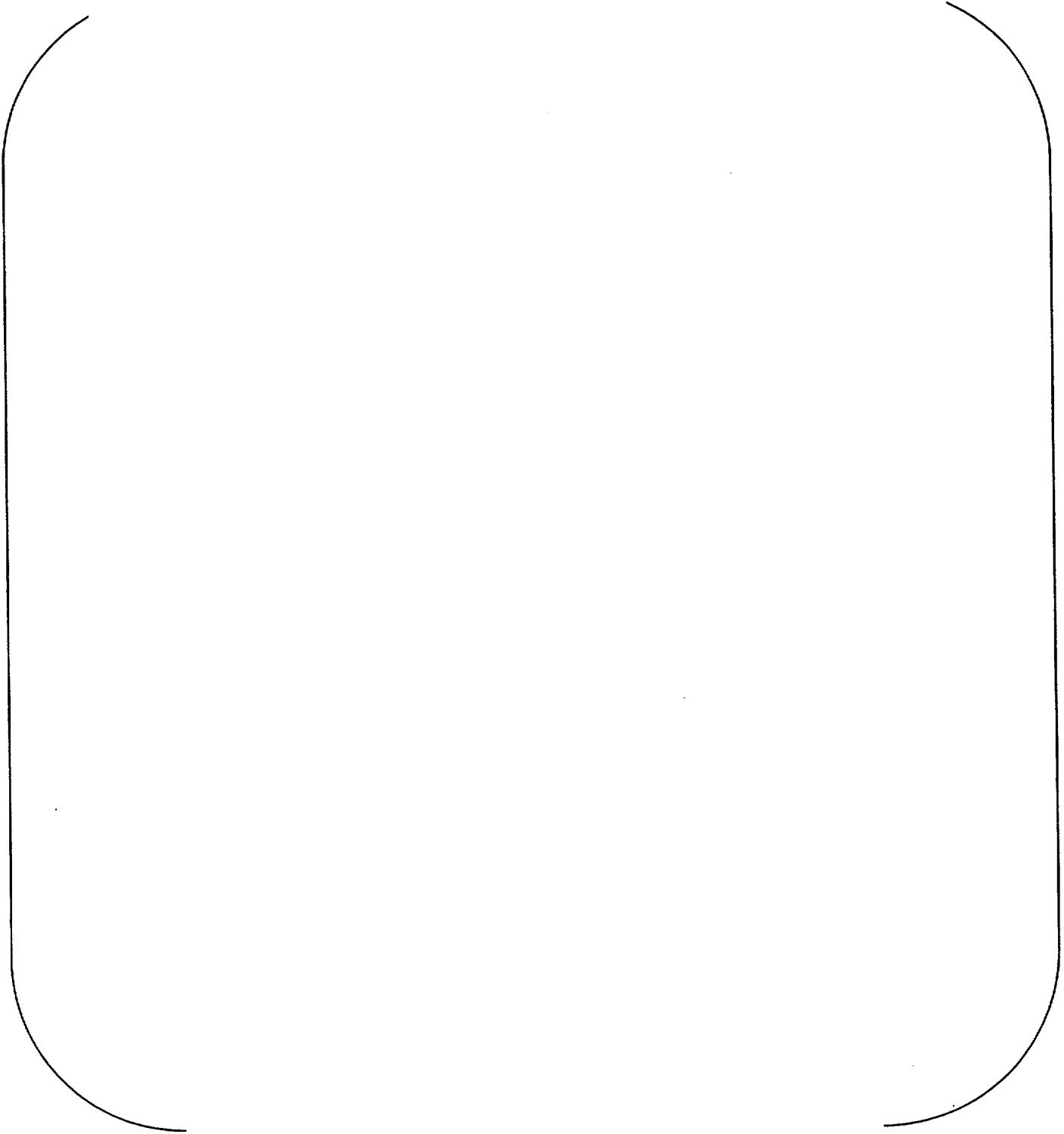
A large, empty rounded rectangular frame with a thin black border, occupying the central portion of the page. It is intended for the content of Table B-44.

Table B-44: Temperature in Rod 513-2 at Bottom Node: TCBOT (continued)

A large, empty rectangular area enclosed by a thin black line, with rounded corners. It is positioned below the caption and above the footer, occupying most of the page's width and height. This area is likely intended for a table or data but is currently blank.

Table B-45: Temperature in Rod 513-2 at Top Node: TCTOP

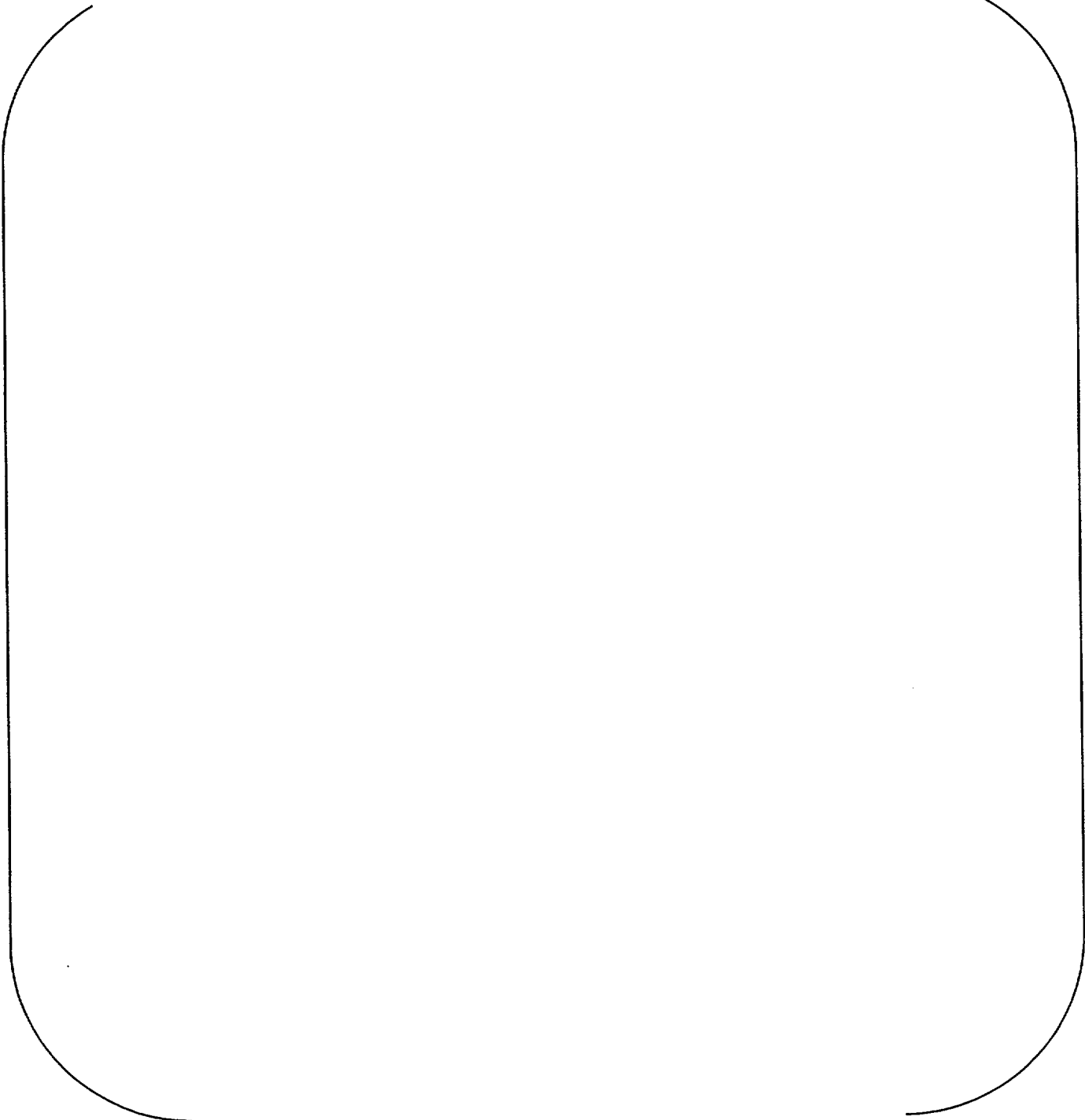
A large, empty rounded rectangular frame with a thin black border, occupying most of the page. It is intended for the content of Table B-45.

Table B-45: Temperature in Rod 513-2 at Top Node: TCTOP (continued)

Table B-46: Temperature in Rod 513-6 at Bottom Node: TCBOT

A large, empty rounded rectangular frame with a thin black border, occupying the central portion of the page. It is intended for the content of Table B-46.

Table B-46: Temperature in Rod 513-6 at Bottom Node: TCBOT (continued)

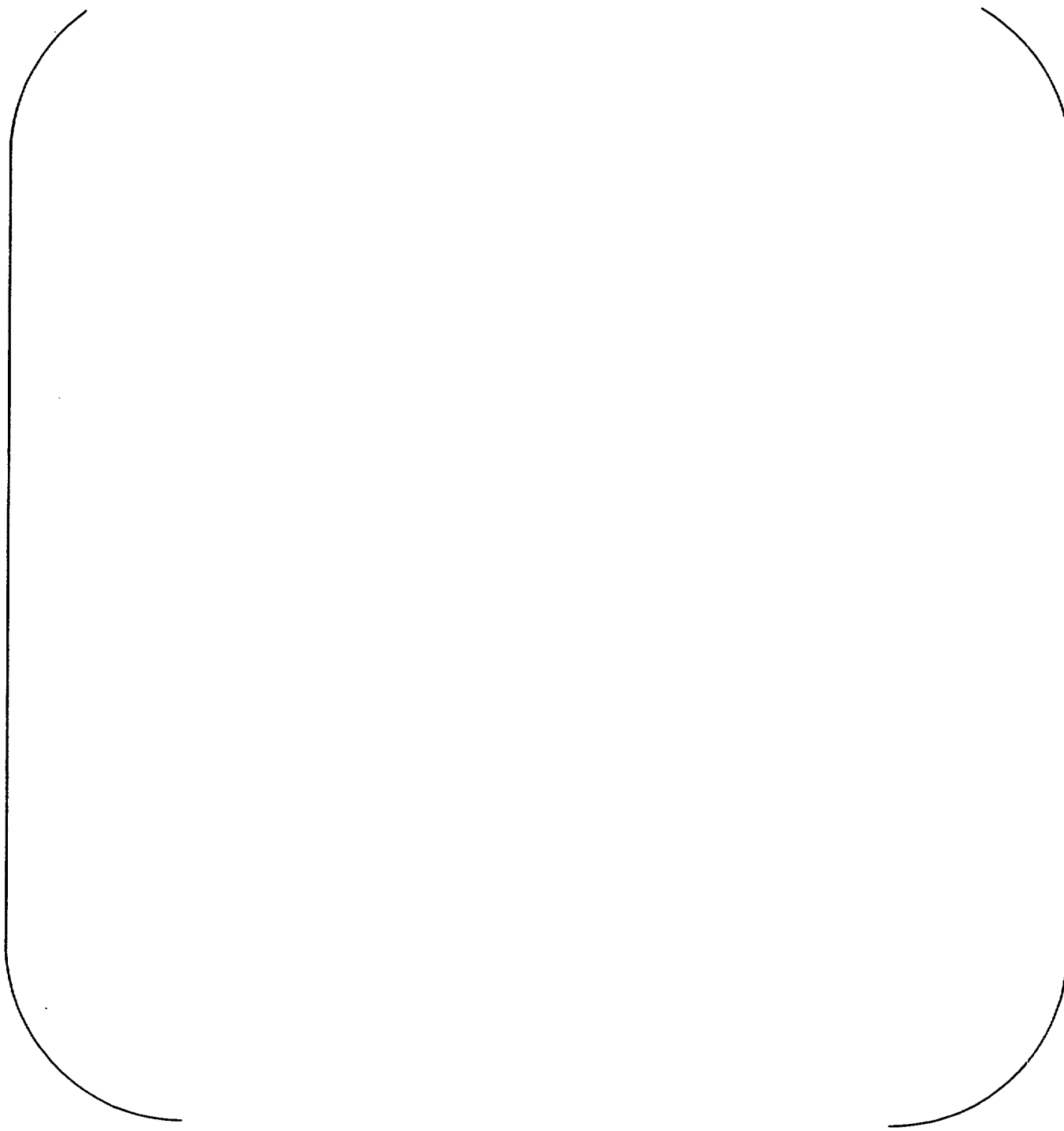
A large, empty rounded rectangular frame that occupies most of the page. It is defined by a single black line with rounded corners at the top and bottom. The interior of the frame is completely blank, suggesting that the table data has been omitted or is otherwise unavailable.

Table B-47: Temperature in Rod 513-6 at Top Node: TCTOP

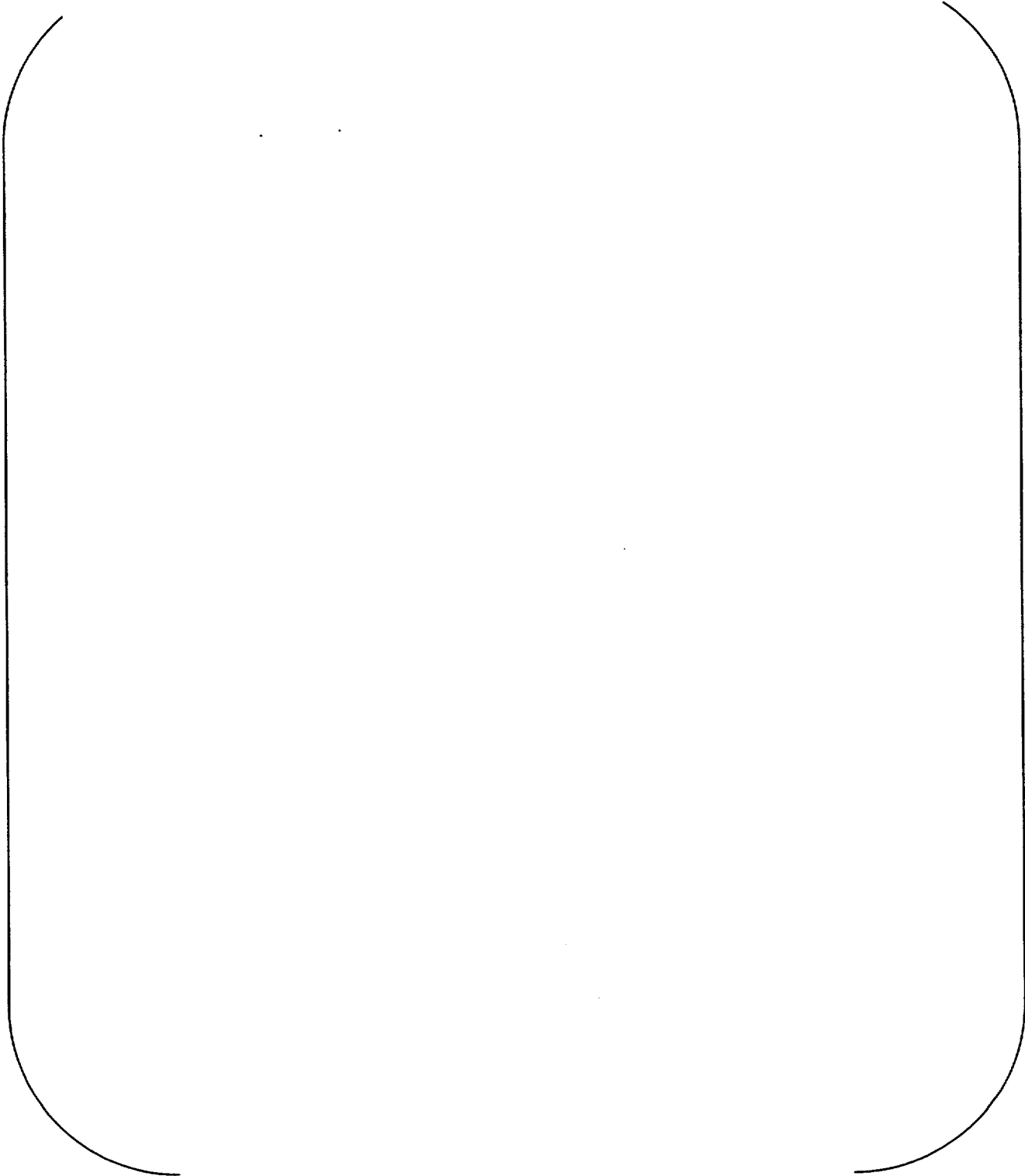


Table B-47: Temperature in Rod 513-6 at Top Node: TCTOP (continued)

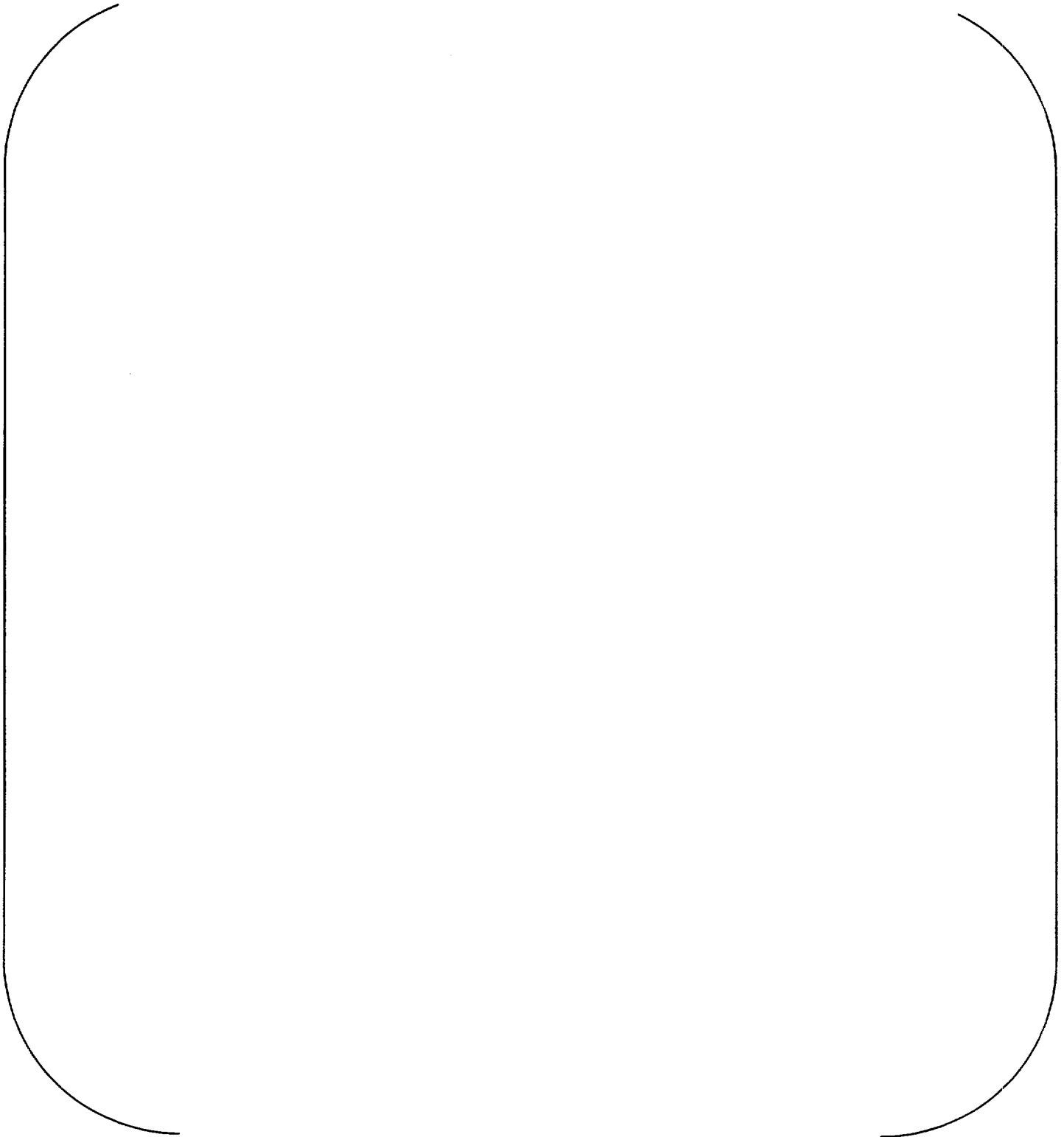
A large, empty rounded rectangular frame with a thin black border, occupying the central portion of the page. It is intended for the content of Table B-47.

Table B-48: Rod Average Temperature in Rod 515-a: TCAVE

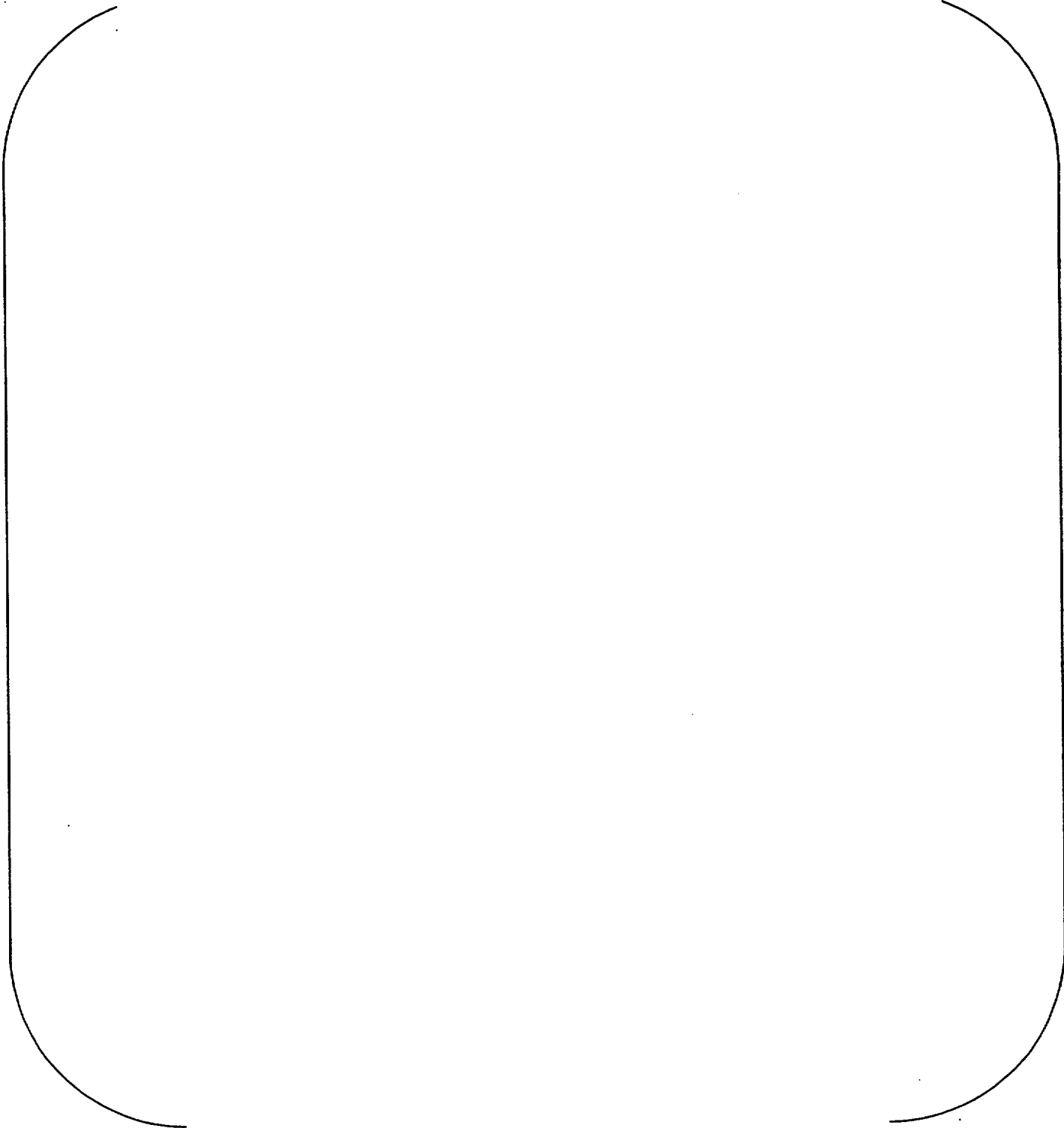
A large, empty rounded rectangular frame with a thin black border, occupying the central portion of the page. It is intended for the content of Table B-48.

Table B-48: Rod Average Temperature in Rod 515-a: TCAVE (continued)

A large, empty rectangular area enclosed by a thin black line with rounded corners, indicating that the table content is missing or redacted.

Table B-49: Rod Average Temperature in Rod 515-a2: TCAVE

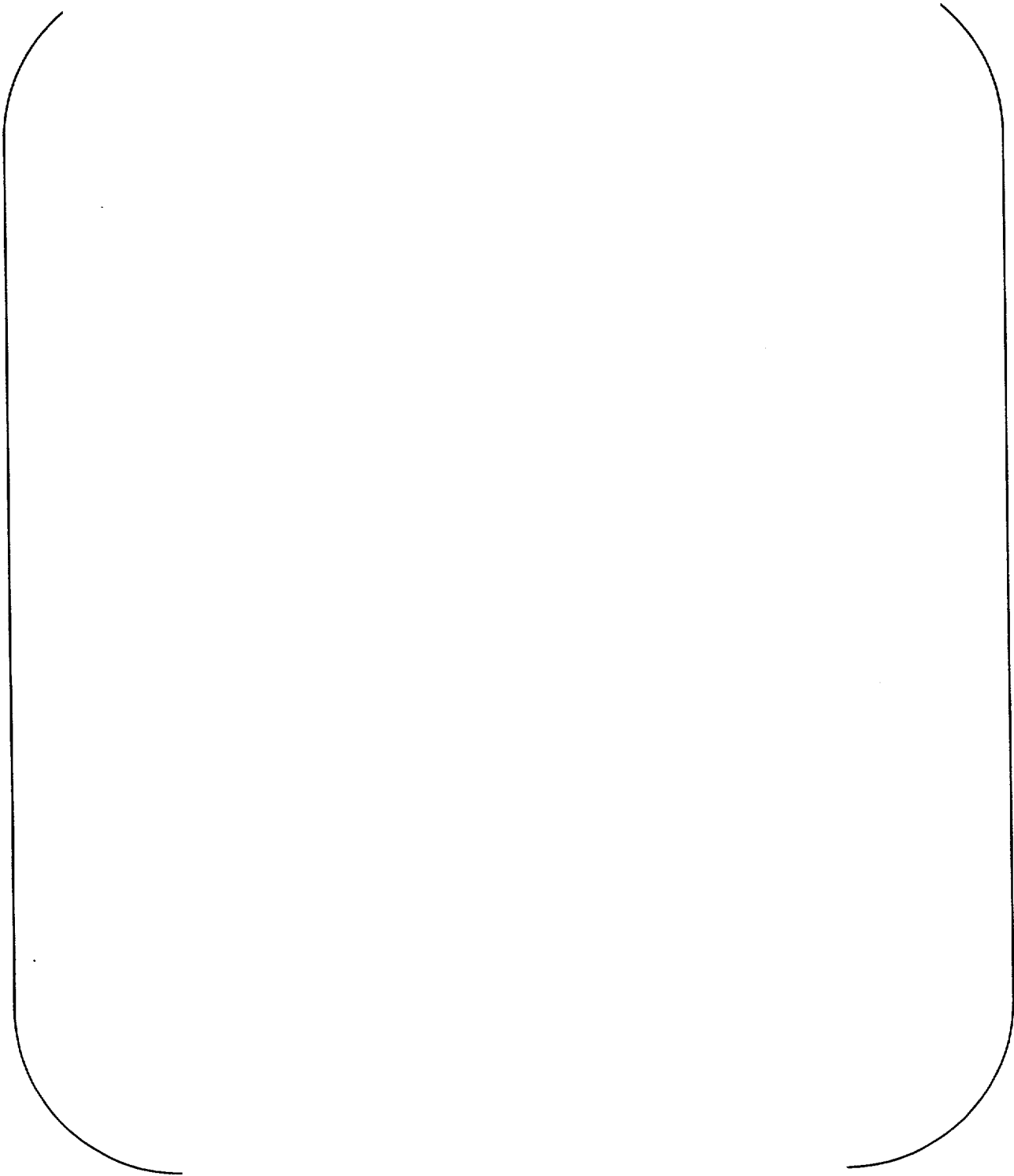
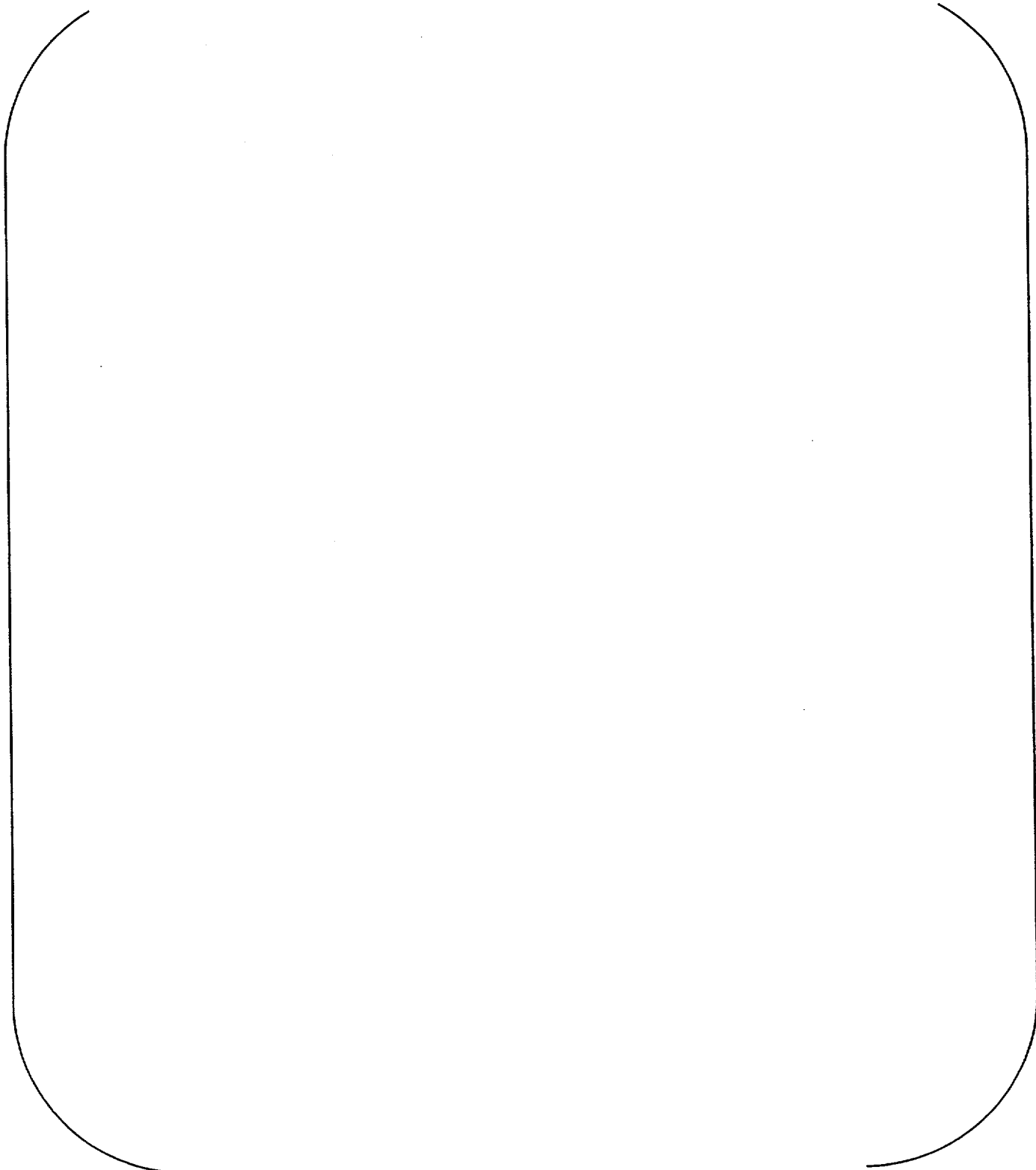
A large, empty rounded rectangular frame with a thin black border, occupying the central portion of the page. It is intended for the content of Table B-49.

Table B-49: Rod Average Temperature in Rod 515-a2: TCAVE (continued)

A large, empty rounded rectangular frame, likely intended for a table or figure, but containing no data.

Table B-50: Rod Average Temperature in Rod 562-2to4ET: TCAVE

A large, empty rounded rectangular frame with a thin black border, occupying the central portion of the page. It is intended for the content of Table B-50.

**Table B-50: Rod Average Temperature in Rod 562-2to4ET: TCAVE
(continued)**

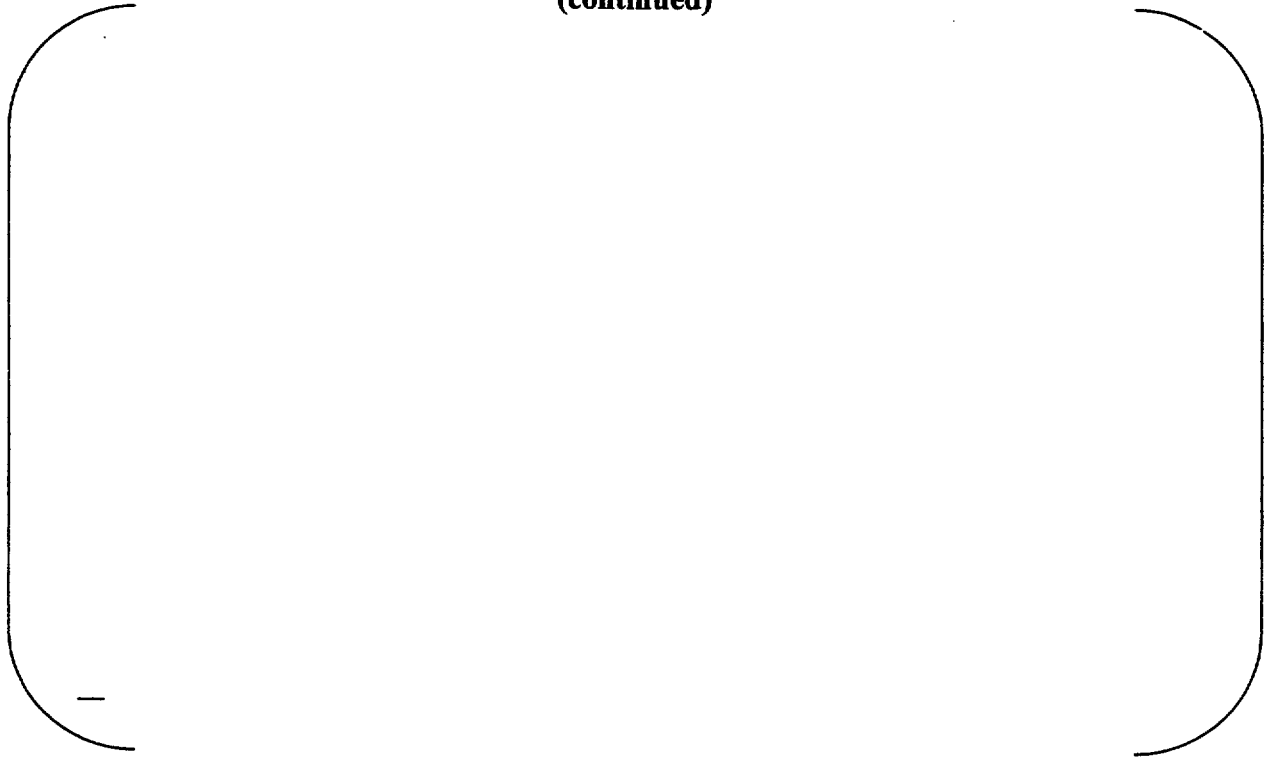
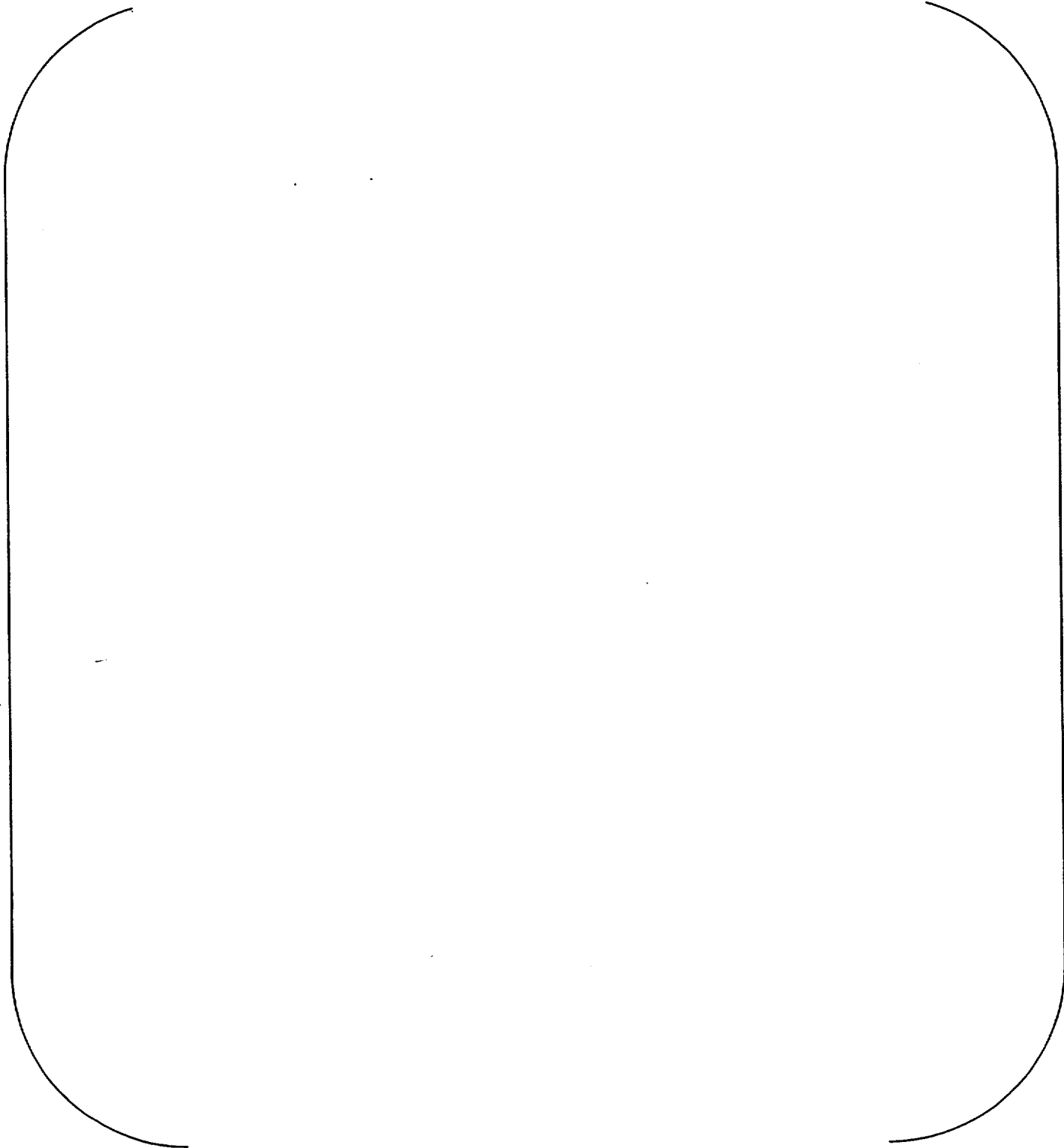


Table B-51: Temperature in Rod 597-d52-wtc at Bottom Node: TCBOT

A large, empty rounded rectangular frame with a thin black border, occupying the central portion of the page. It is intended for the content of Table B-51.

**Table B-51: Temperature in Rod 597-d52-wtc at Bottom Node: TCBOT
(continued)**

[]

Table B-52: Temperature in Rod 597-d53-wtc at Bottom Node: TCBOT

A large, empty rounded rectangular frame with a thin black border, occupying the central portion of the page. It is intended for the data from Table B-52.



Figure B-1: BOL Fuel Centerline Temperature: IFA-432-1

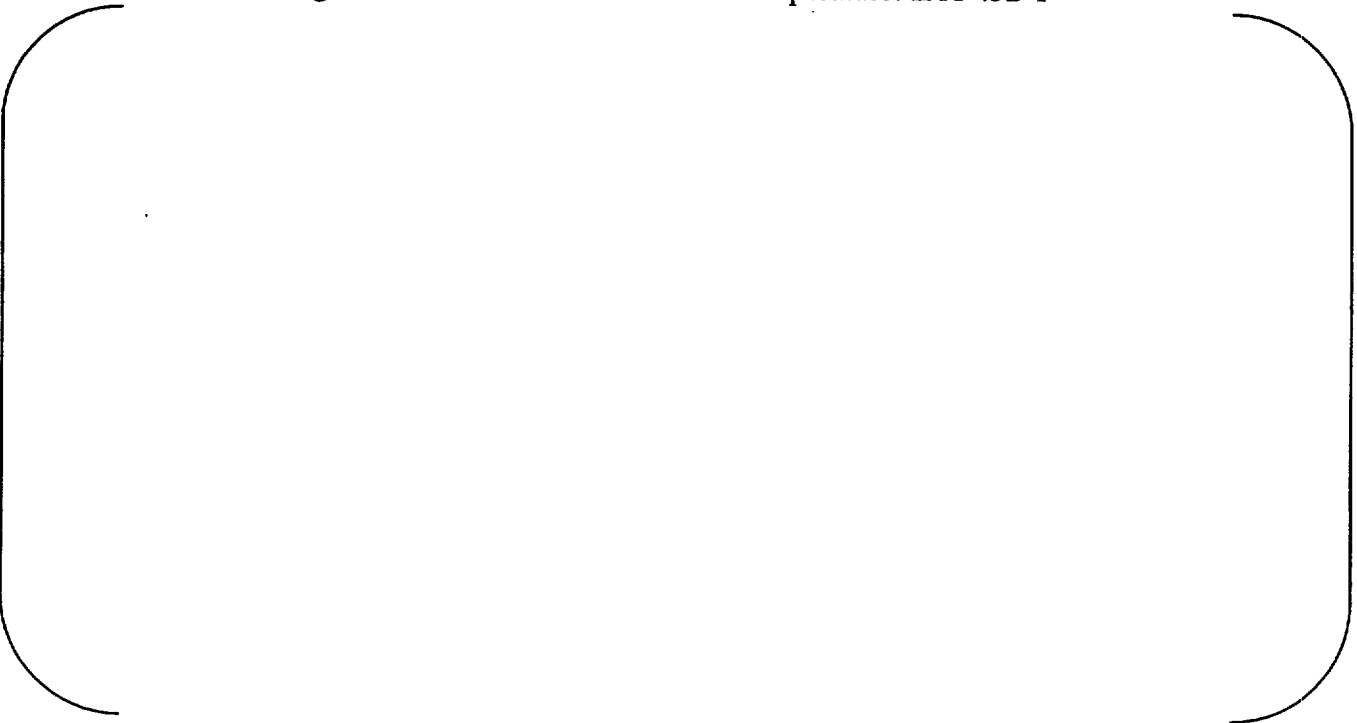


Figure B-2: BOL Fuel Centerline Temperature: IFA-432-2



Figure B-3: BOL Fuel Centerline Temperature: IFA-432-3



Figure B-4: BOL Fuel Centerline Temperature: IFA-432-5



Figure B-5: BOL Fuel Centerline Temperature: IFA 504-1-ar



Figure B-6: BOL Fuel Centerline Temperature: IFA 504-1-he

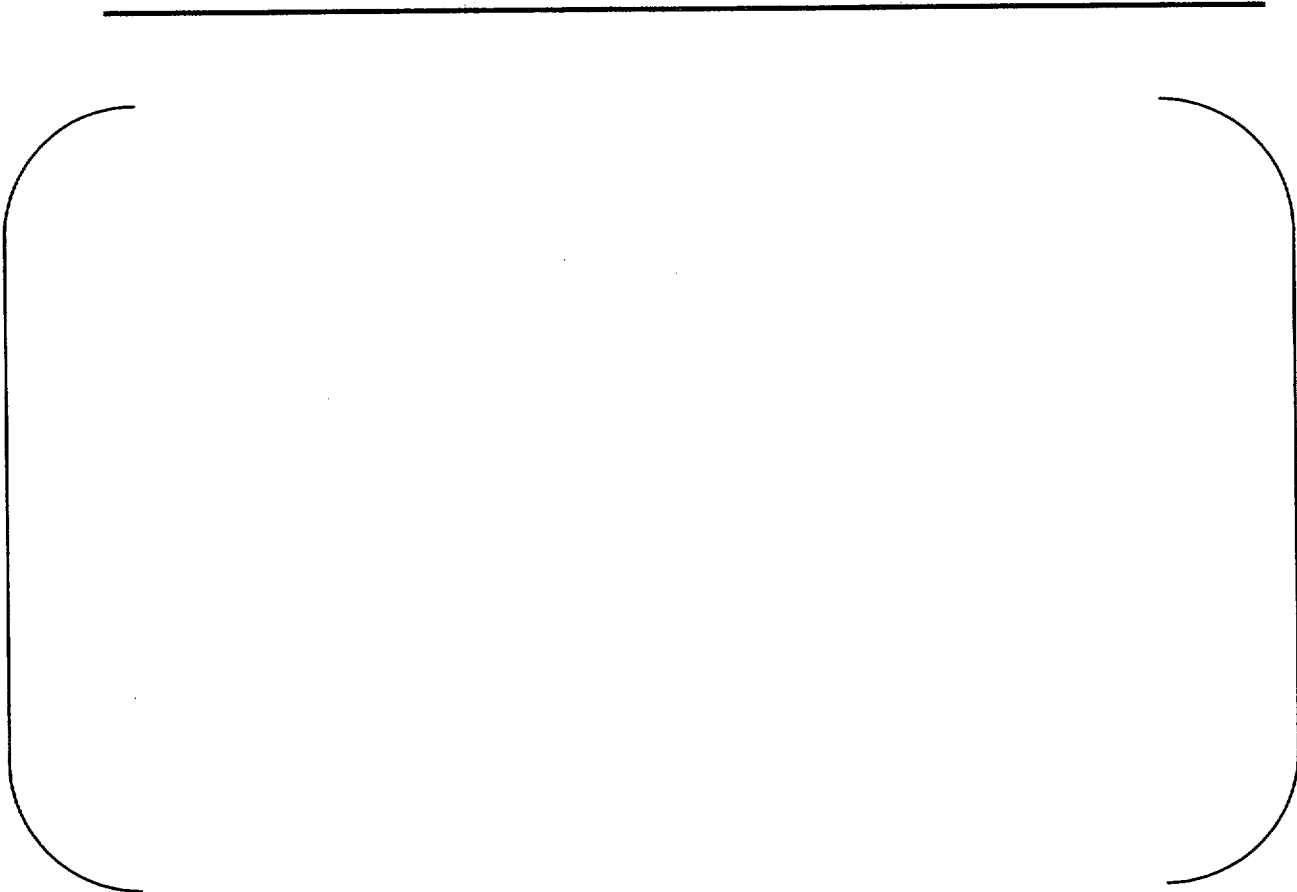


Figure B-7: BOL Fuel Centerline Temperature: IFA 504-1-Xe



Figure B-8: BOL Fuel Centerline Temperature: IFA 505-911A

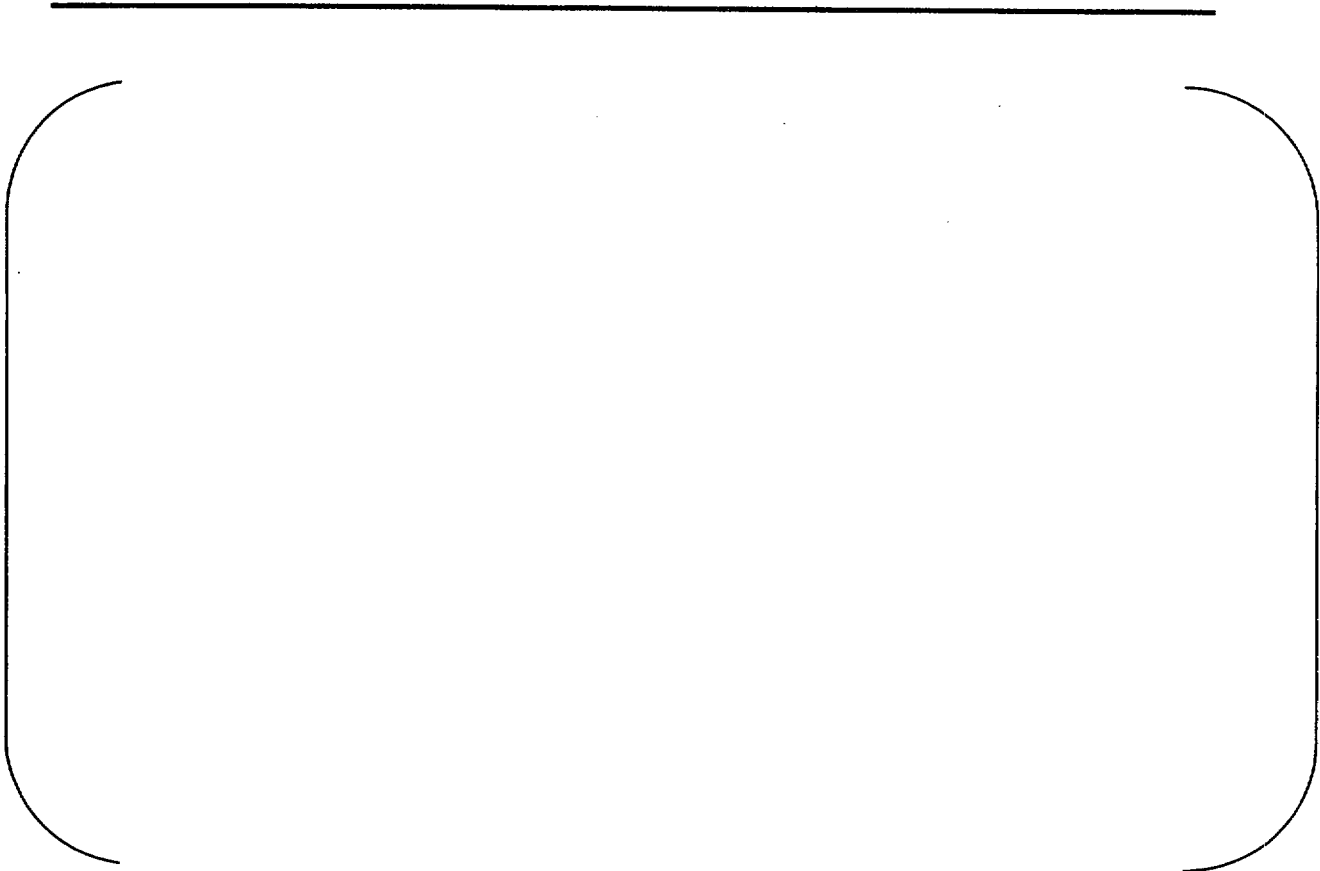


Figure B-9: BOL Fuel Centerline Temperature: IFA 505-911B



Figure B-10: BOL Fuel Centerline Temperature: IFA 505-912A



Figure B-11: BOL Fuel Centerline Temperature: IFA 505-913A



Figure B-12: BOL Fuel Centerline Temperature: IFA 505-913B

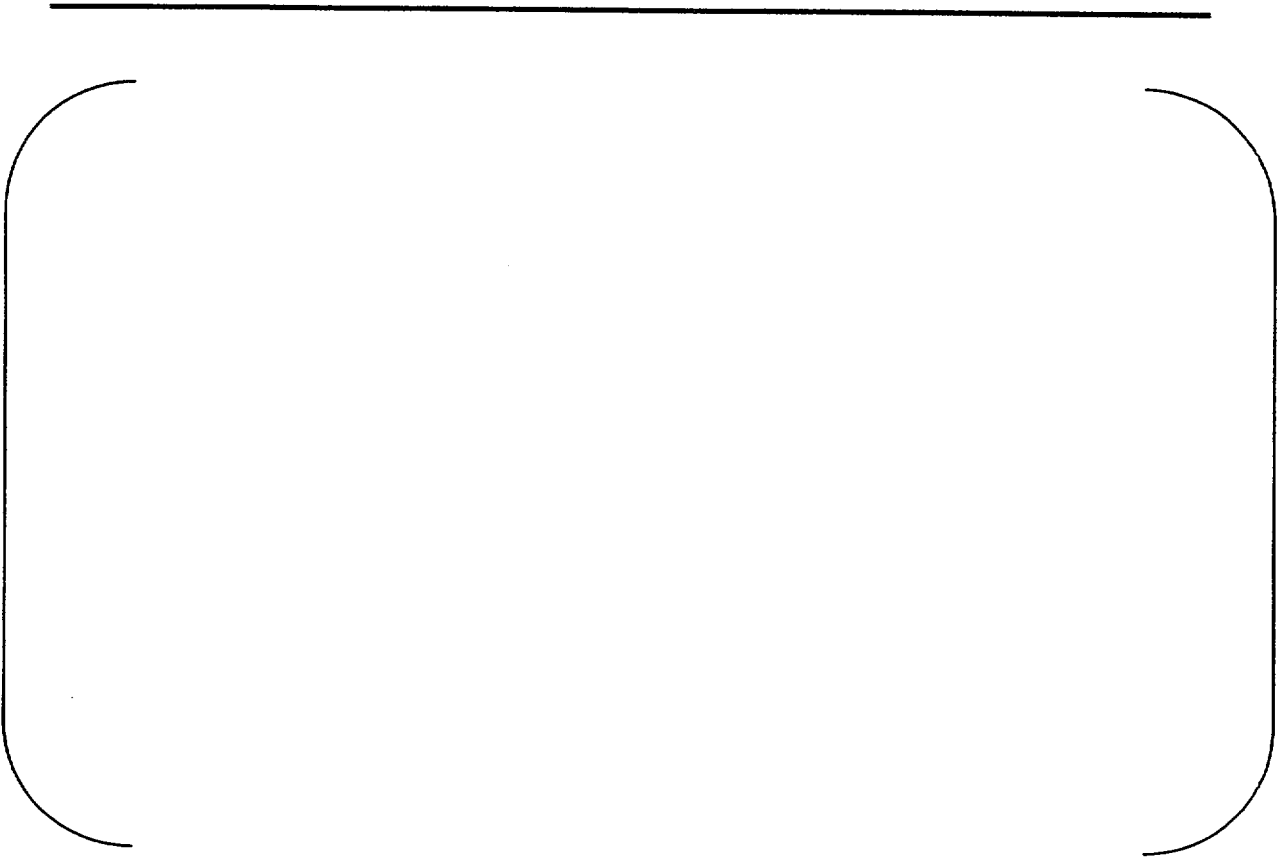


Figure B-13: BOL Fuel Centerline Temperature: IFA 505-914A

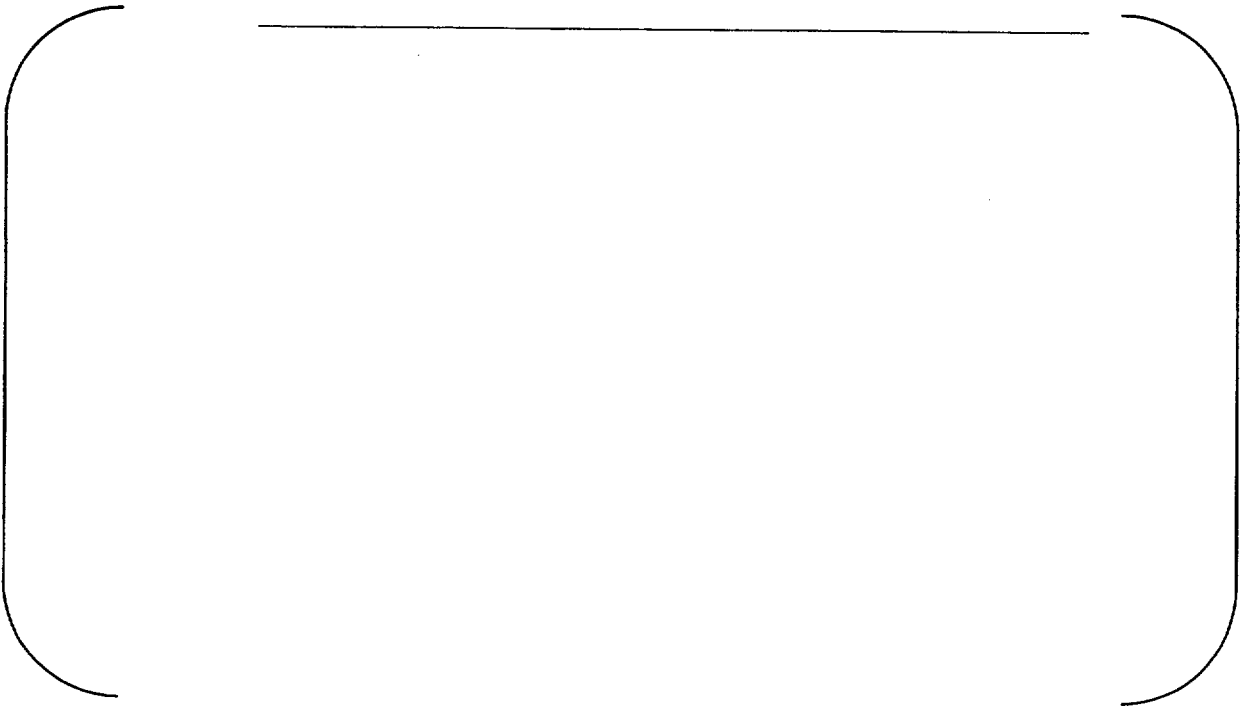


Figure B-14: BOL Fuel Centerline Temperature: IFA 505-915A



Figure B-15: BOL Fuel Centerline Temperature: IFA 505-915B




Figure B-16: BOL Fuel Centerline Temperature: IFA 505-916A

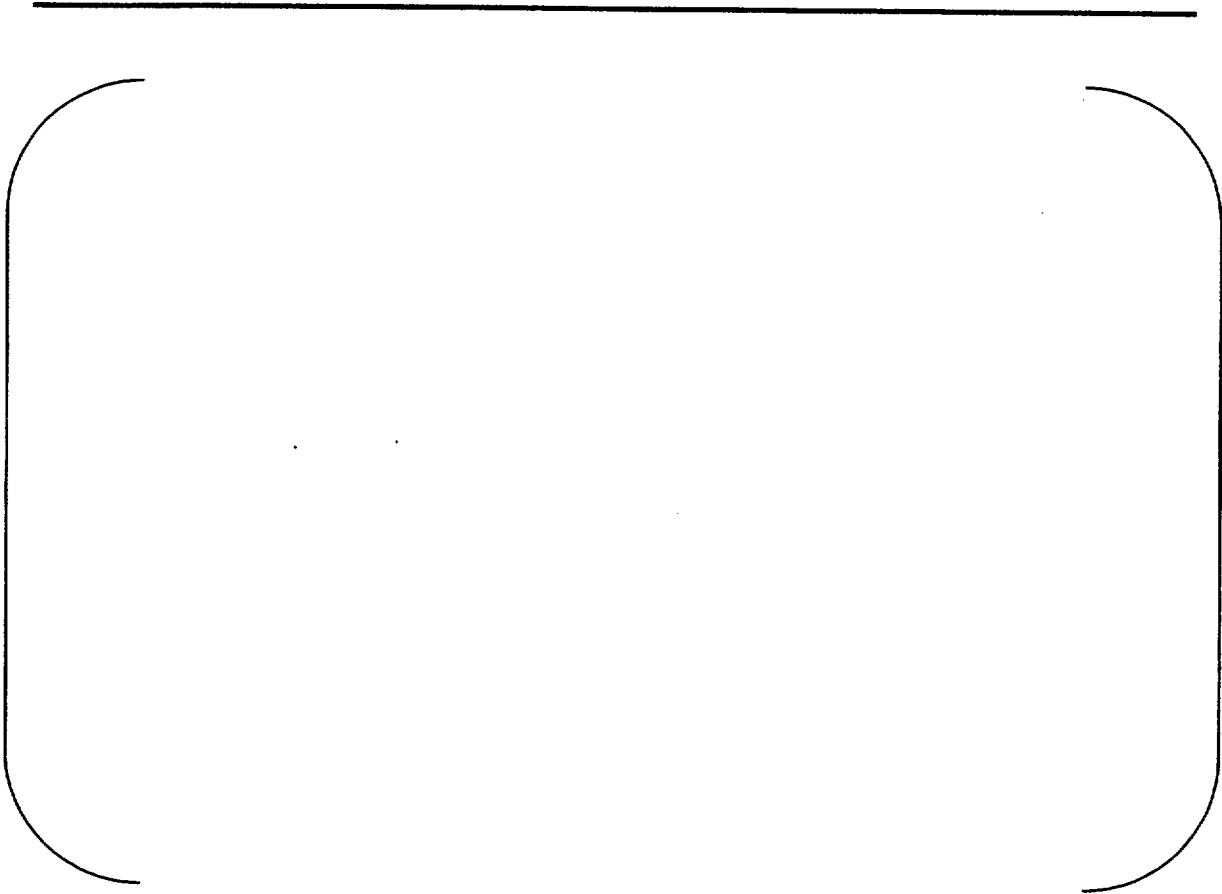


Figure B-17: BOL Fuel Centerline Temperature: IFA 505-922C



Figure B-18: BOL Fuel Centerline Temperature: IFA 505-922D

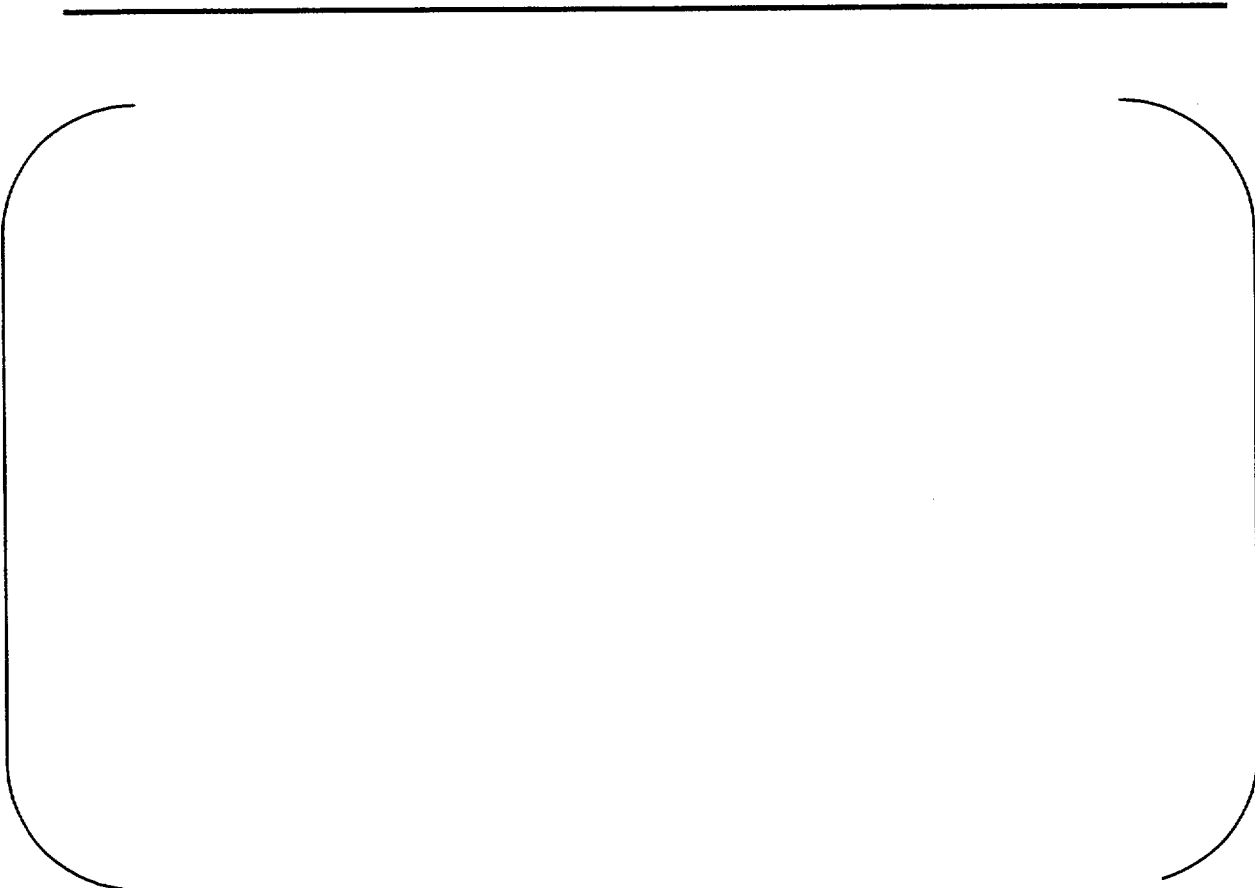


Figure B-19: BOL Fuel Centerline Temperature: IFA 505-923D



Figure B-20: BOL Fuel Centerline Temperature: IFA 505-924C



Figure B-21: BOL Fuel Centerline Temperature: IFA 505-924D



Figure B-22: BOL Fuel Centerline Temperature: IFA 505-926C



Figure B-23: BOL Fuel Centerline Temperature: IFA 505-926D



Figure B-24. BOL Fuel Centerline Temperature: IFA 507-1_3_5

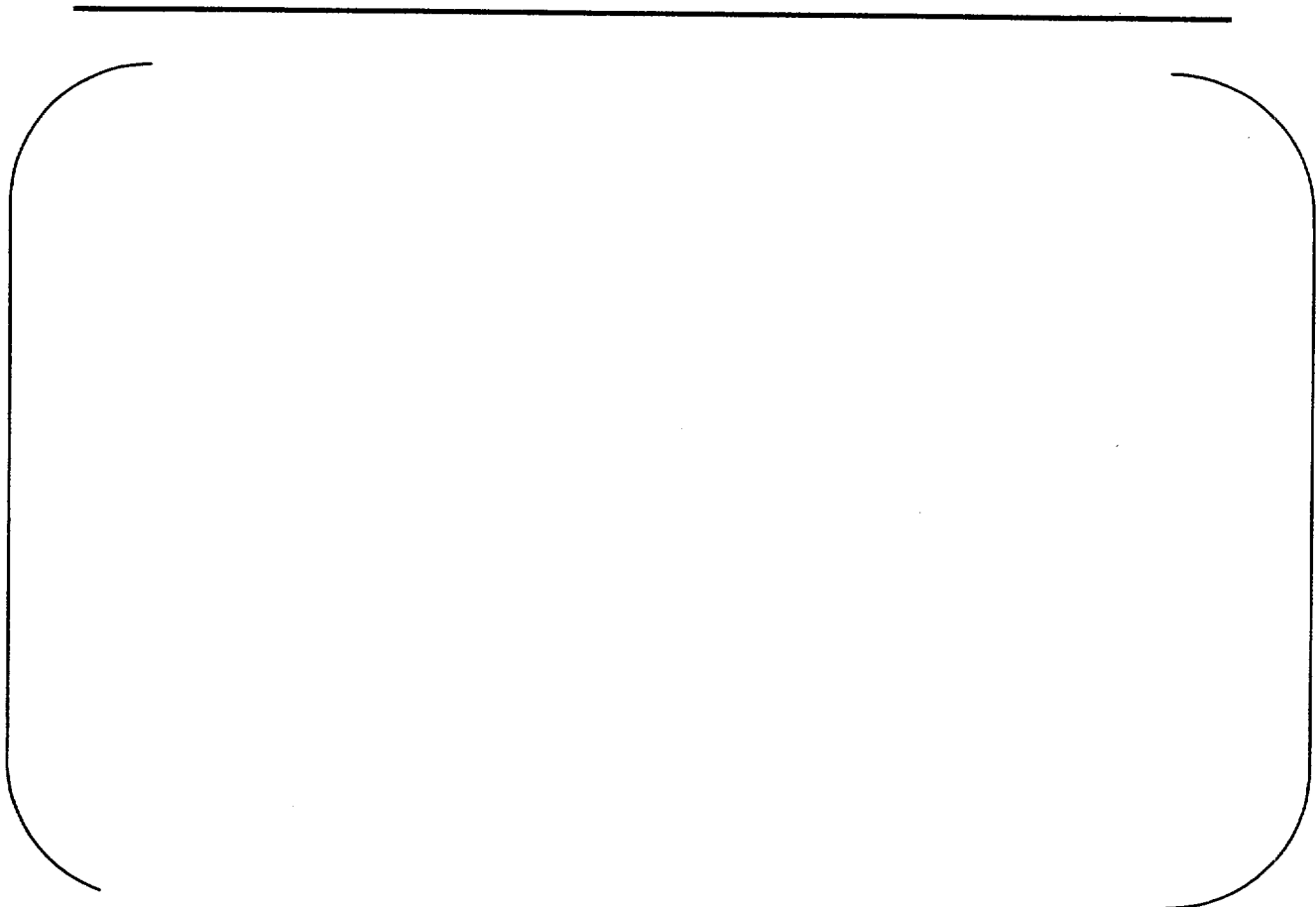


Figure B-25: BOL Fuel Centerline Temperature: IFA 507-2_4_6



Figure B-26: BOL Fuel Centerline Temperature: IFA 513-1

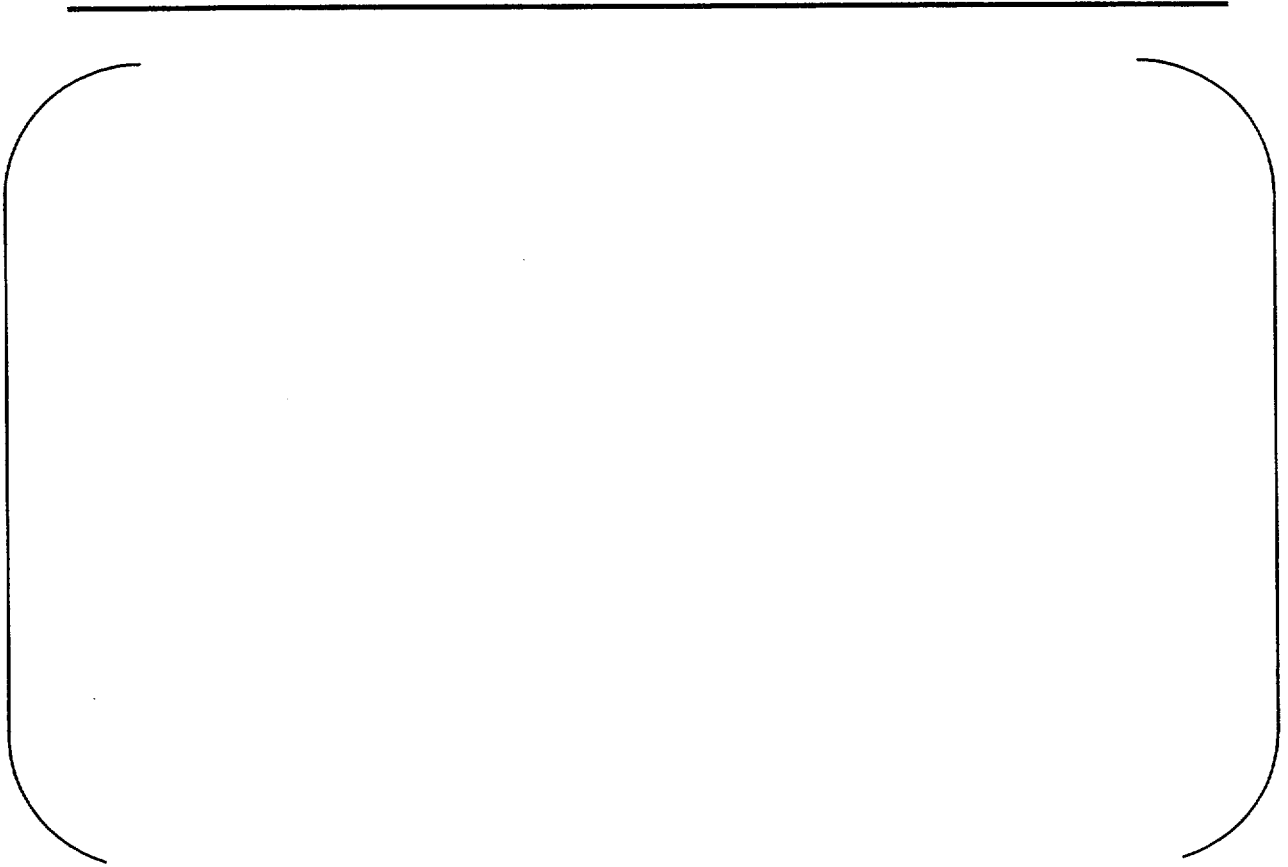


Figure B-27: BOL Fuel Centerline Temperature: IFA 513-2

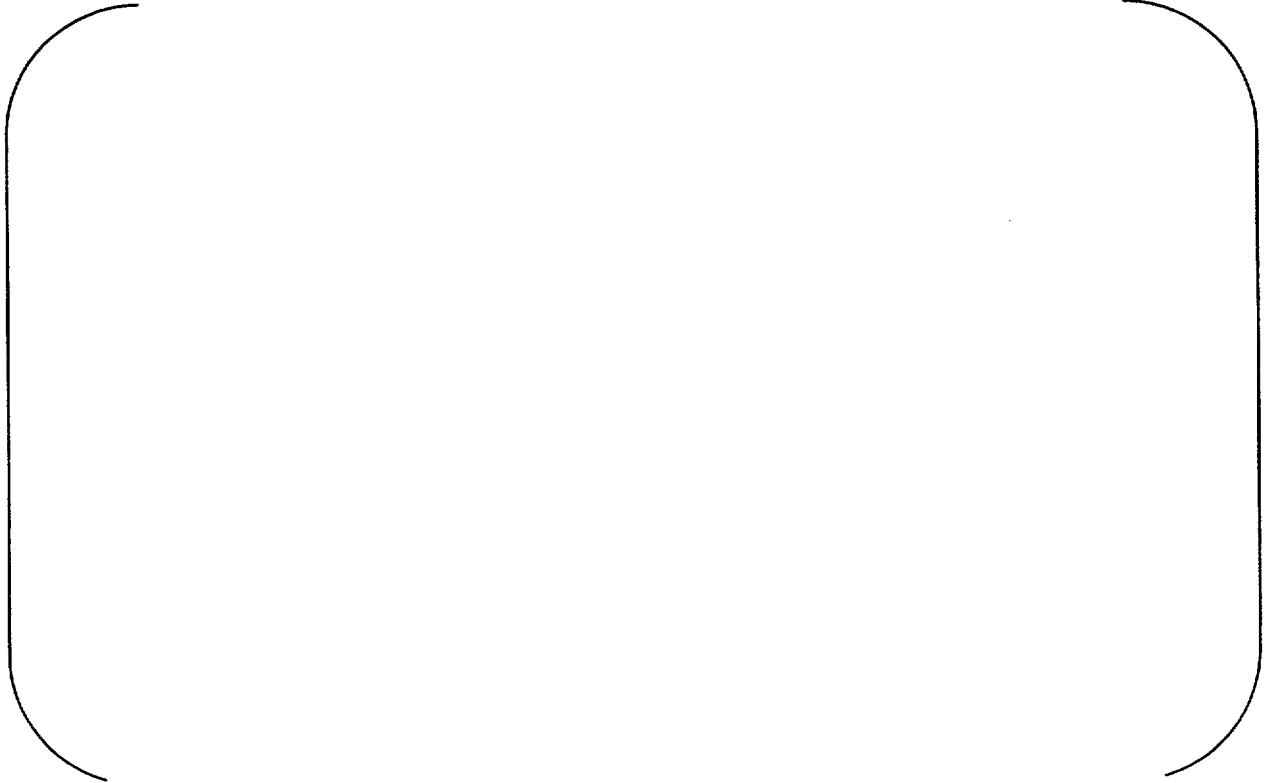


Figure B-28: BOL Fuel Centerline Temperature: IFA 513-6

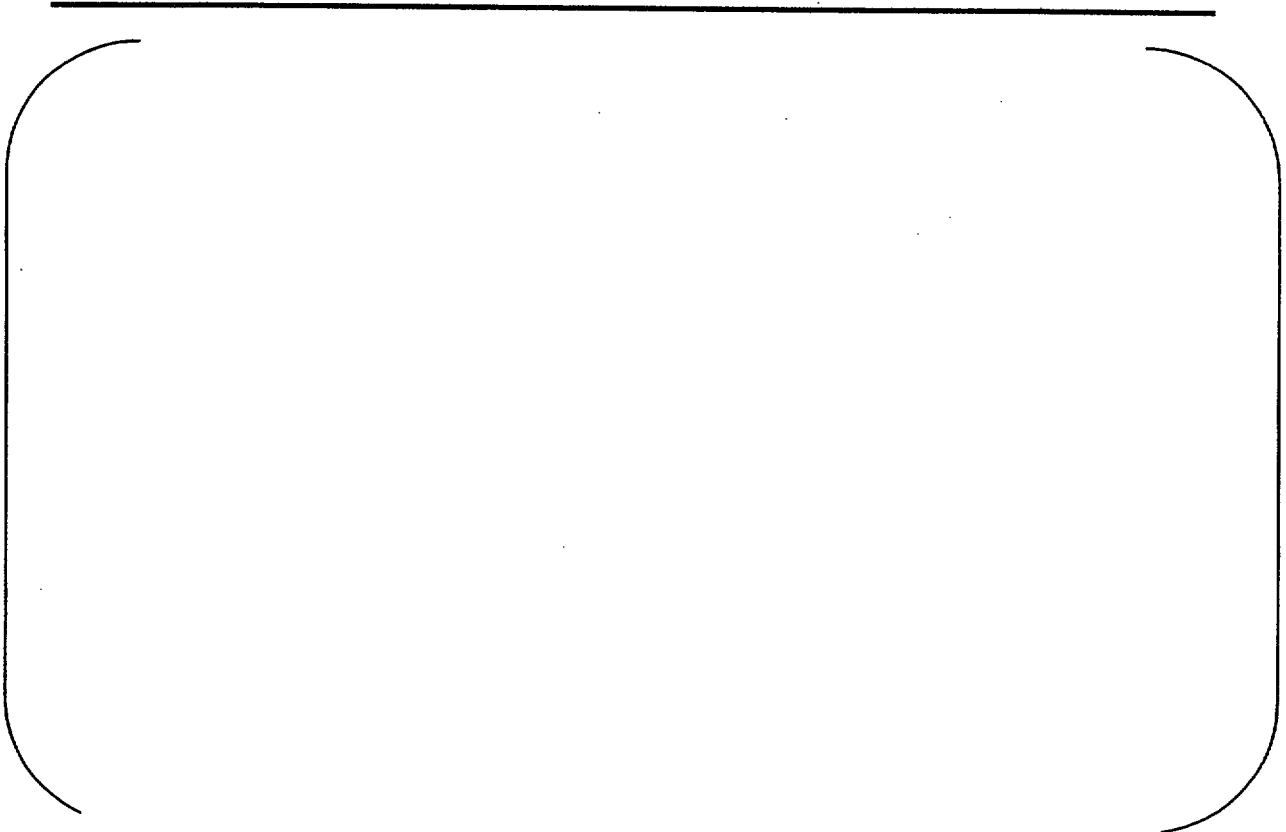


Figure B-29: BOL Fuel Centerline Temperature: IFA 515-a1

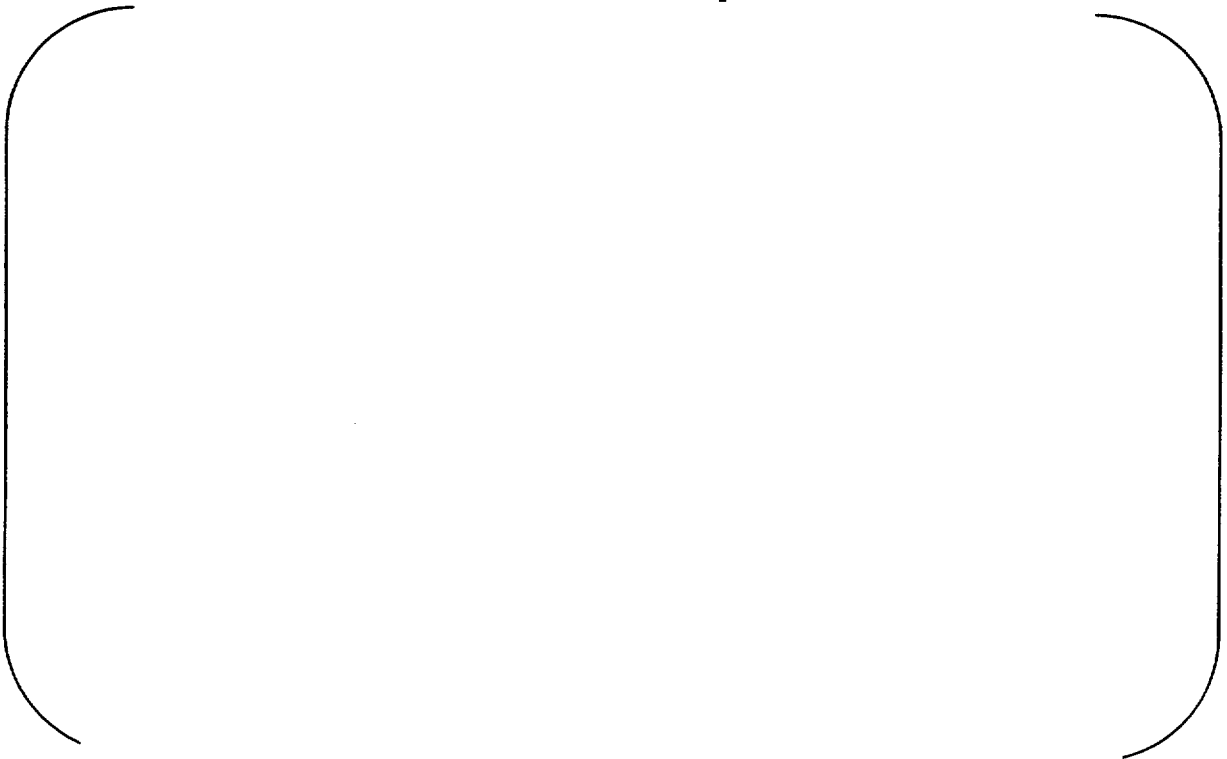


Figure B-30: BOL Fuel Centerline Temperature: IFA 515-a2



Figure B-31: BOL Fuel Centerline Temperature: IFA 522-1



Figure B-32: BOL Fuel Centerline Temperature: IFA 522-2

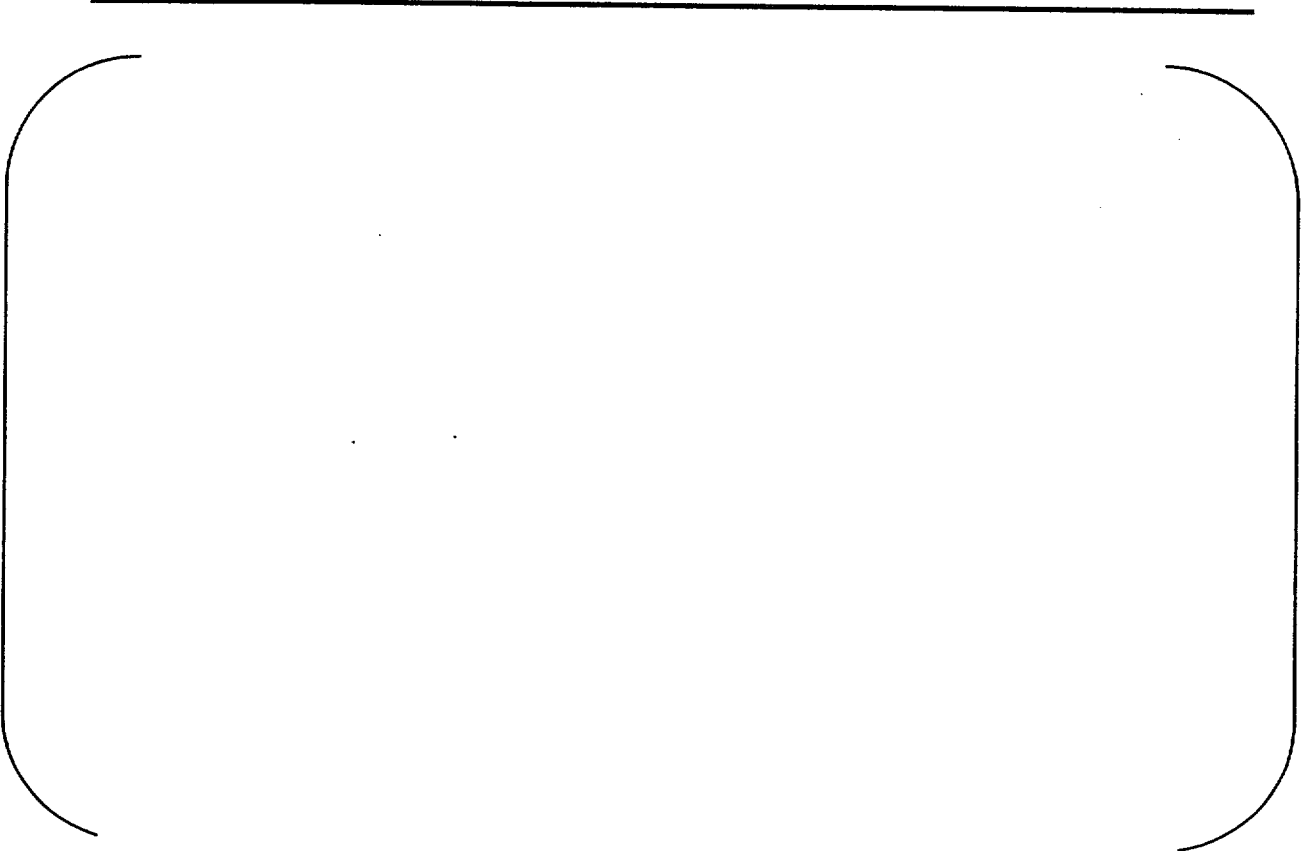


Figure B-33: BOL Fuel Centerline Temperature: IFA 562-1rod1L



Figure B-34: BOL Fuel Centerline Temperature: IFA 562-1rod5L



Figure B-35: Rod nodal power histories for the bottom node in IFA 432

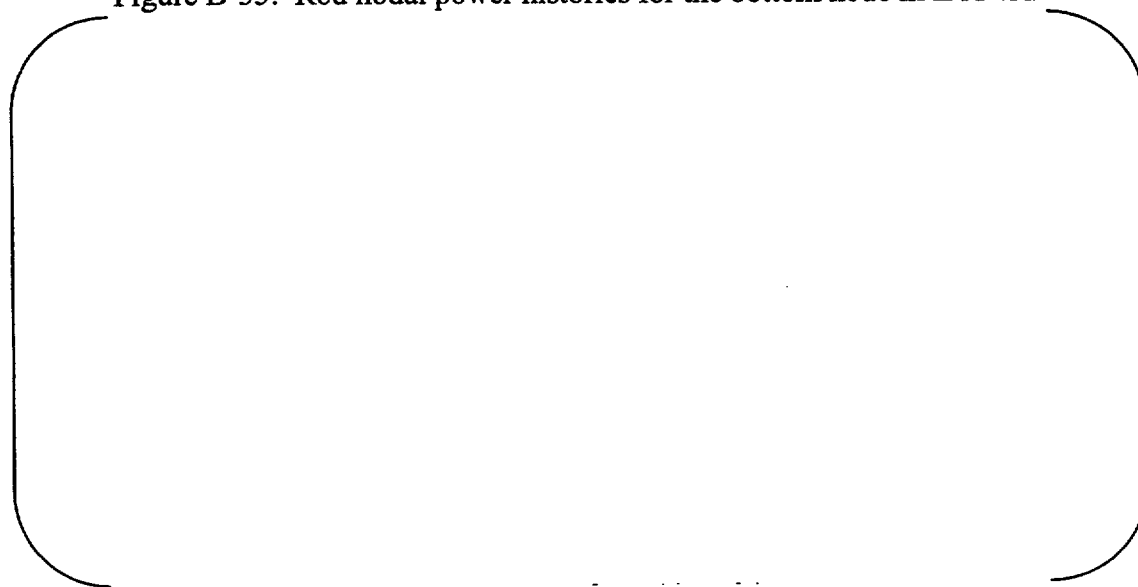


Figure B-36: Rod nodal power histories for the top node in IFA 432



Figure B-37: Rod nodal power histories for the bottom node in IFA 513

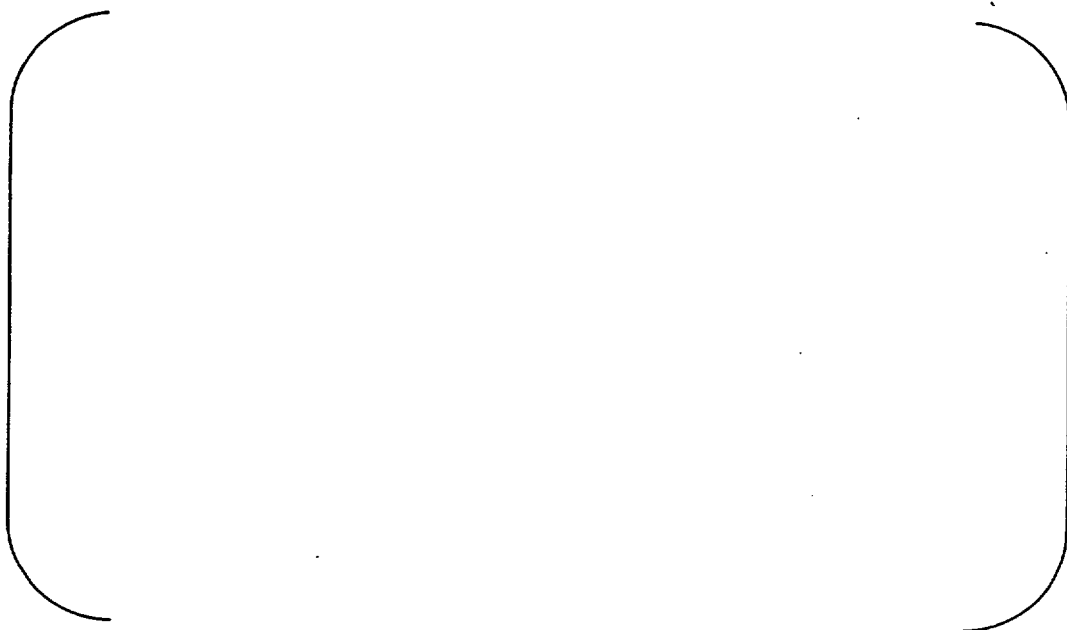


Figure B-38: Rod nodal power histories for the top node in IFA 513



Figure B-39: Rod nodal power histories for IFA 597



Figure B-40: Rod nodal power histories for IFA 515 and 562

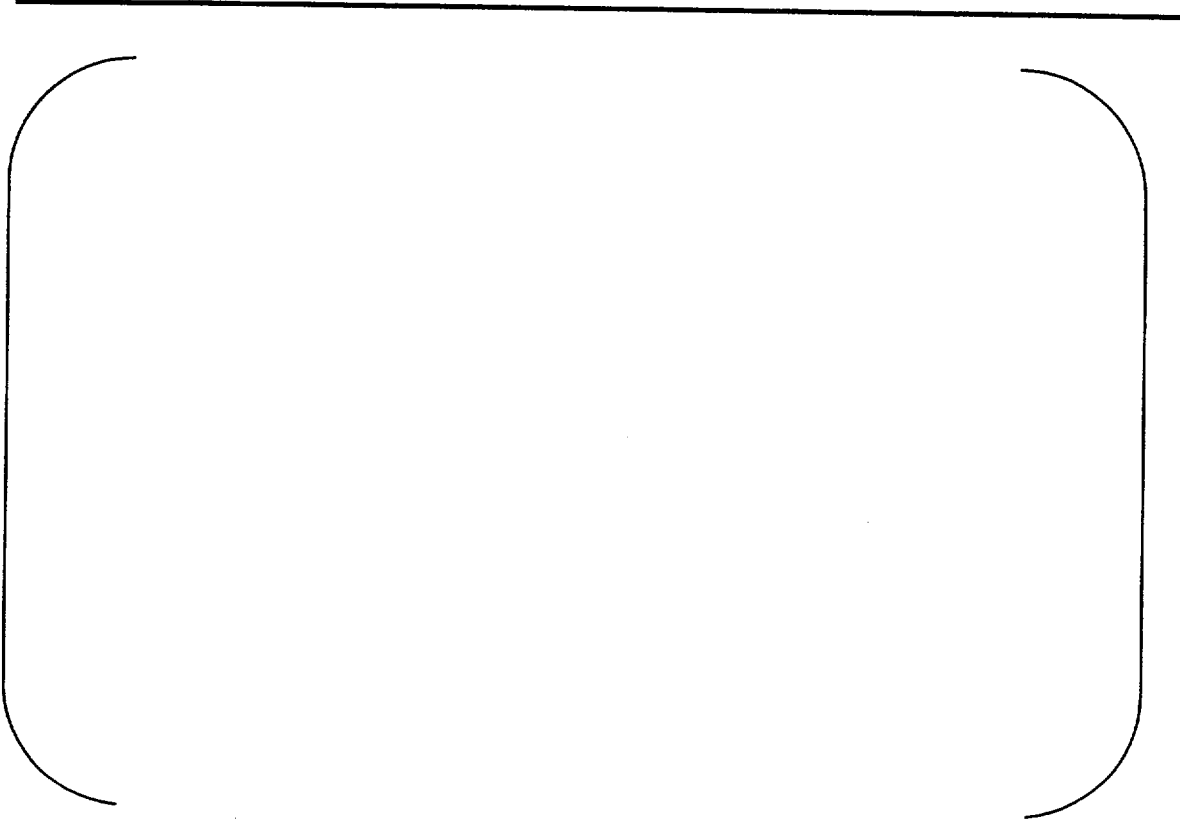


Figure B-41: Calculated and measured fission gas release vs. irradiation time for rod IFA 432-1

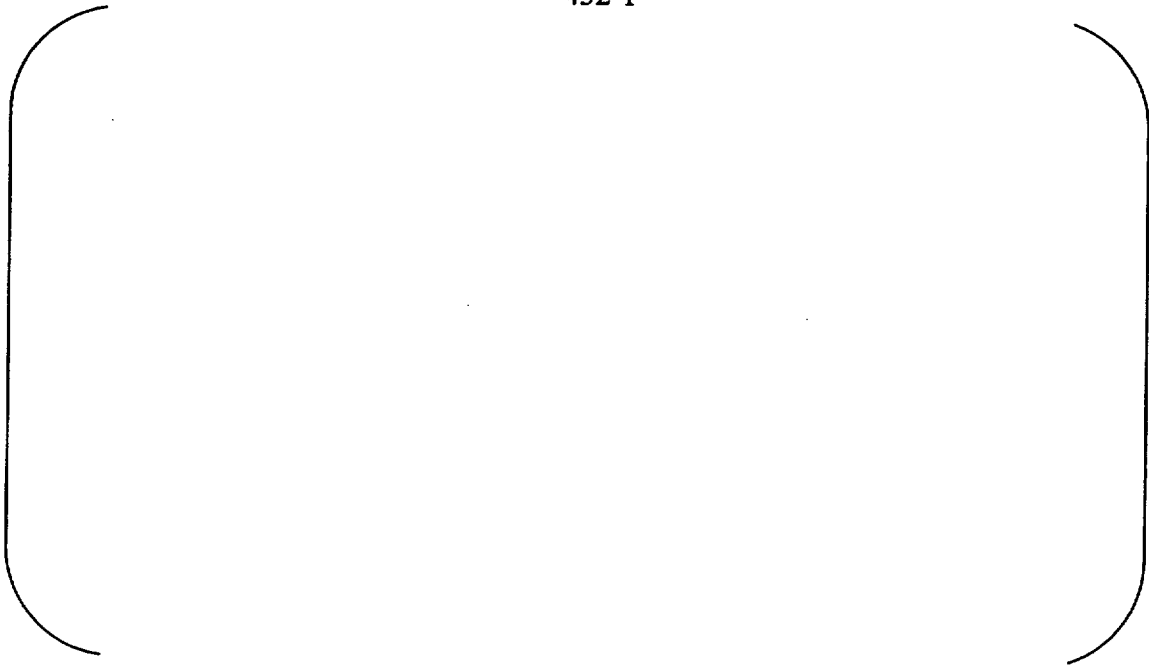


Figure B-42: Calculated and measured fuel temperature vs. irradiation time for rod IFA 432-1 at bottom node



Figure B-43: Calculated and measured fuel temperature vs. irradiation time for rod IFA 432-2 at bottom node



Figure B-44: Calculated and measured fuel temperature vs. irradiation time for rod IFA 432-3 at top node



Figure B-45: Calculated and measured fuel temperature vs. irradiation time for rod IFA 432-3 at bottom node

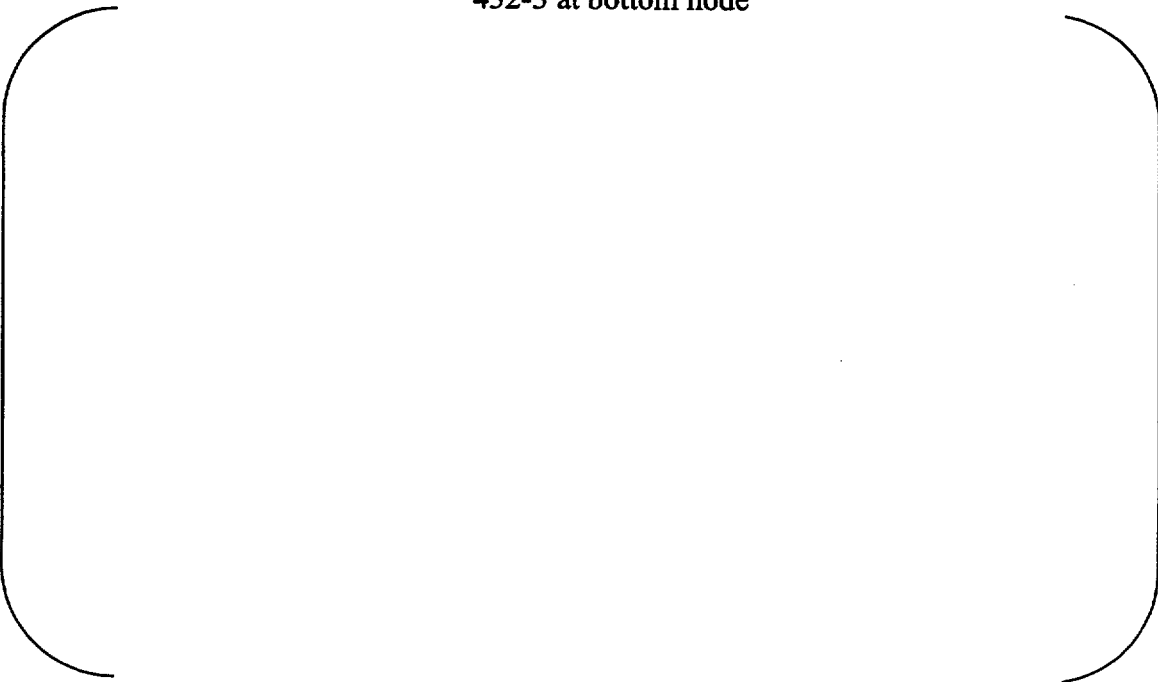


Figure B-46: Calculated and measured fuel temperature vs. irradiation time for rod IFA 432-5 at bottom node



Figure B-47: Calculated and measured fuel temperature vs. irradiation time for rod IFA 513-1 at top node

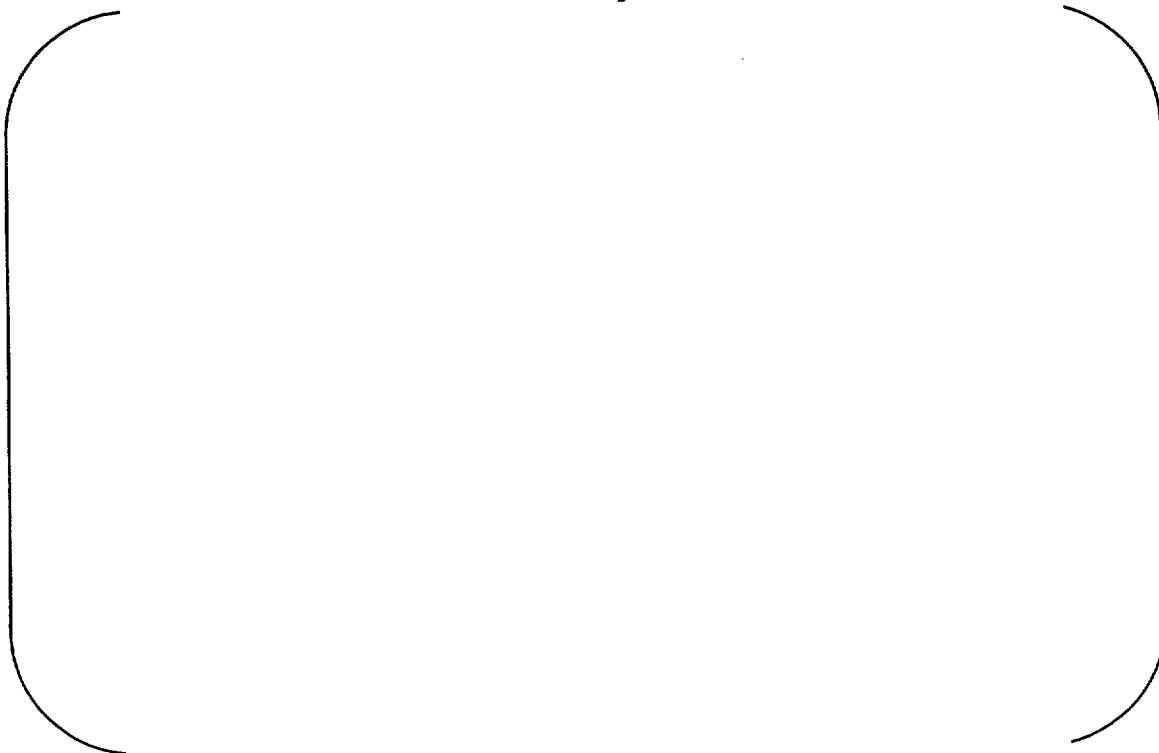


Figure B-48: Calculated and measured fuel temperature vs. irradiation time for rod IFA 513-1 at bottom node



Figure B-49: Calculated and measured fuel temperature vs. irradiation time for rod IFA 513-2 at top node

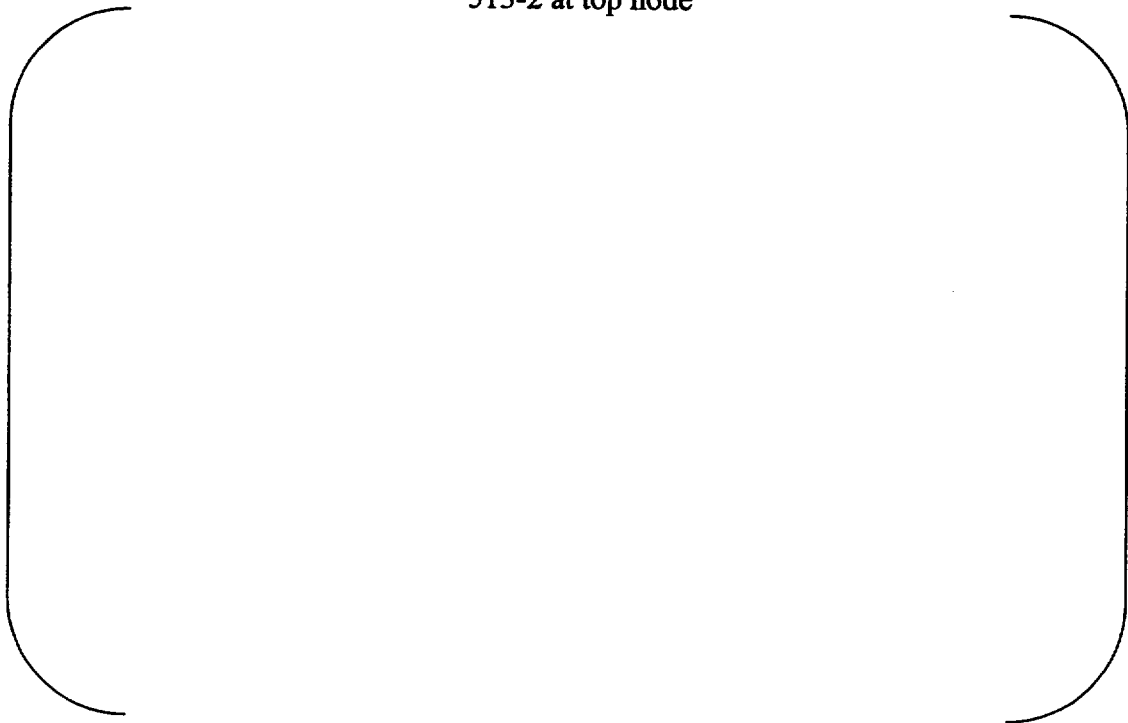


Figure B-50: Calculated and measured fuel temperature vs. irradiation time for rod IFA 513-2 at bottom node



Figure B-51: Calculated and measured fuel temperature vs. irradiation time for rod IFA 513-6 at top node

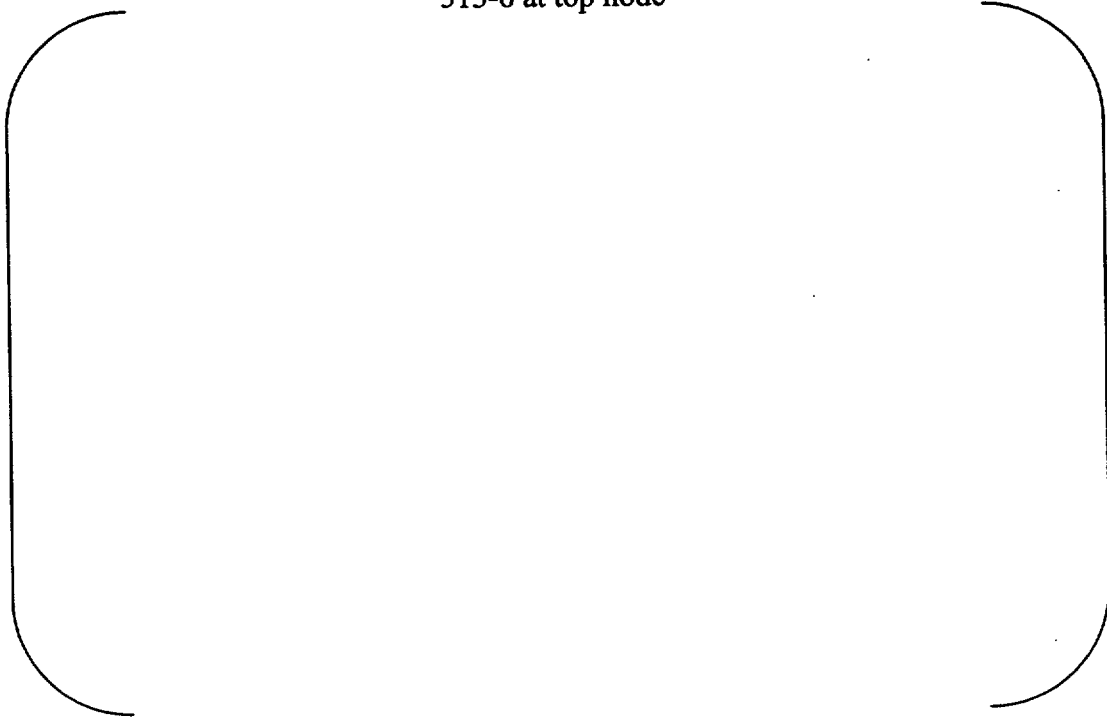


Figure B-52: Calculated and measured fuel temperature vs. irradiation time for rod IFA 513-6 at bottom node

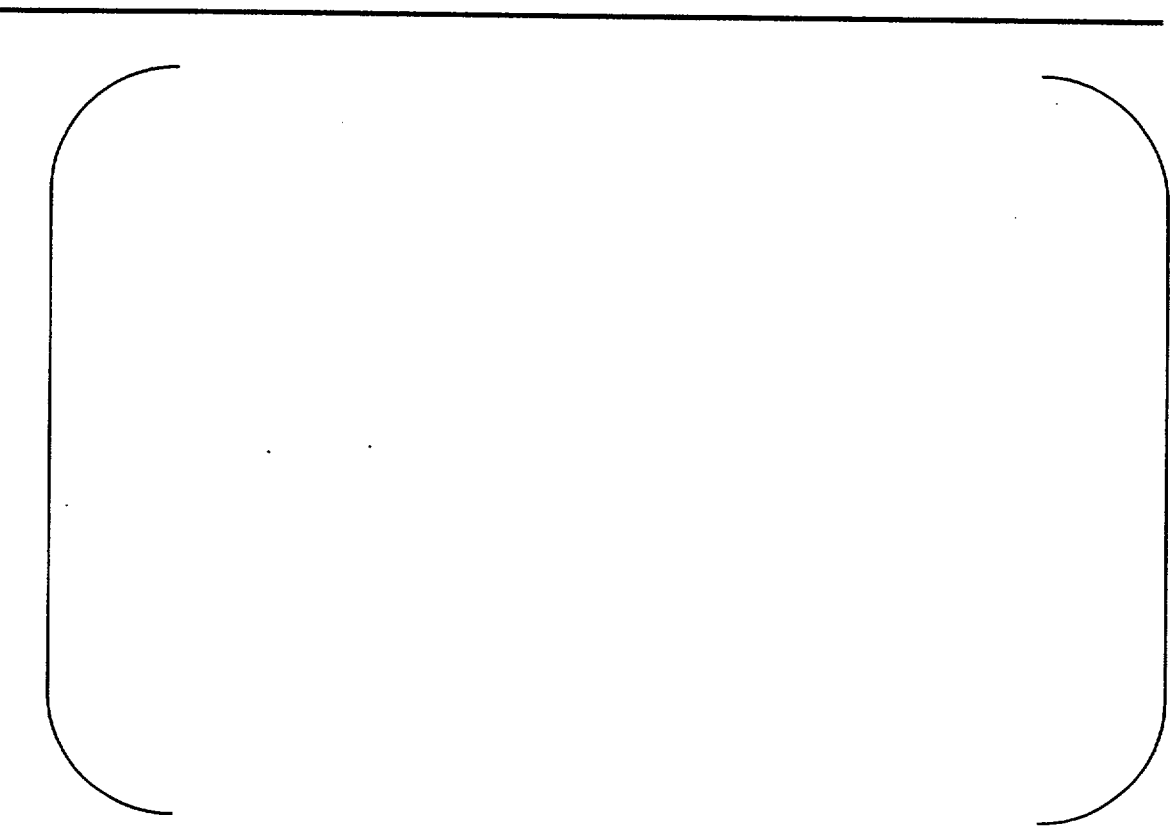


Figure B-53: Calculated and measured average fuel temperature vs. irradiation time for rod IFA 515-a1

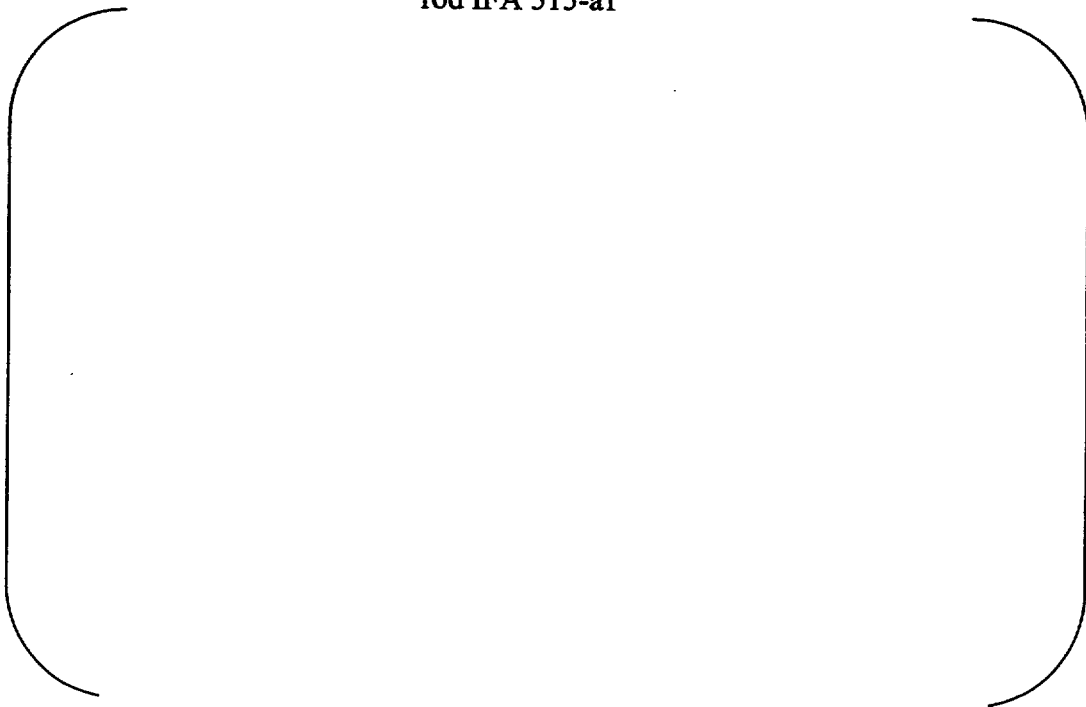


Figure B-54: Calculated and measured average fuel temperature vs. irradiation time for rod IFA 515-a2




Figure B-55: Calculated and measured average fuel temperature vs. irradiation time for rod IFA 562to4ET




Figure B-56: Calculated and measured average fuel temperature vs. irradiation time for rod IFA 597-d52-wtc



**Figure B-57: Calculated and measured fuel temperature vs. irradiation time for rod IFA
597-d53-wtc at bottom node**

APPENDIX C DATA BASE CHARACTERISTICS

The description of generalized mean values of cracked pellet gap conductance in Appendix C of Reference (1-1) applies to STAV7.2. Therefore, the information in Appendix C of Reference (1-1) is not repeated in this document.

This appendix summarizes the source of the data used for the calibration and verification of STAV7.2 in Section 3 and provides tables identifying the actual fuel rods used in the calibration and verification. The convention for fuel rod identification within an assembly is described in Figure C-1. The acronym "W-Atom" refers to Westinghouse-Atom, which is the former ABB-Atom (ASEA Atom).

C.1 Fuel Rods Irradiated in Research Reactors

C.1.1 Halden HBWR Fuel Experiments

An extensive OECD Halden Reactor Project data base of temperature measurements is available. Experiments IFA-432, IFA-504, 505, 507, 513, 515, 522, and 562 have been selected for beginning of life temperature calibration of STAV7.2. [

Through-life pellet temperature data were obtained from tests IFA-432, 513, 515, 562, and 597.]

A-504

IFA-504 is one of the most sophisticated and well-known of all Halden experiments. [

IFA-505

[]

IFA-507.1

[

]

[

]

[

]

IFA-522.1 and 522.2

[

]

IFA-562.1

[

]

[

]

IFA-432

[

]

[

]

[

]

[

]

[

]

The irradiation power histories used in the STAV7.2 calibration and verification for these rods were provided by PNL during the STAV6.2 review process.

IFA-513

[

]

Irradiation power histories used in the STAV7.2 calibration and verification for these rods were also provided by PNL for this test series during the STAV6.2 review process.

IFA-562.2-4

[

]

[

]

IFA-597.2

[

]

[

]

[

]

IFA 404.1

[

]

C.1.2 Studsvik R-2 BWR Irradiation Experiment S268/S269

[

]

[

]

[

]

[

]

[]

C.1.3 SCK/CEN BR-3

[]

The rods were operated at power levels substantially in excess of powers experienced in normal power reactor operation which resulted in very high burnups.

[]

PIE was performed at SCK/CEN hot cells in Belgium. []

C.2 Boiling Water Reactor Irradiated Rods

The BWR fuel performance data base includes fuel rods of W-Atom open lattice 8x8, SVEA-64, SVEA-100, and SVEA-96 designs on which pool-side measurements and PIE have been performed following power reactor operation.

[]

[]

[

]

Another extensive examination program was the international High Burnup Effects Program, HBEP. The HBEP was a joint project for investigating effects on fuel irradiated to high burnups. It was managed by Pacific Northwest Laboratory in the USA and co-sponsored by research institutes and fuel vendors including W-Atom. [

]

Data have also been gathered from single fuel rods irradiated in various reactors. Several of these rods were irradiated with the co-sponsorship of the W-Atom High Burnup Program (forerunner of the present W-Atom Fuel Technology Program). These data are primarily fission gas release measurements on punctured rods. A number of plenum gamma-scanning measurement campaigns to establish fission gas release have been performed within the Fuel Technology Program. Rod puncturing with associated measurements is considered to provide information more appropriate for fission gas release calibration than gamma scanning. The gamma-scanning data are only used for fission gas release verification purposes.

Finally, several rods in the data base were irradiated in [

]

C.2.1 Barsebäck 2

Barsebäck 2 Initial Core Fuel

[

]

Barsebäck 2 Reload 2

[

]

Barsebäck 2 Reload 5

[

]

C.2.2 Ringhals 1

Ringhals 1 Reloads 1 and 3A

[

]

C.2.3 Oskarshamn 2

Oskarshamn 2 Reloads 1-4

[

]

[

]

[

]

Oskarshamn 2 Reload 7

[

]

Oskarshamn 2 Reload 11

[

]

C.2.4 Oskarshamn 3

Oskarshamn 3 Reload 1

[

]

[

]

Oskarshamn 3 Reload 6

[

]

C.2.5 Forsmark 3

Forsmark 3 Reload 3

[

]

Forsmark 3 Reload 2

[

]

C.2.6 Olkiluoto 1

Olkiluoto 1 Reloads 1 and 3

[

]

Olkiluoto 2 (OL2) Reload 8

[

]

C.2.7 Leibstadt

[

]

C.3 Pressurized Water Reactor Irradiated Rods

The Westinghouse PWR data base includes data obtained by W-Atom, Westinghouse, and the former Combustion Engineering. Data include poolside measurements and PIE of Westinghouse 17x17 rods irradiated in Surry as well as earlier designs such as 15x15

and 14x14 irradiated in the Zion, Zorita and Saxton plants. Extensive pre-characterization, measurements in the course of irradiation and PIE make the data highly qualified for calibration and validation use. The CE 14x14 fuel rods included in the data base were irradiated in Calvert Cliffs, Unit 1.

C.3.1 Ringhals 3 and 4

[

]

Some of the fuel rods were subjected to irradiation in experimental reactors. For example, two rods were included in the ZODIAC post-irradiation examination project, one rod was irradiated in the ROPE-II project after prefabrication, and two of the eight stringer rods were analyzed after power ramping in Studsvik.

C.3.2 Surry

[

]

[

]

[

]

[

]

C.3.3 Zion

[]

[]

[]

[]

[]

[]

[]

[]

C.3.4 Zorita

The Zorita PWR Research and Development Program was initiated in 1966 as a joint venture between Westinghouse, Union Electrica Madrilenia S A (UESA), and Junta de Energia Nuclear (JEN). The program objective was to demonstrate improved fuel rod designs for high-power and high-burnup application. []

Irradiation took place in the Jose Cabrera (Zorita) reactor owned and operated by UESA. JEN provided hot cell facilities for both non-destructive and destructive examinations. []

[]

[]

[]

The Zorita fuel rods are of an early design and manufacture. []

[]

C.3.5 Saxton

[

]

C.3.6 Calvert Cliffs 1

[

]

C.4 Power Ramp Data Base

A relatively substantial data base obtained from various power ramp tests on BWR and PWR rods made in test reactors are available for evaluation. In particular, the fission gas release data obtained from these tests were used to calibrate and verify the transient fission gas release model in STAV7.2. The tests providing these data can be summarized as follows:

- The Studsvik Inter-Ramp project
- The Studsvik Over-Ramp project
- The Studsvik Super-Ramp project
- The Risö Transient Fission Gas Release project
- The Third Risö Fission Gas Release project

C.4.1 Studsvik Inter-Ramp Project

The Studsvik Inter-Ramp project was intended to investigate fuel behavior in general and the propensity for failure of unpressurized 8x8 BWR fuel rods when subjected to fast transients in particular. [

Following this irradiation, the rods were subjected to power ramps in pressurized water loops. Post irradiation examinations were performed at the hot cell laboratory at Studsvik.

[

]

[

]

[
]
Destructive examination of the rods included fission gas release measurements. [
]

C.4.2 Studsvik Over-Ramp Project

The objective of the Studsvik Over-Ramp project was to experimentally investigate fuel rod behavior in general and the propensity for failure of typical PWR fuel rods caused by pellet-cladding interaction when subjected to power transients in particular.

[
]
]
]
]
]
]
]
]

C.4.3 Studsvik Super-Ramp Project

The primary objective of the Studsvik Super-Ramp project was to experimentally investigate fuel rod behavior in general with particular focus on understanding the failure

mechanism caused by pellet-cladding interaction when subjected to power transients. The test rods in the Super-Ramp program were initially irradiated to relatively high burnups in commercial BWR and PWRs. [

]

[

]

(

)

[

]

The Westinghouse test rods consisted of two groups with the following primary characteristics:

(

)

[

]

The power ramping of the test rods was performed in the Studsvik R2 reactor in the pressurized water loop with forced-circulation cooling simulating PWR coolant temperature and pressure conditions. [

]

[

]

C.4.4 The Risö Transient Fission Gas Release Project

The principal objective of the Risö Transient Fission Gas Release Project (Risö 2) was to investigate experimentally the kinetic behavior of fission gas release during power transients for UO₂ fuel. The fuel was initially irradiated in a BWR to sufficiently high burnup. In addition, a project goal was to provide detailed characterization of local fission product gas distribution and fuel structure. Such data are useful for validation of fuel performance codes and the formulation of appropriate models for fission gas release during power transients.

[

]

[

]

C.4.5 The Third Risö Fission Gas Release Project

The first two Risö projects generated a comprehensive base data for transient behavior of fission gas releases up to a fuel burnup of about 44 MWd/kgU. At the time of the first two Risö projects, technology for direct measurement of the fuel temperature during a power transient for fuel that had been irradiated to significantly burnup in a power reactor did not exist.

Previously irradiated power reactor fuel was re-fabricated into test fuel pins that were instrumented with pressure transducers and fuel thermocouples for the Third Risö Fission Gas Release Project (FGP3). This enabled continuous monitoring of fission gas release and fuel temperature during power transients. As in the previous Risö 2 projects, extensive hot cell examinations before and after testing provided detailed local fission product distribution and fuel structure data.

[

]

(1) [

]

(2) [

]

(3) [

]

[

]

[

]

The destructive examination of the rods included fission gas release measurements.

**Table C-1: Beginning-of-life Center line Temperature Calibration Data Base
from the Halden Test Reactor**

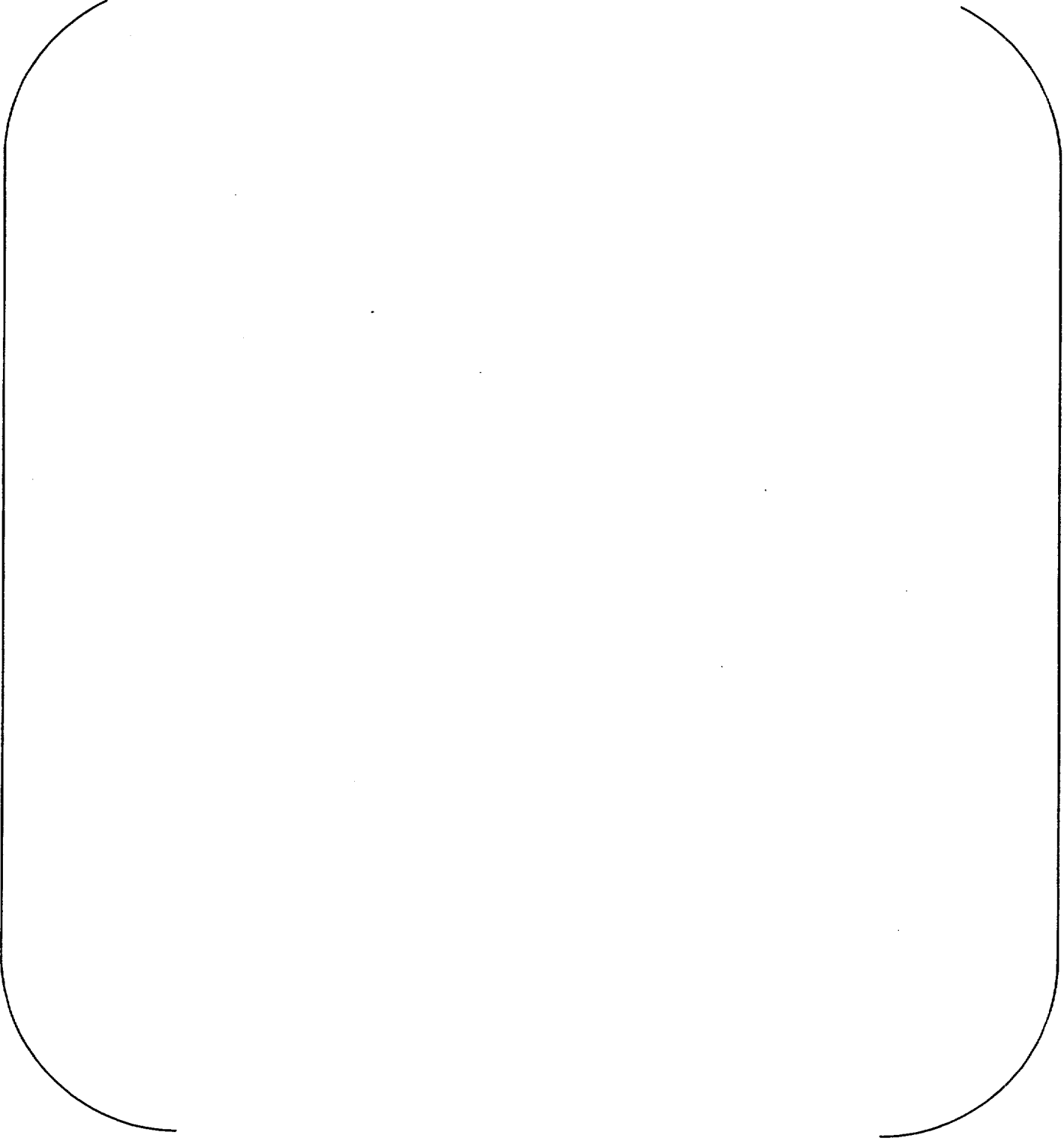


Table C-2: In-Life Temperature Verification Data

A large, empty rounded rectangular frame, likely intended for a table or figure, but currently blank.

Table C-3: BWR Calibration Data Base and Results

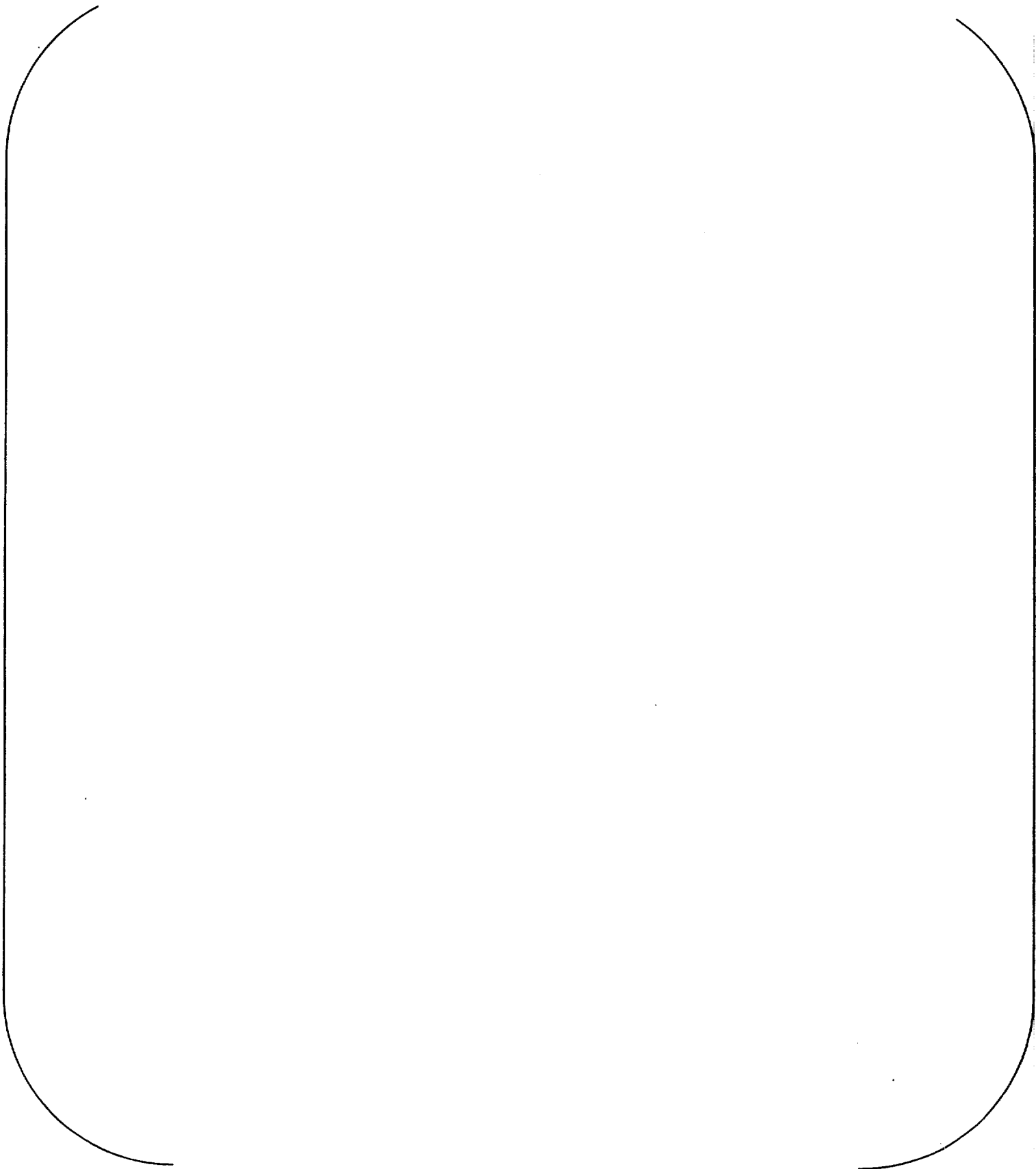


Table C-3: BWR Calibration Data Base and Results (continued)

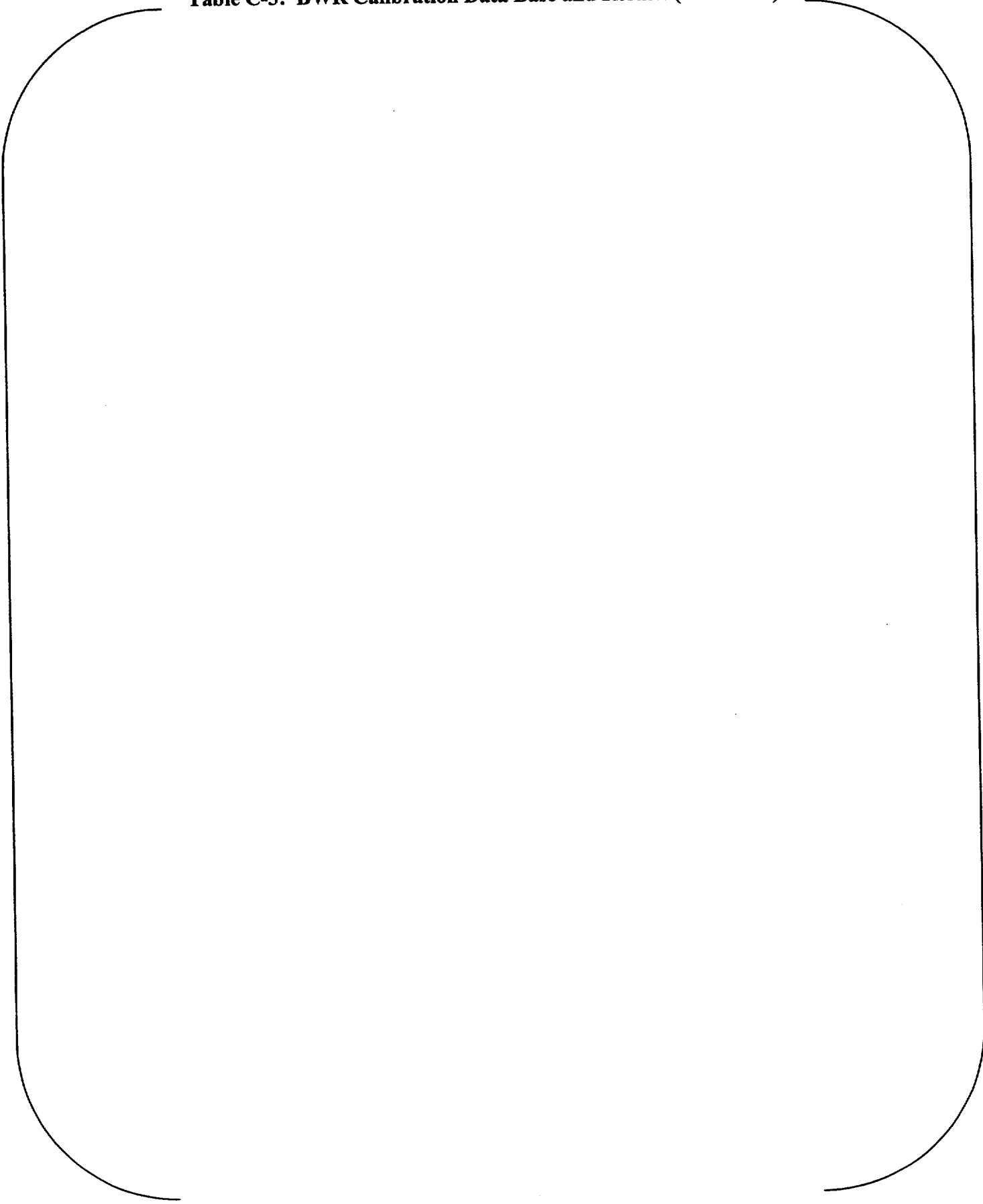


Table C-3: BWR Calibration Data Base and Results (continued)

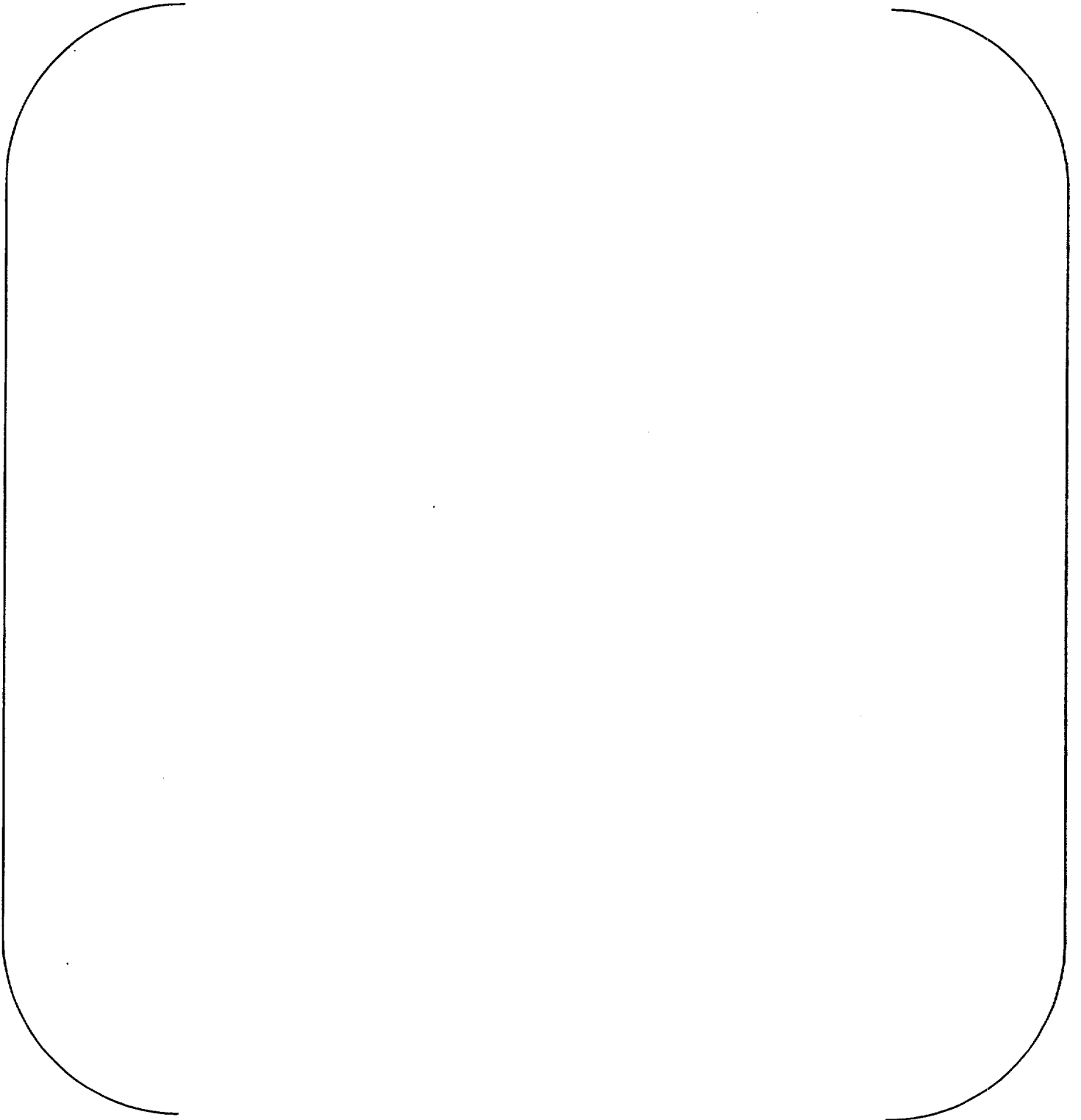


Table C-3: BWR Calibration Data Base and Results (continued)

Table C-4: PWR Calibration Data Base and Results

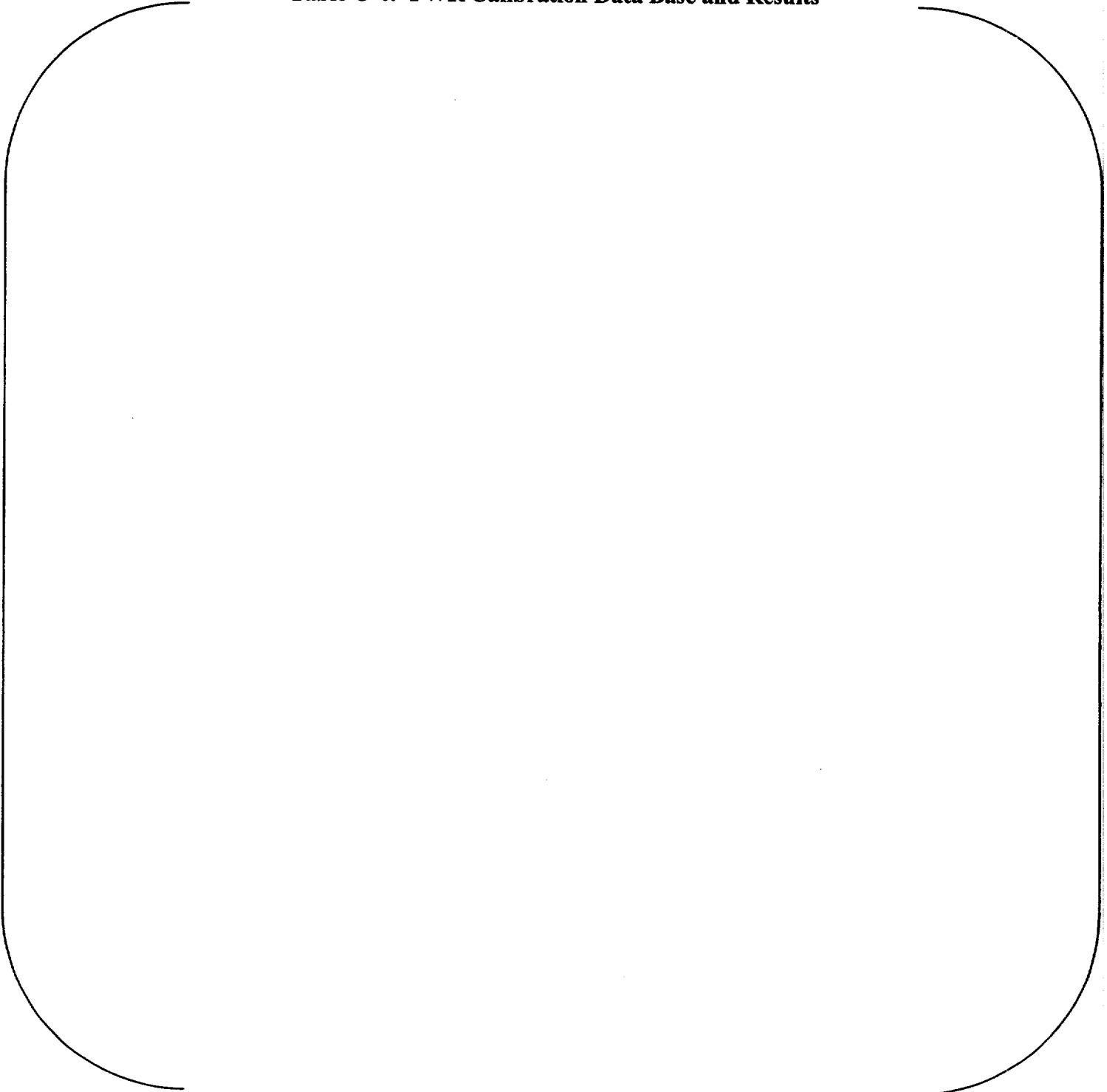


Table C-4: PWR Calibration Data Base and Results (continued)

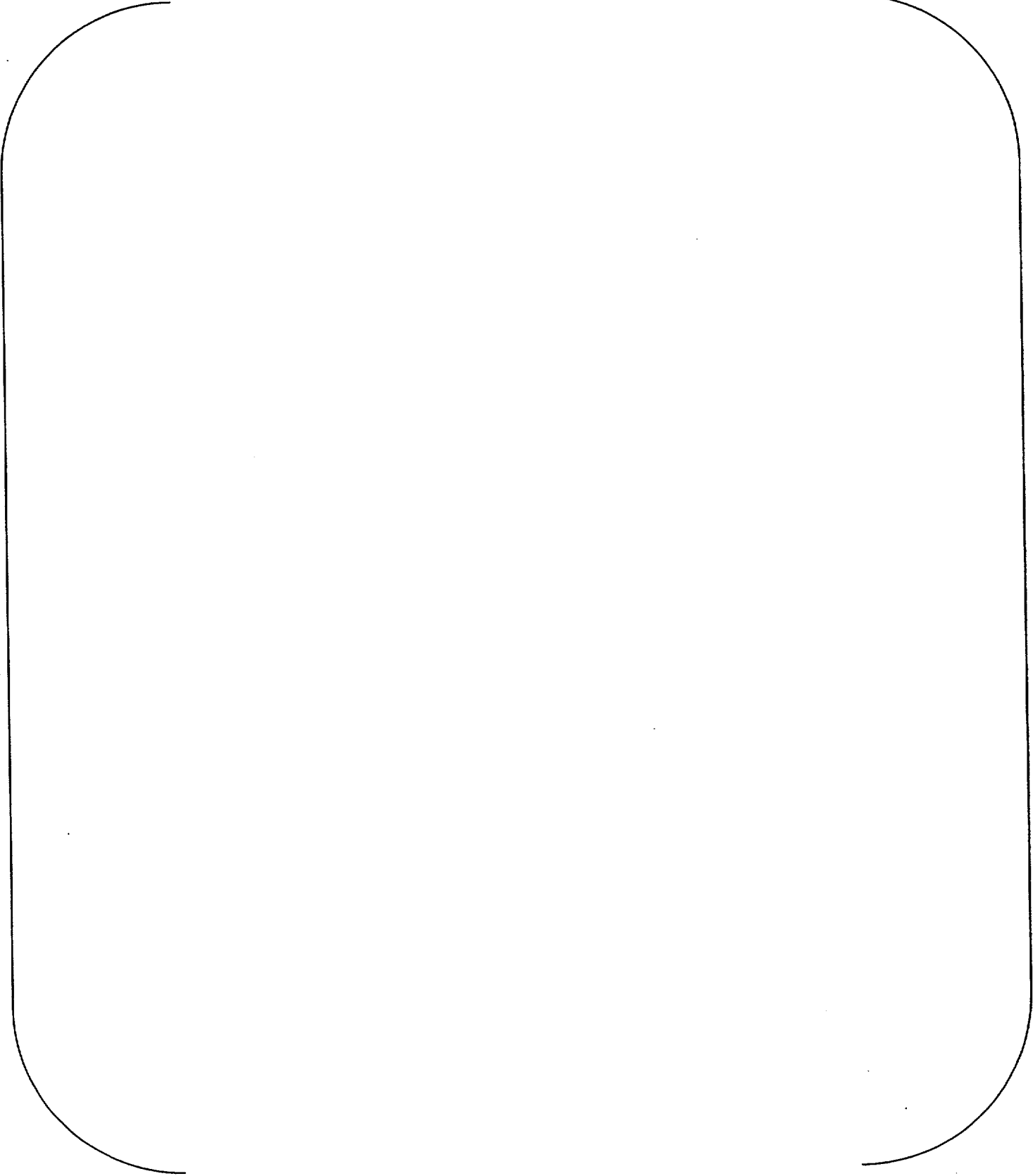


Table C-5: BWR Verification Data Base and Results

Table C-5: BWR Verification Data Base and Results (continued)

Table C-6: PWR Verification Data Base and Results

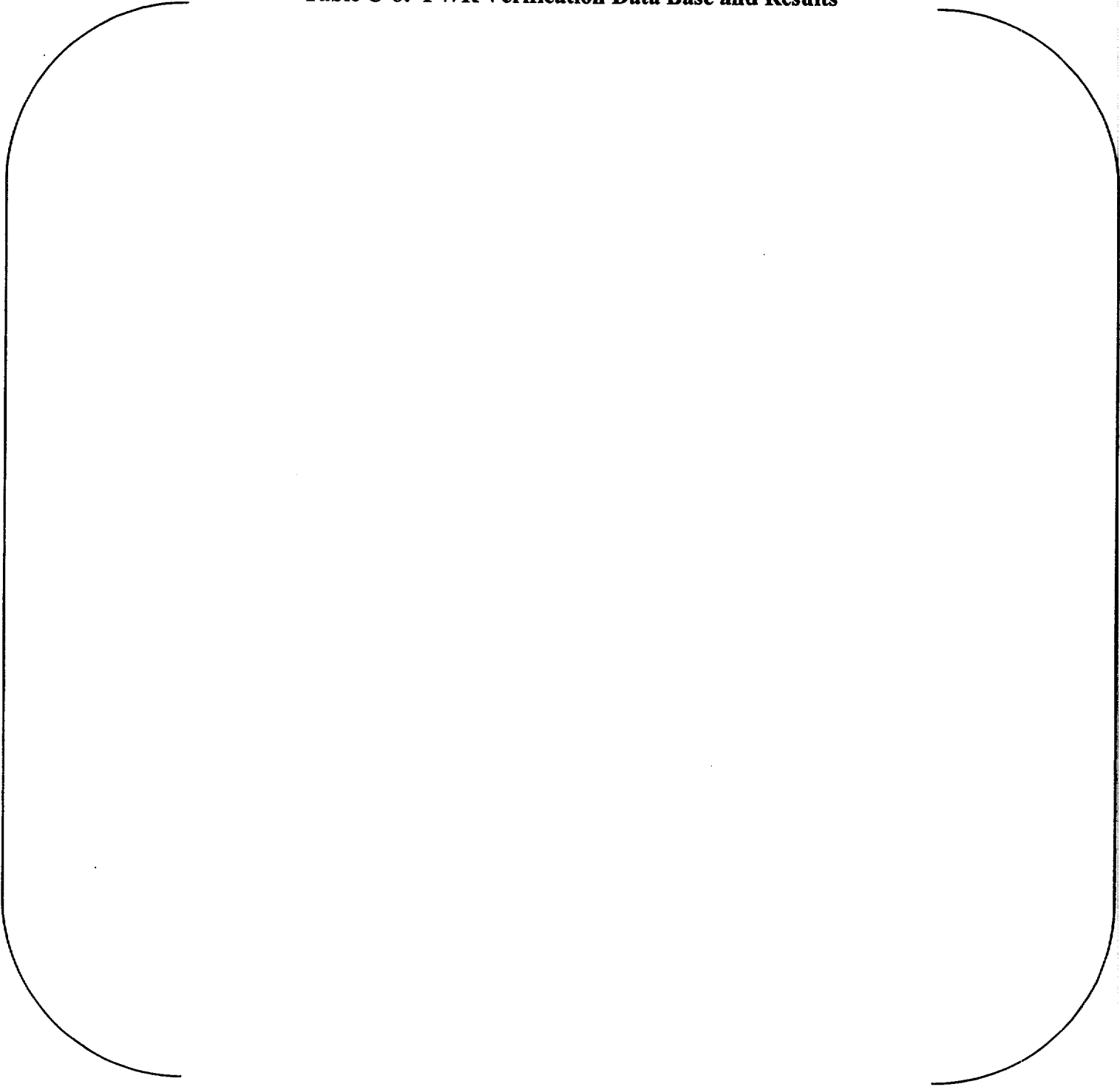


Table C-6: PWR Verification Data Base and Results (continued)



Table C-7: BWR Older 8x8 Assemblies

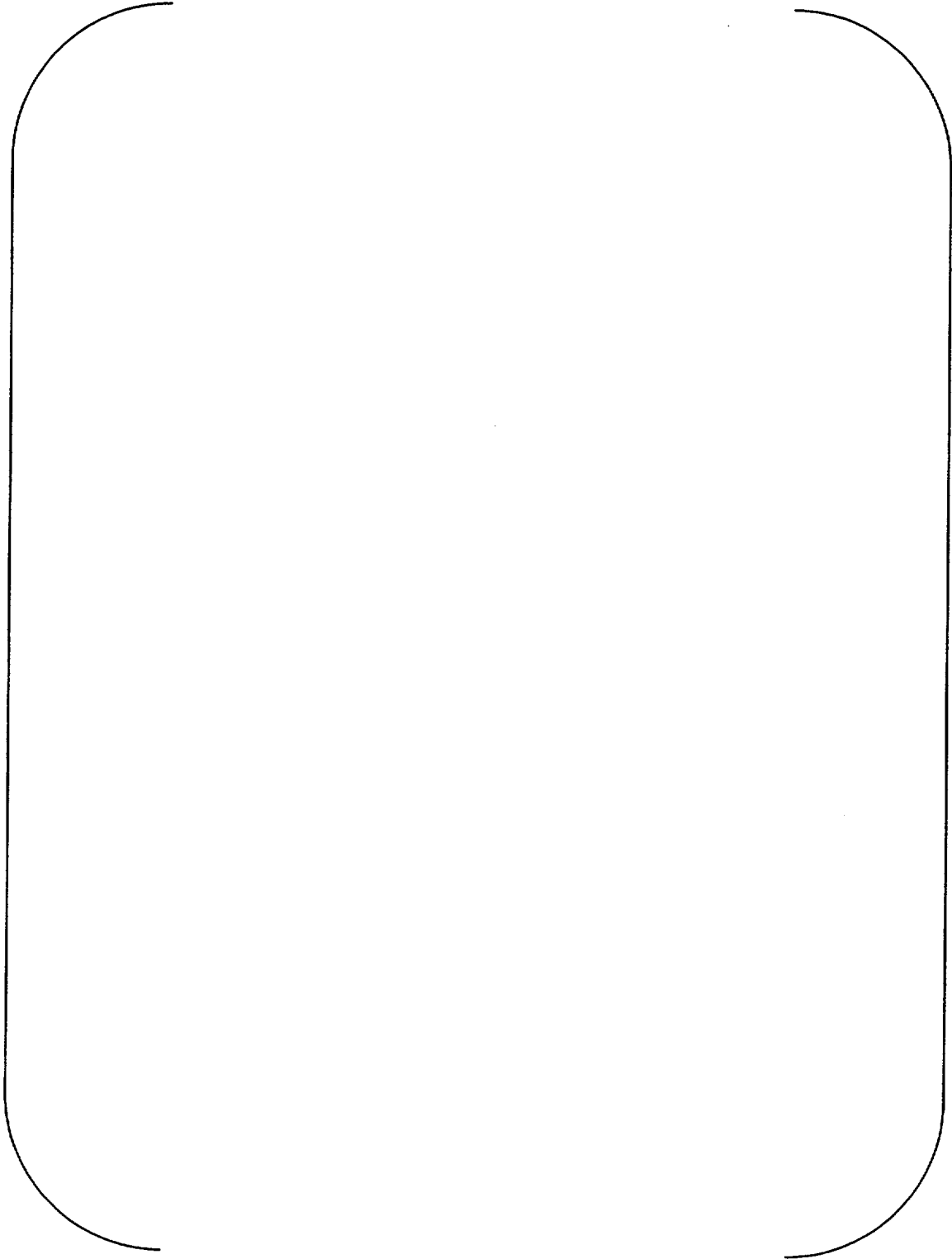
A large, empty rounded rectangular frame with a thin black border, occupying most of the page. It is intended for the content of Table C-7.

Table C-8: Transient FGR Data Base and Results

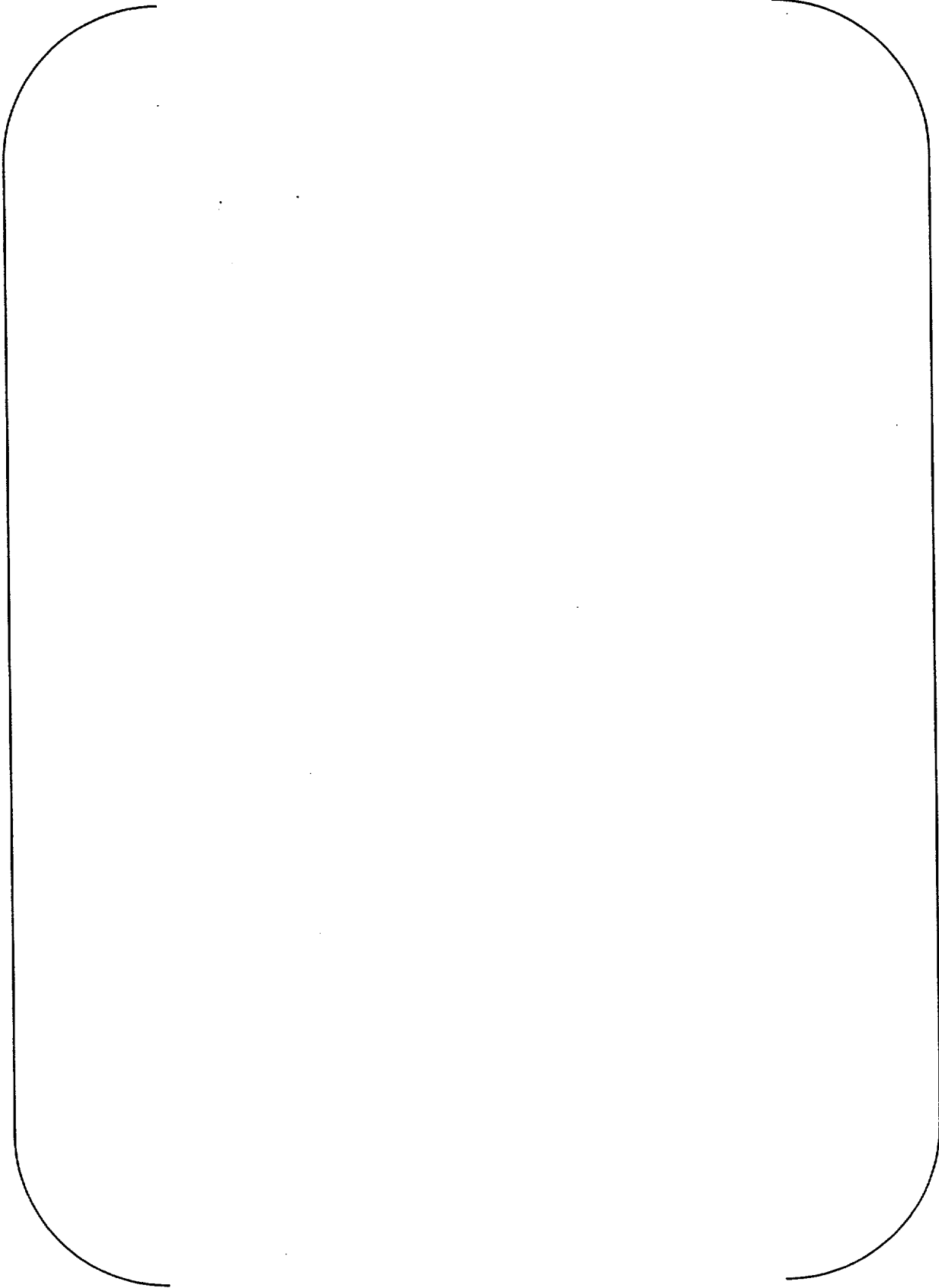


Table C-8: Transient FGR Data Base and Results (continued)

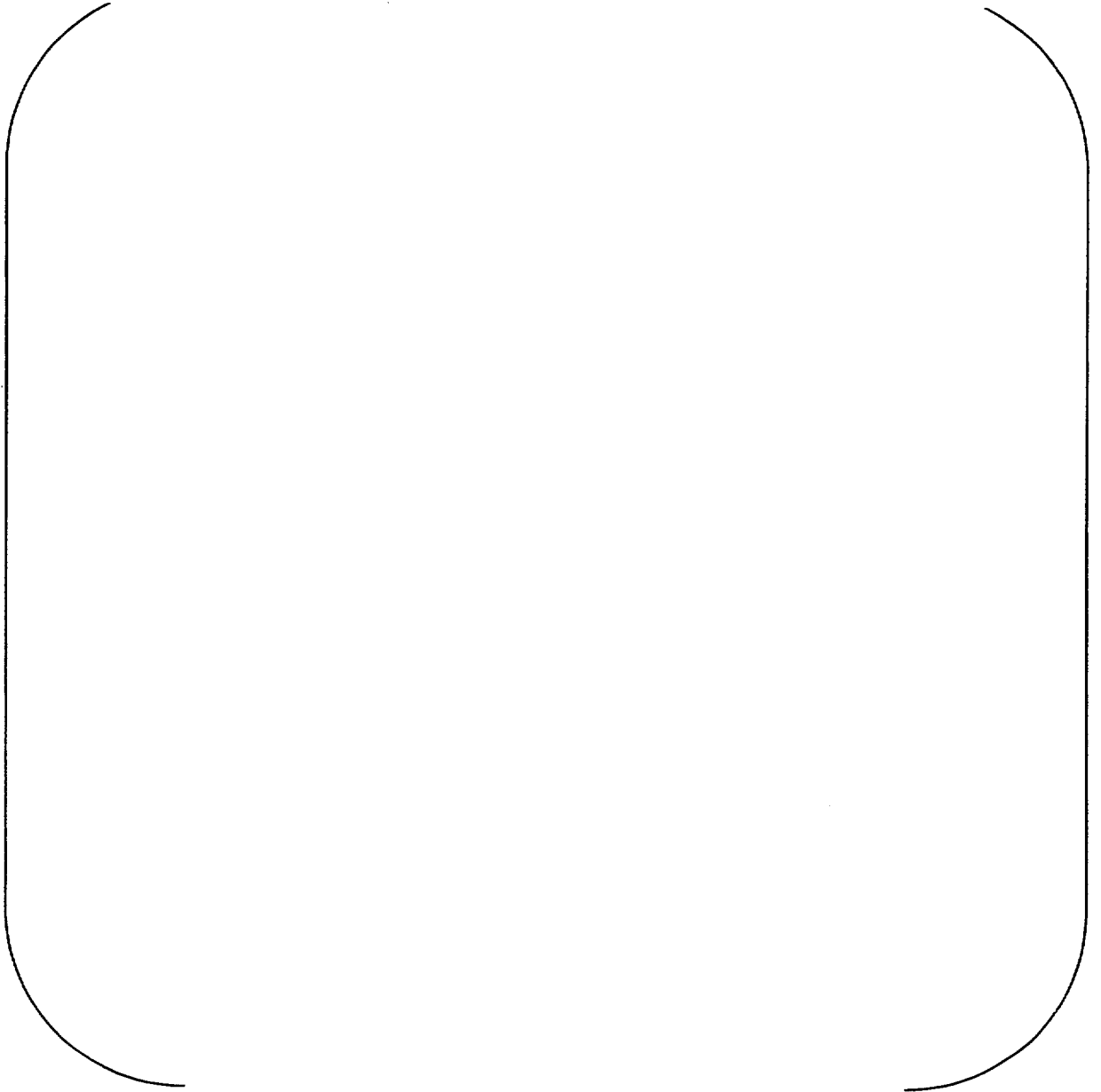
A large, empty rounded rectangular frame that occupies most of the page. It is defined by a single black line with rounded corners at the top and bottom. The interior of the frame is completely blank, suggesting that the table content has been omitted or is otherwise unavailable.

Table C-9: BWR Cladding Creep Verification

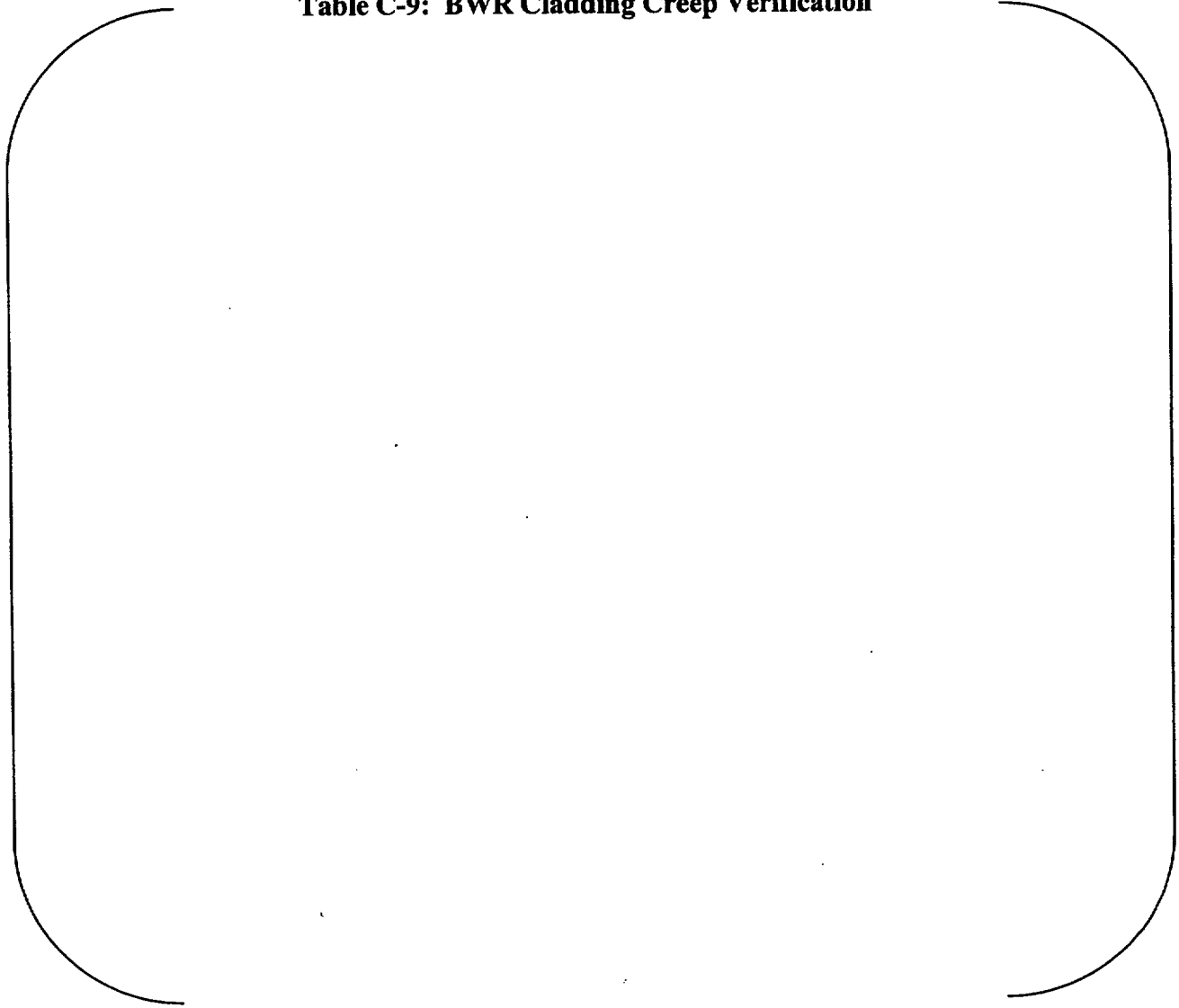
A large, empty rounded rectangular frame with a thin black border, centered on the page. It is intended for the content of Table C-9.

Table C-10: BWR Cladding Creep Verification in Studsvik Test Reactor

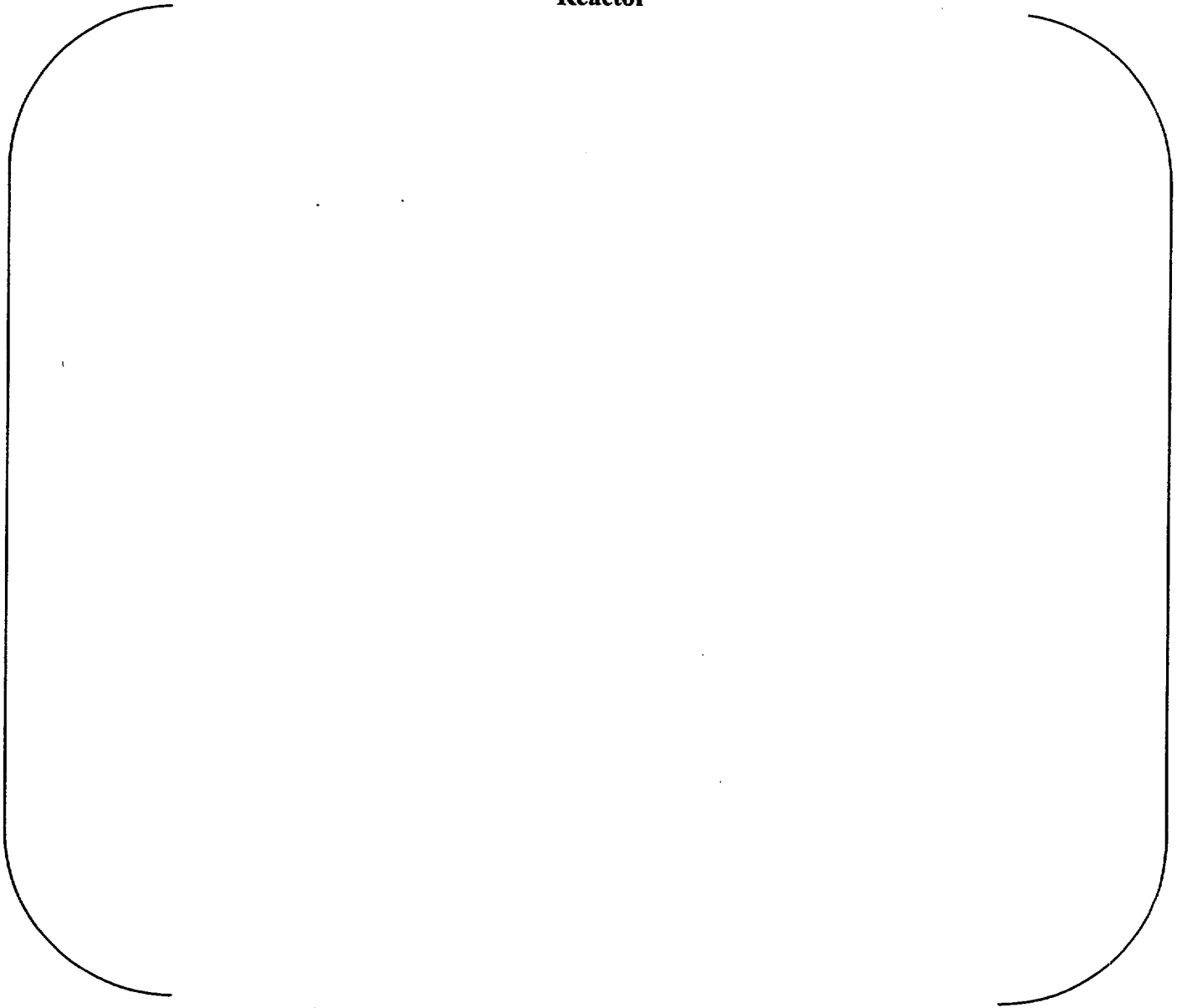
A large, empty rounded rectangular frame with a thin black border, occupying the central portion of the page. It is intended for the content of Table C-10.

Table C-11: PWR Cladding Creep Verification

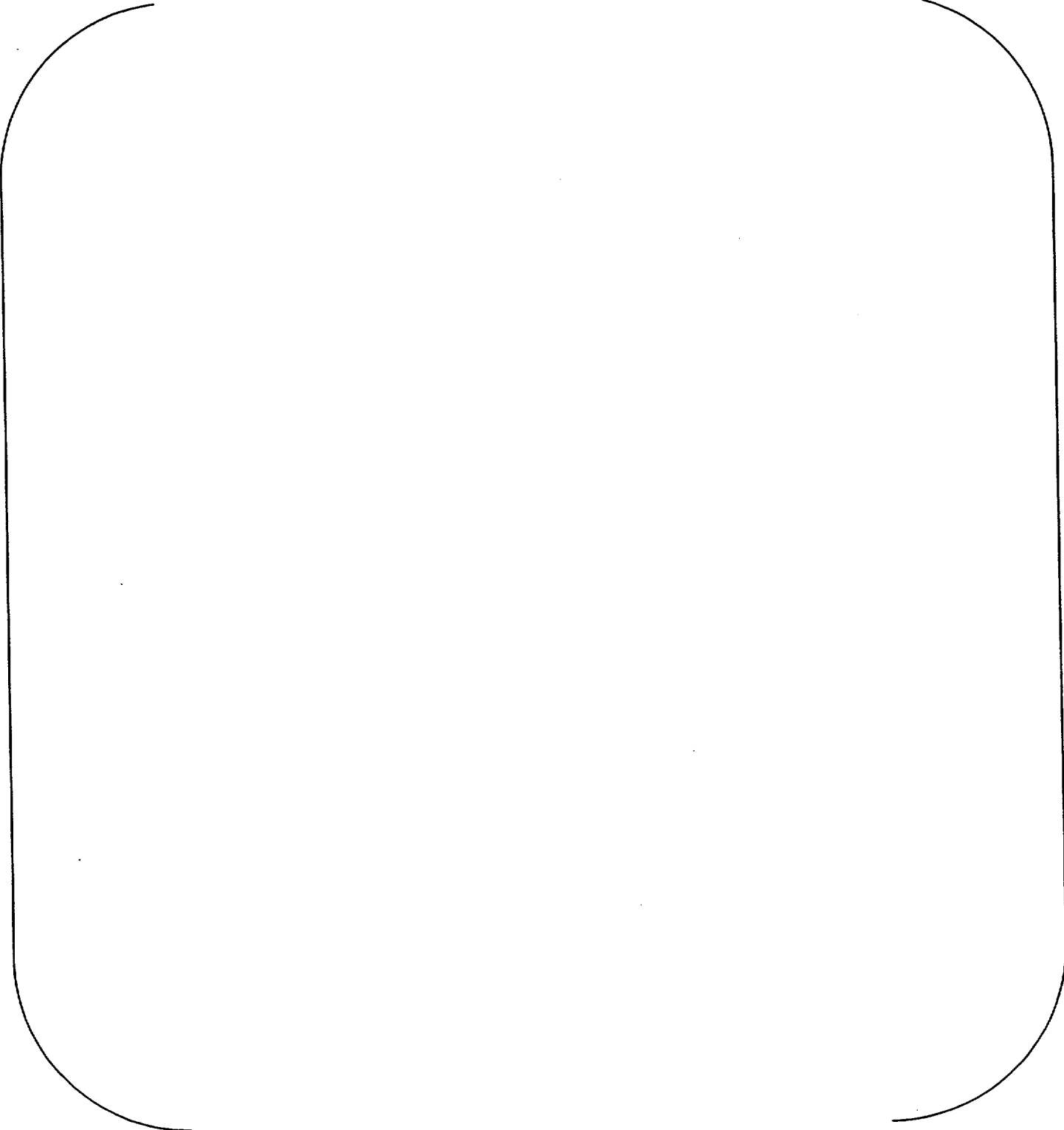
A large, empty rounded rectangular frame with a thin black border, occupying most of the page. It is intended for the content of Table C-11.

Table C-11: PWR Cladding Green Verification (continued)

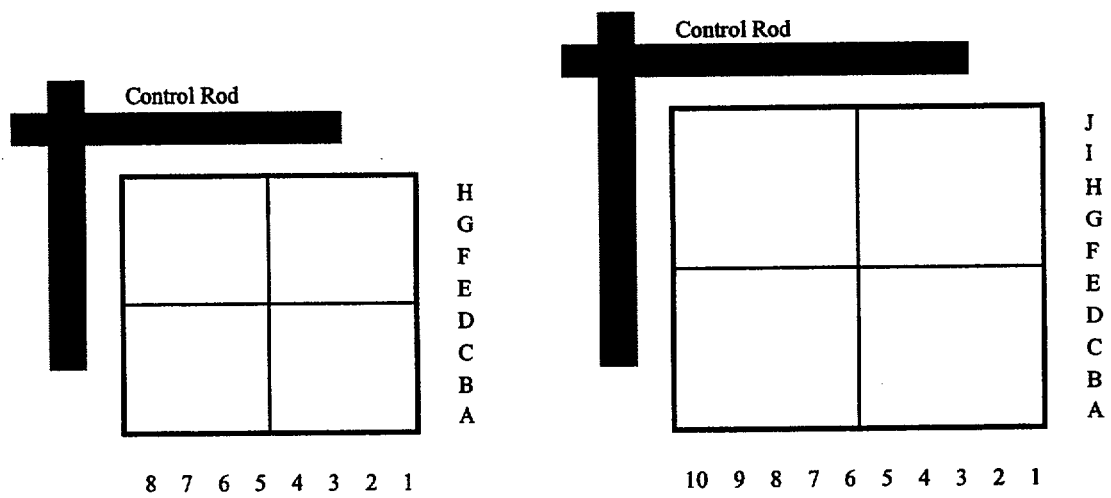


Figure C-1: Rod Positions Designations for 8x8 (including SVEA-64) and 10x10 Westinghouse BWR Fuel

APPENDIX D BWR FUEL ROD POWER HISTORIES

This appendix contains the BWR fuel rod power histories supporting the calibration and verification calculations in Section 3.

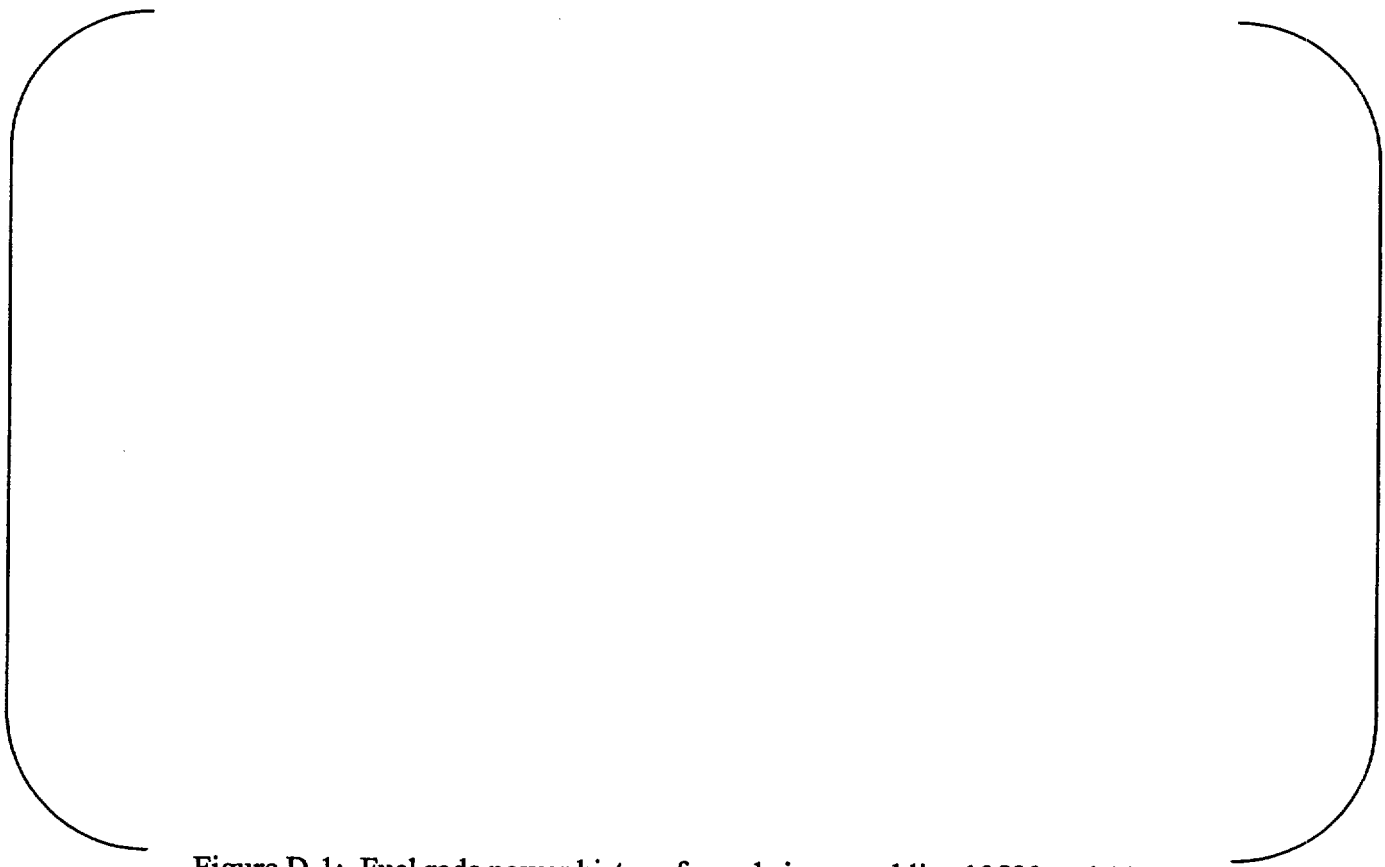


Figure D-1: Fuel rods power history for rods in assemblies 10580 and 10624

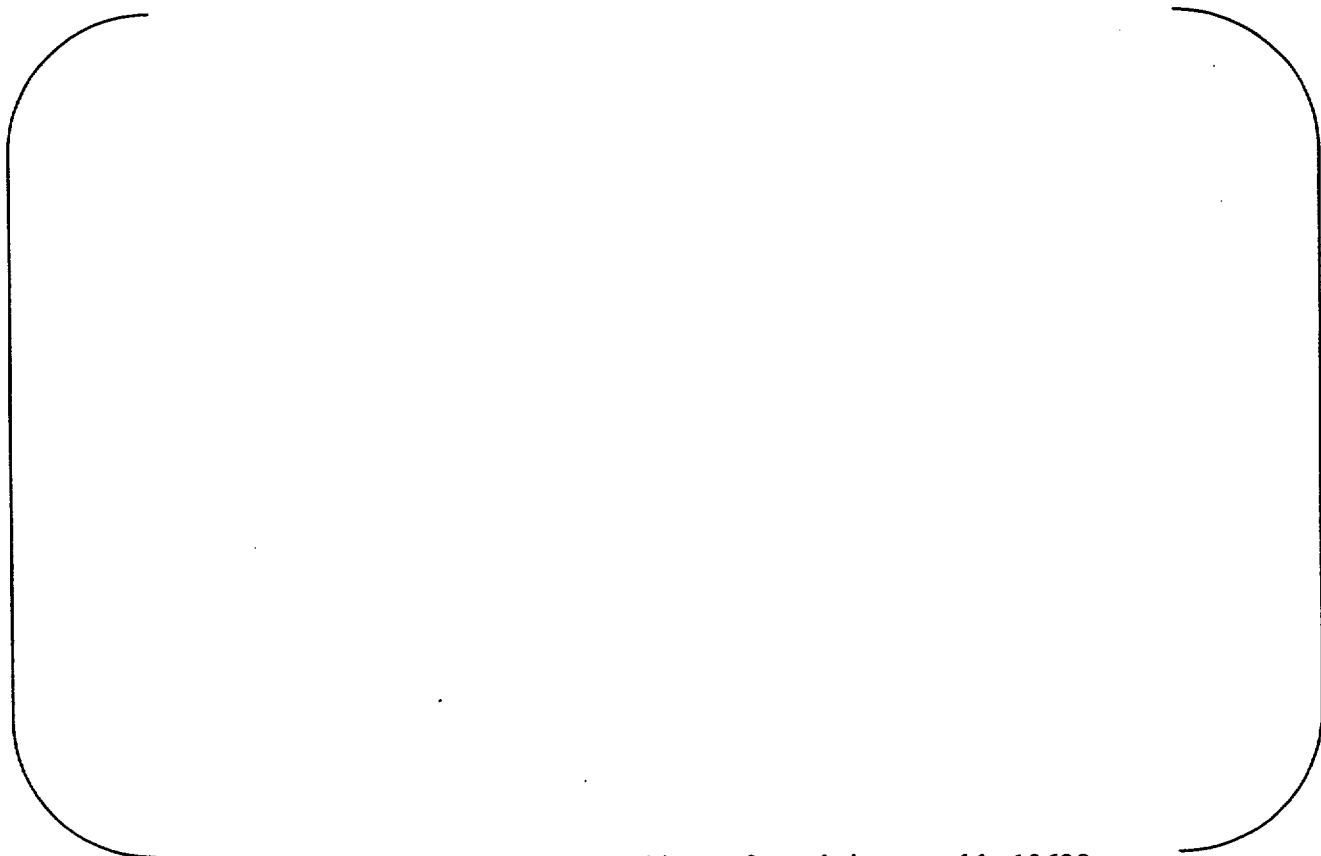


Figure D-2: Fuel rods power history for rods in assembly 13629

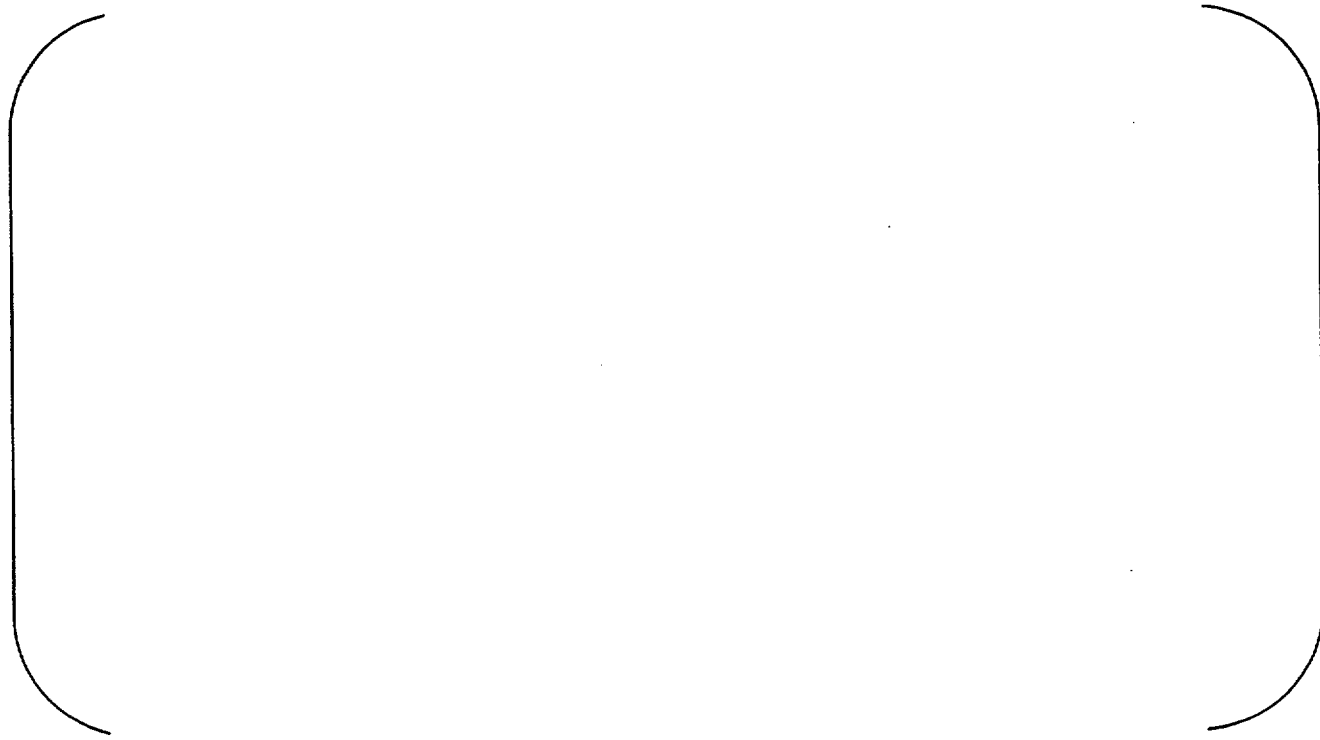


Figure D-3: Fuel rods power history for rods in assembly 14595



Figure D-4: Fuel rods power history for rods in assembly 14695



Figure D-5: Fuel rods power history for rods in assembly 14713



Figure D-6: Fuel rods power history for in assembly 14735



Figure D-7: Fuel rods power history for rods in assembly 14740




Figure D-8: Fuel rods power history for rods in assembly 15466

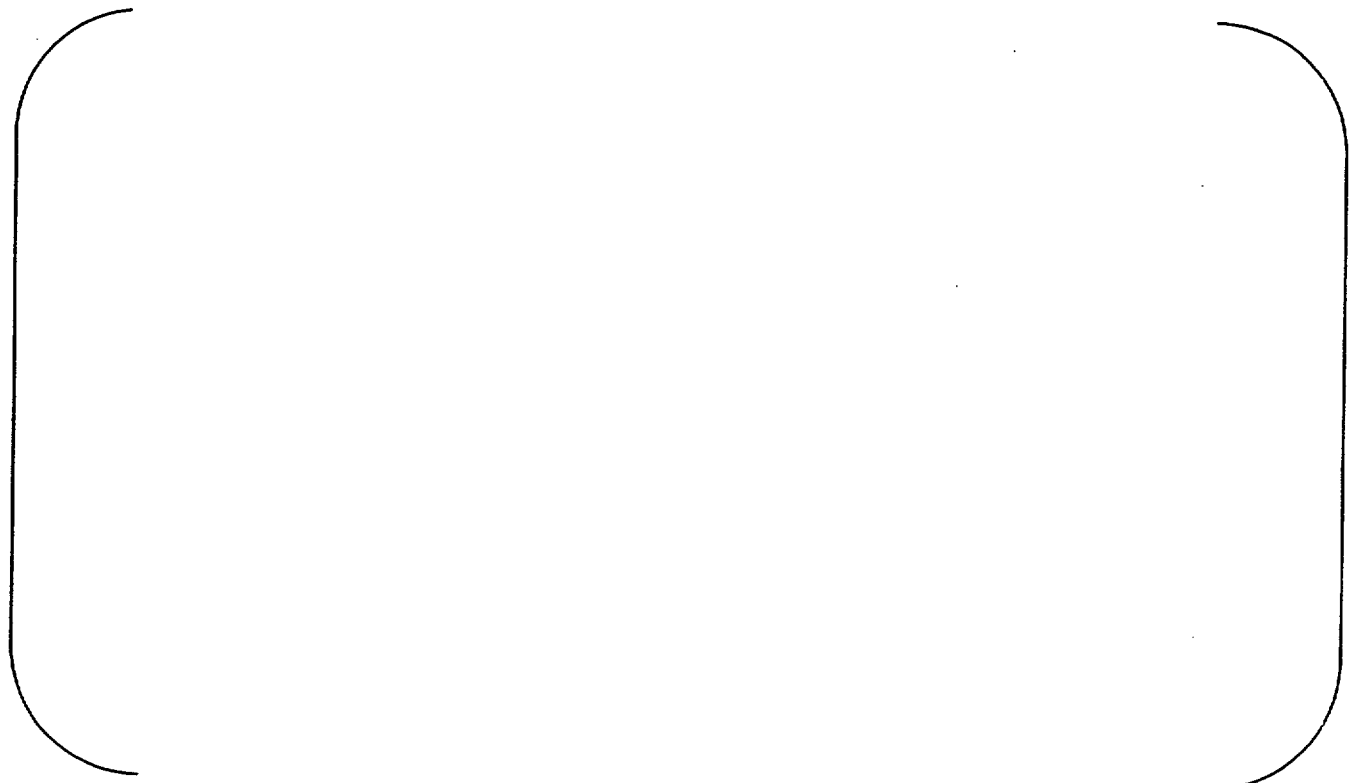


Figure D-9: Fuel rods power history for rods in assembly 15581



Figure D-10: Fuel rods power history for rods in assembly 15582



Figure D-11: Fuel rods power history for rods in assembly 15586



Figure D-12: Fuel rods power history for rods in assemblies 2538, 2818, 17684 and 17745



Figure D-13: Fuel rods power history for rods in assembly 20461

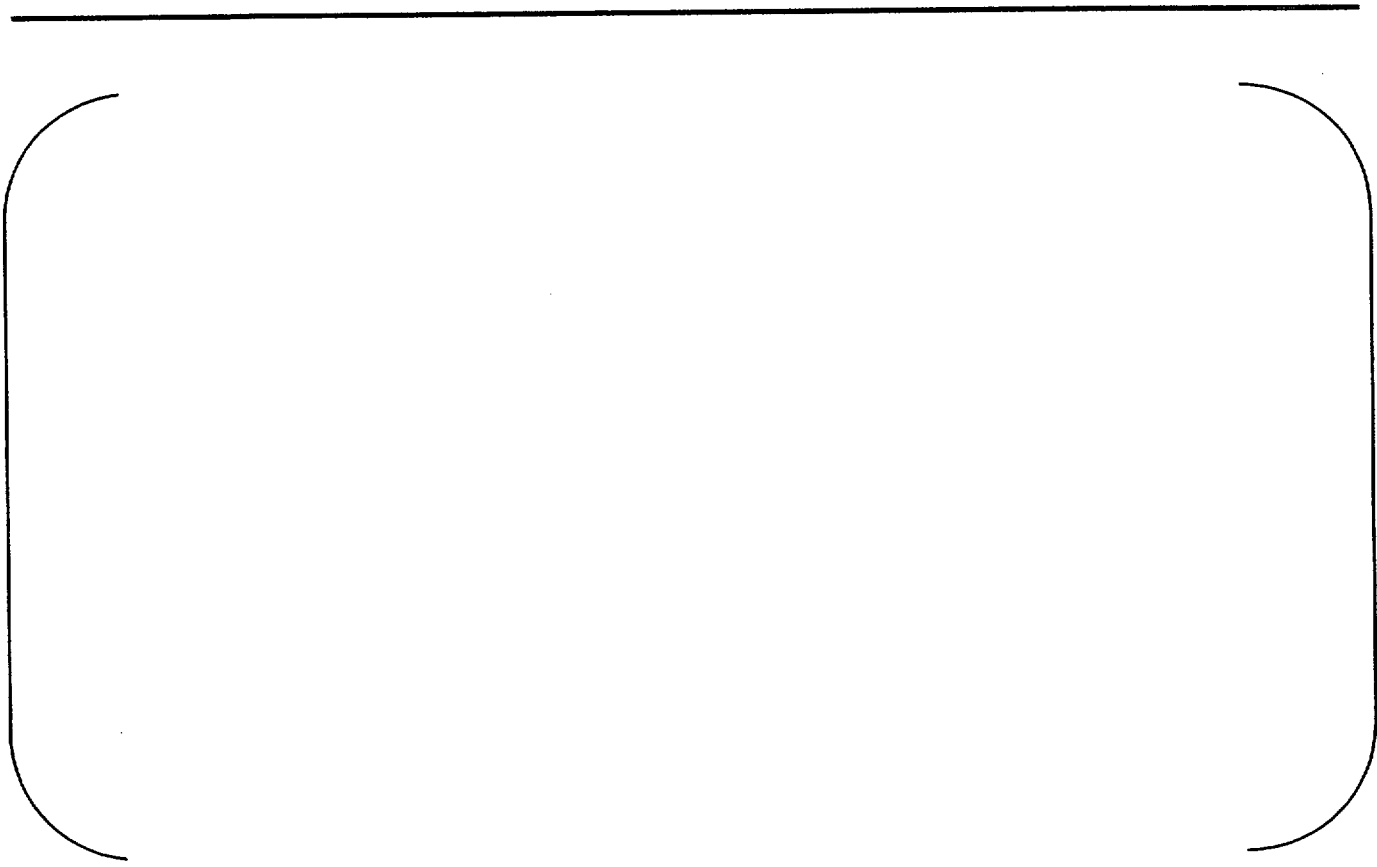


Figure D-14: Fuel rods power history for rods in assembly 2952



Figure D-15: Fuel rods power history for rods in assemblies 3013, 3120 and 3160



Figure D-16: Fuel rods power history for rods in assemblies 4698, 4885, 4896 and 4925



Figure D-17: Fuel rods power history for rods in assembly 6116



Figure D-18: Fuel rods power history for rods in assemblies 6472, 6478, 6537 and 6576



Figure D-19: Fuel rods power history for rods in assembly 6704



Figure D-20: Fuel rods power history for rods in assembly 6782



Figure D-21: Fuel rods power history for rods in assembly 7560



Figure D-22: Fuel rods power history for rods in assembly aaa006



Figure D-23: Fuel rods power history for rods in assembly aba047



Figure D-24: Fuel rods power history for rods in assembly acc119

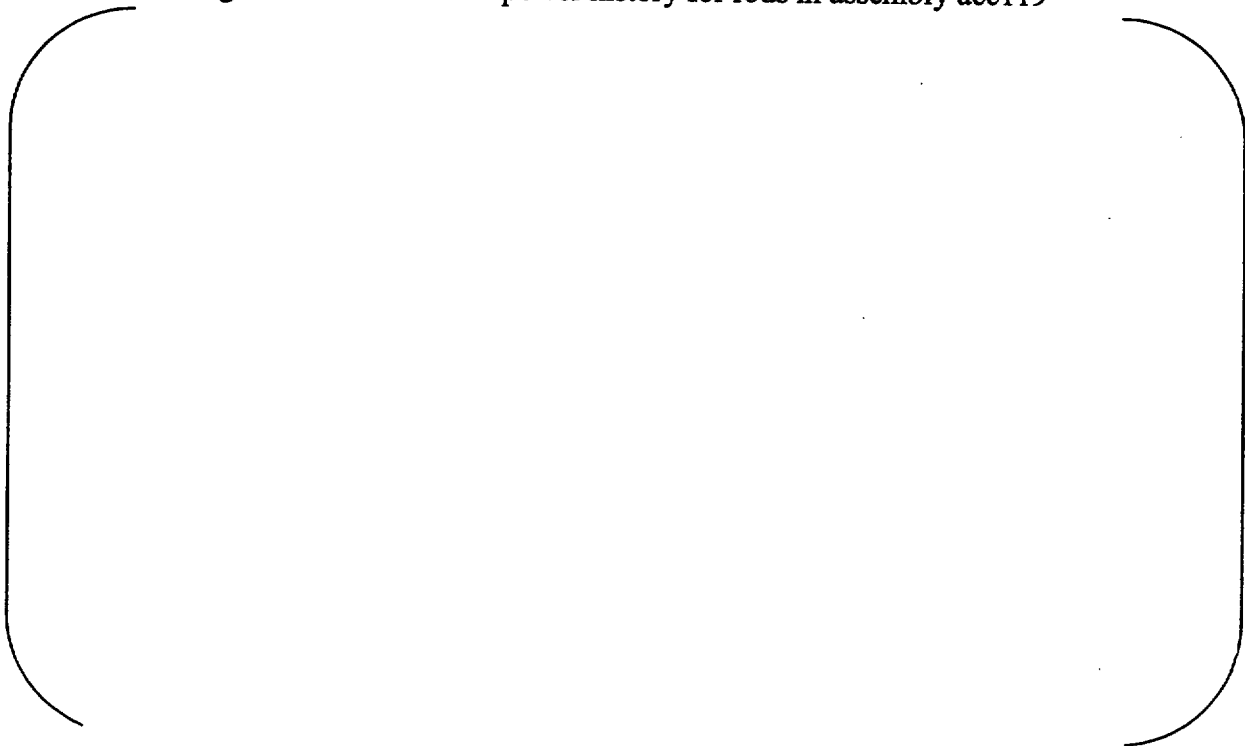


Figure D-25: Fuel rods power history for rods in assemblies aaa045, abb073, ada008 and aeb070



Figure D-26: Fuel rods power history for rods a1 – d8 in assembly s22



Figure D-27: Fuel rods power history for rods e1-h8 in assembly s22

APPENDIX E PWR FUEL ROD POWER HISTORIES

This appendix contains the PWR fuel rod power histories supporting the calibration and verification calculations in Section 3.

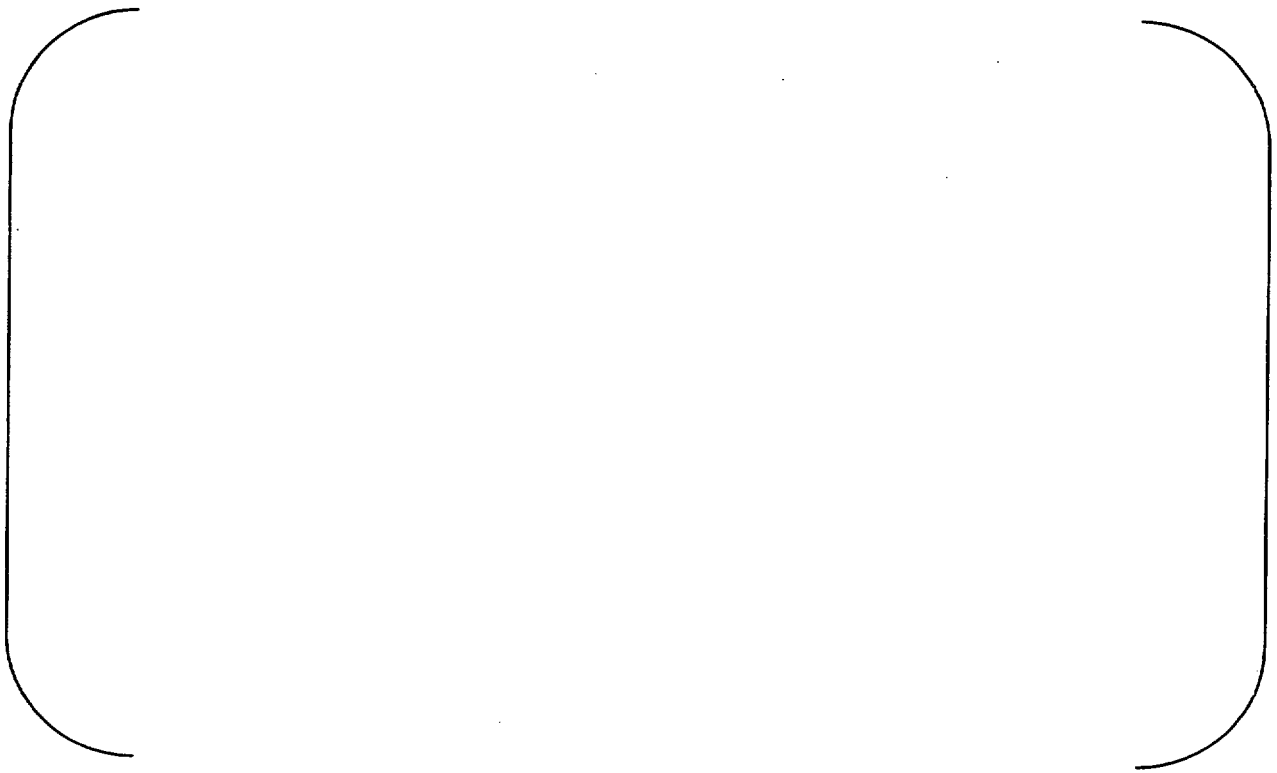


Figure E-1: Rod power histories for rods 266, 281, 285 and 294

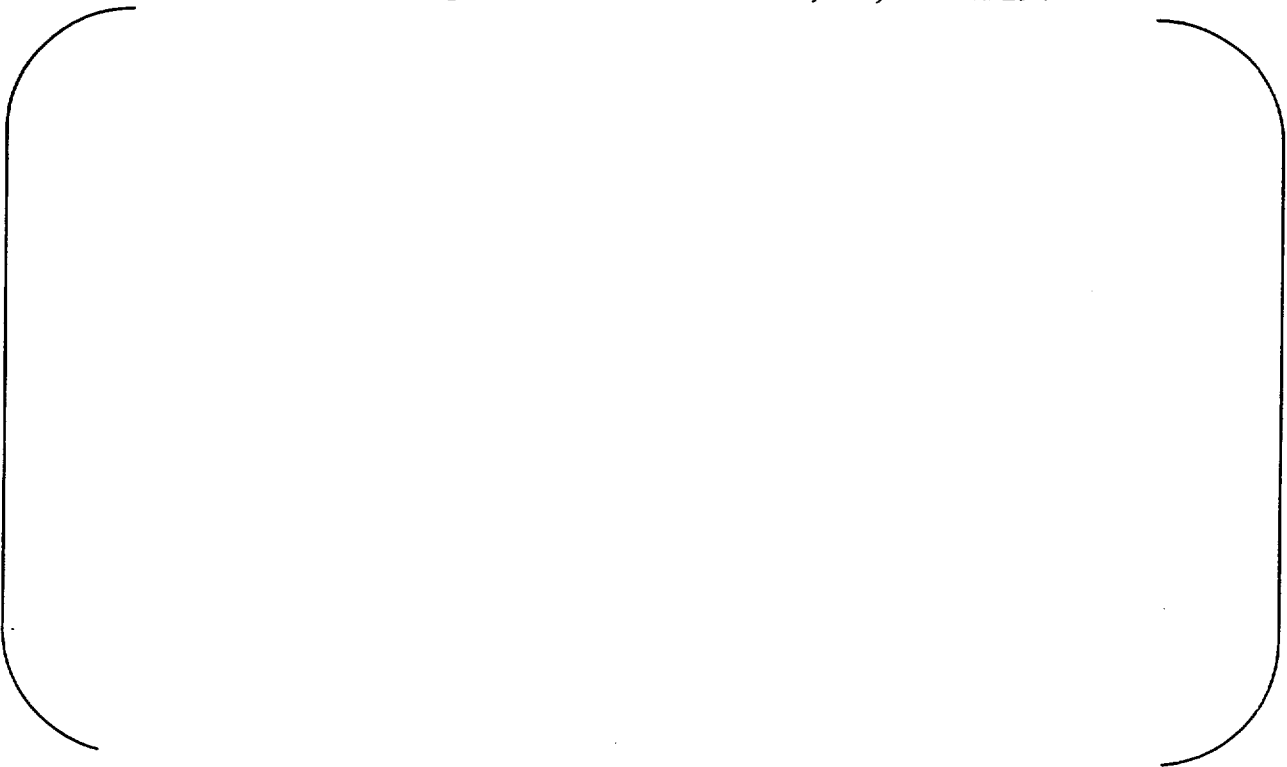


Figure E-2: Rod power histories for rods 313, 318, 328 and 344

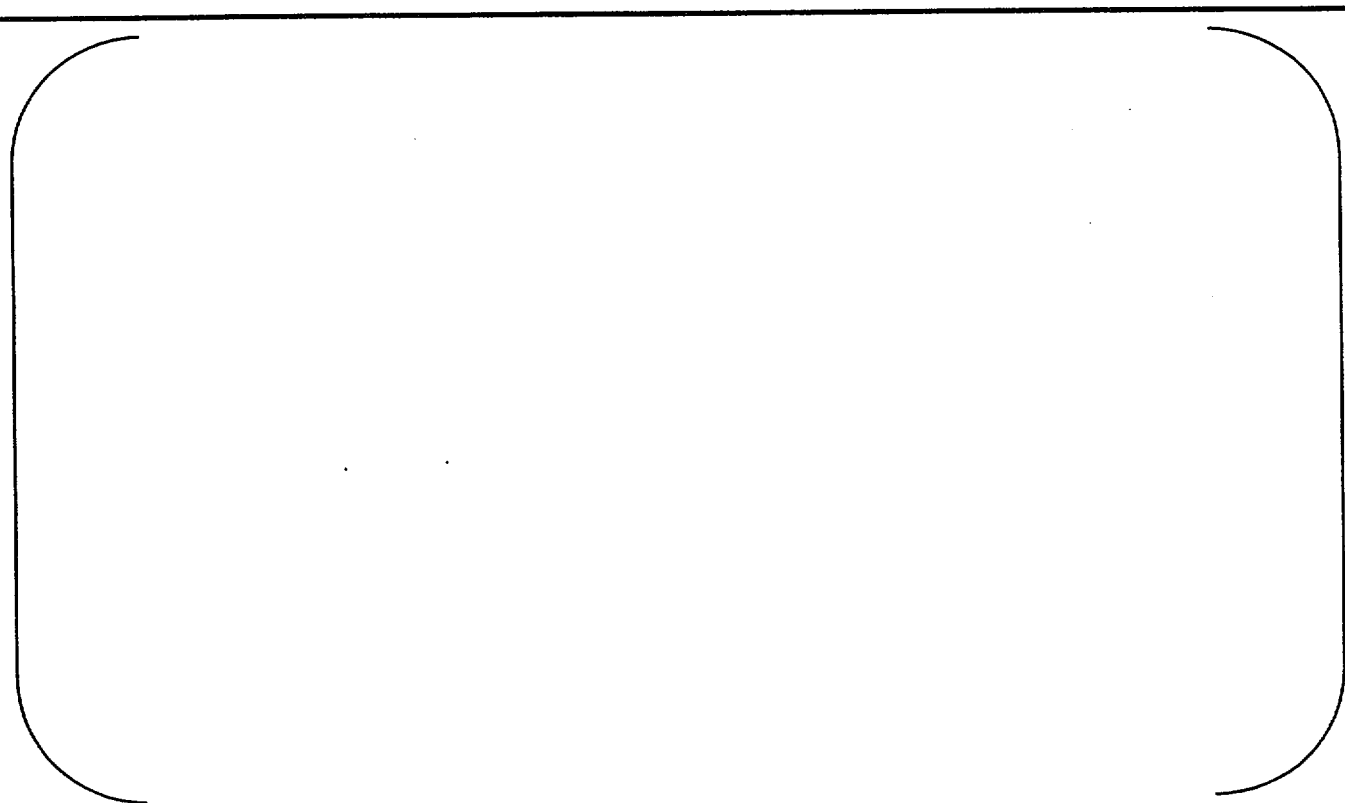


Figure E-3: Rod power histories for rods 331, 332 and 335

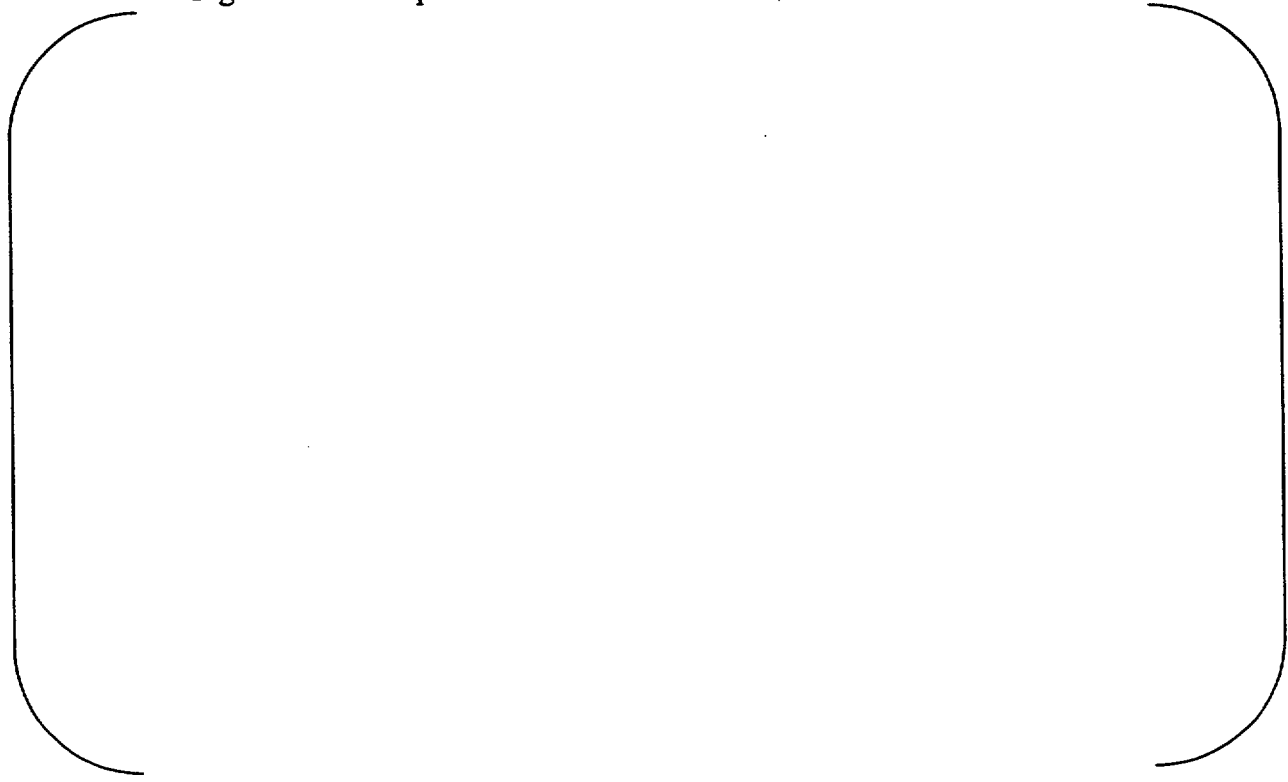


Figure E-4: Rod power histories for rods 363, 365, 368, 385 and 386



Figure E-5: Rod power histories for rods in assemblies 4i7 and 4i8



Figure E-6: Rod power histories for rods in assembly 4m1



Figure E-7: Rod power histories for rods in assembly 4m4



Figure E-8: Rod power histories for rods 501, 502, 507 and 509



Figure E-9: Rod power histories for rods 511 – 513 and 515



Figure E-10: Rod power histories for rods in assembly 5f1



Figure E-11: Rod power histories for rods in assembly 5f2



Figure E-12: Rod power histories for rods 603, 610, 612 and 613

Figure E-13: Rod power histories for rods 620, 622, 624 and 638

Figure E-14: Rod power histories for rods 640, 642, 646 and 648




Figure E-15: Rod power histories for rods 650, 653, 654, 657 and 659




Figure E-16: Rod power histories for rods 661, 663, 665, 677 and 679

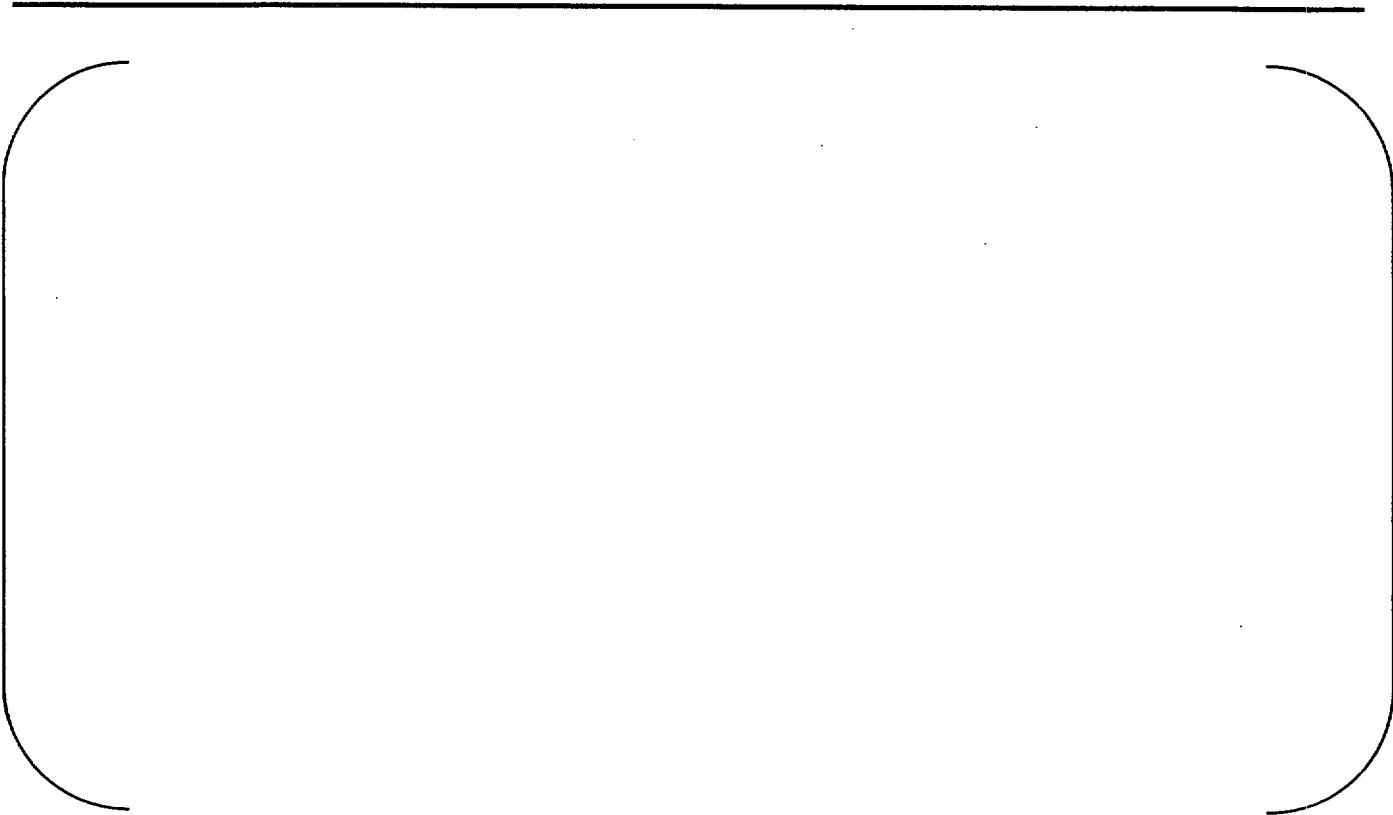


Figure E-17: Rod power histories for rods 681, 683, 685, 687 and 689



Figure E-18: Rod power histories for rods 691, 693, 696, 697 and 699




Figure E-19: Rod power histories for rods 700 - 703

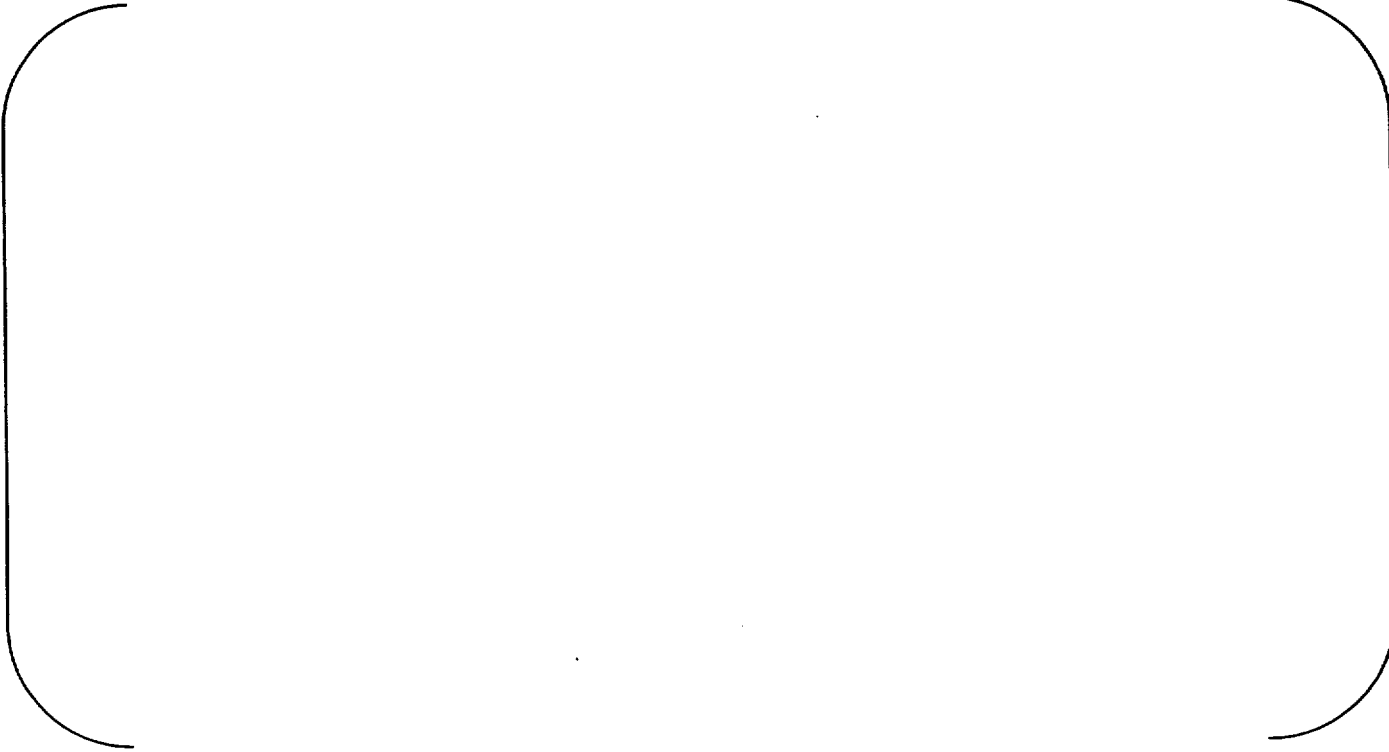


Figure E-20: Rod power histories for rods 704 - 707




Figure E-21: Rod power histories for rods 708 - 711



Figure E-22: Rod power histories for rods 823, 824, 838 and 846




Figure E-23: Rod power histories for rods 869, 871, 872 and 876



Figure E-24: Rod power histories for rods 881, 885 and 886

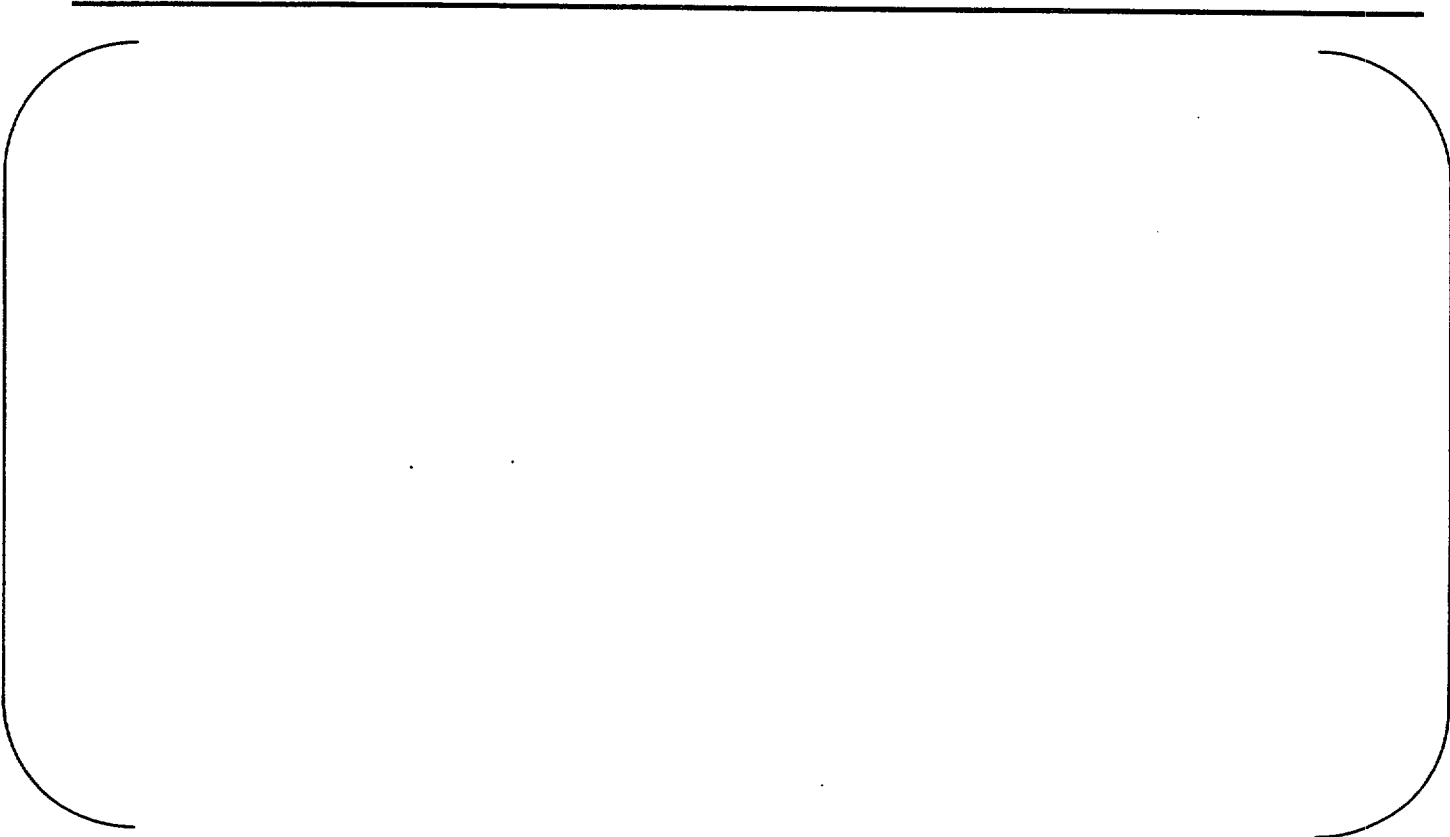


Figure E-25: Rod power histories for rods 888e9, 888m13, 889d7 and 889m9



Figure E-26: Rod power histories for rods 893, 896, 897 and 908




Figure E-27: Rod power histories for rods bge-ben013, bfg092 and bfj027

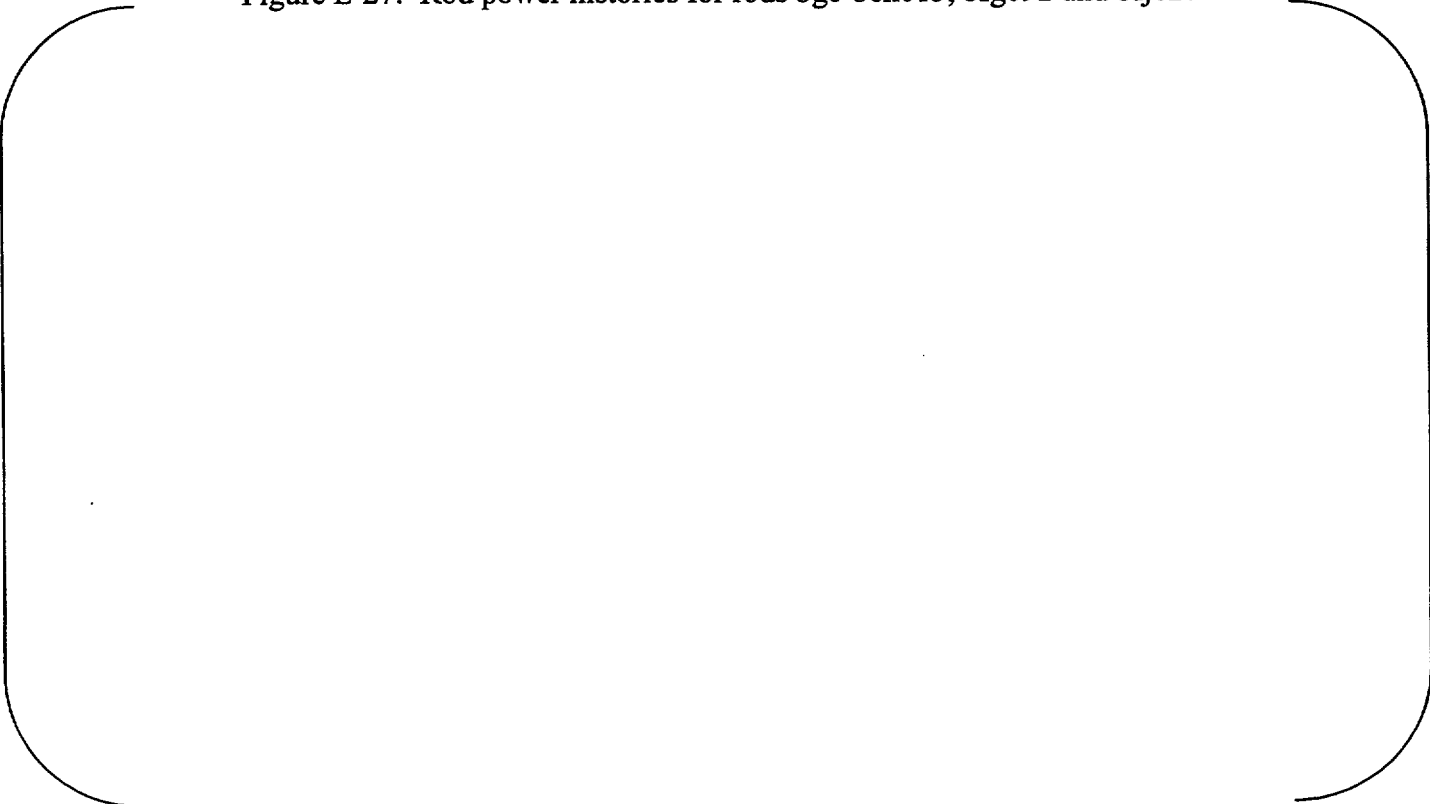


Figure E-28: Rod power histories for rods bge-bf1009 and bf1031, me47-d11 and k17

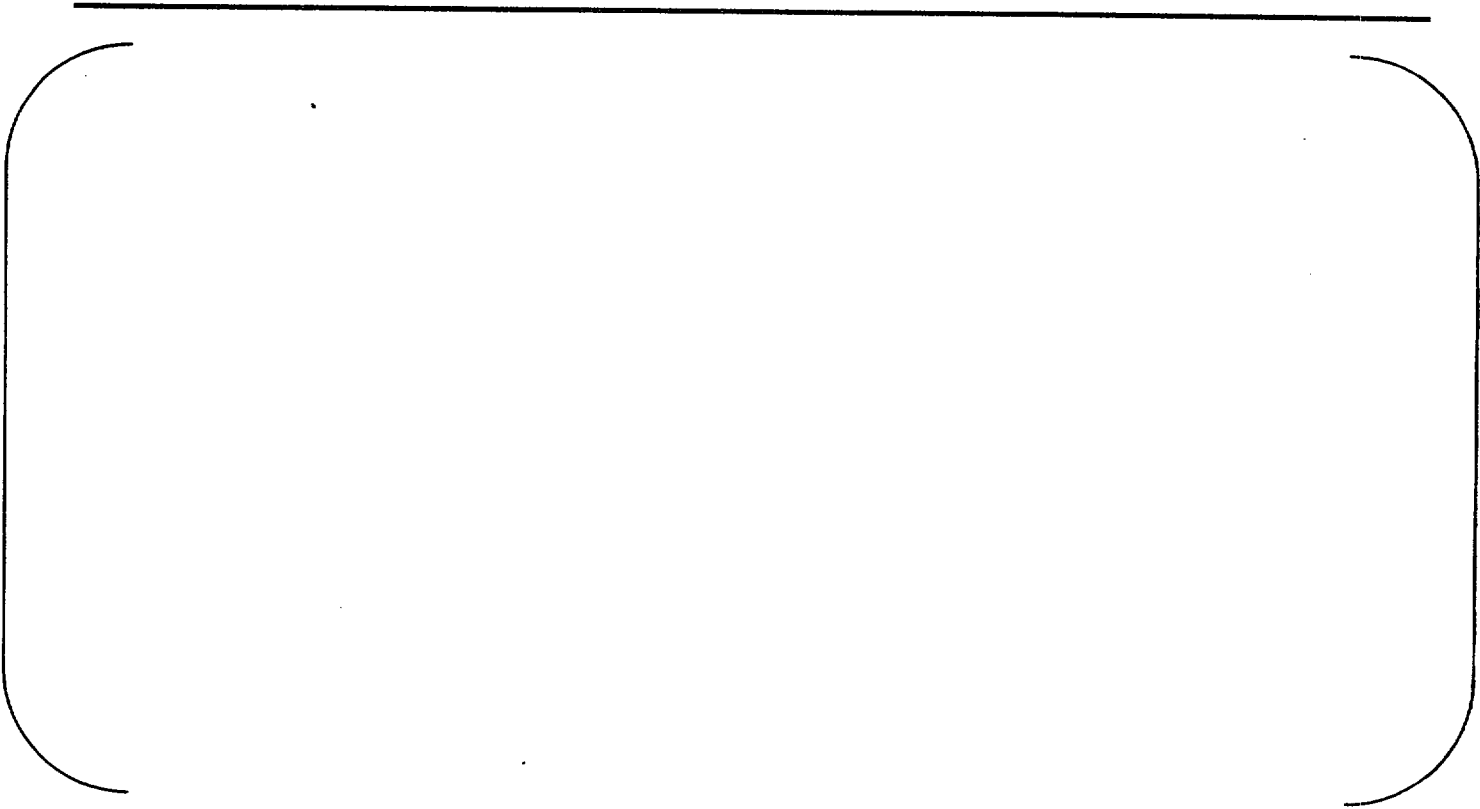


Figure E-29: Rod power histories for rods bge-bfm034 and 043 and bge-ufe019 and 067



Figure E-30: Rod power histories for rods bge-bfm070, 071, 073, and 156